Lincoln University Digital Thesis

Electrospinning nanofiber insert for anterior ocular drug delivery for cataract treatment

A thesis

submitted in partial fulfilment

of the requirements for the Degree of

Doctor of Philosophy

at

Lincoln University,

Lincoln, New Zealand

By

Jayanthi Swaminathan

Lincoln University

2023

DEDICATION

This thesis is dedicated to my wonderful husband, son, and daughter-in-law

Mr Ganesan Swaminathan

Dr Akhilesh Swaminathan

&

Dr Sharanya Sankaran

Who motivated me to follow my passion and dream

And

To my mother and late father

Mrs Saroja Srinivasan

&

Late Mr P K Srinivasan

Who taught me the value of education

Acknowledgements

First and foremost, I would like to express my deepest appreciation to my supervisor, **Professor Craig Bunt** who was my friend, philosopher, and guide throughout this journey. He shifting to Otago University during the last 1.5+ year of this journey did throw some challenges, but he saw to that we reached the finish line without any roadblocks. I would also like to extend my sincere thanks to my Associate Supervisor, **Professor James Morton** for his invaluable input whilst drafting my thesis. I'd like to acknowledge **Dr Thilini Thrimawithana** (lecturer, RMIT University, Melbourne, Australia) associate co-supervisor for her expert suggestions at the start of this journey.

I would like to acknowledge **Lincoln University** for offering me a position as a part-time Teaching Fellow position over the past five years that allowed me to pursue my passion to undertake PhD research along with gaining teaching experience.

Many thanks to my fellow laboratory colleagues, Dr Weiyi Liu and Dr Sally Price for their brainstorming discussions, ideas, and input. I would also like to acknowledge the support given by Ara internship students along this journey with special mention of Jarred Kidwell, Jessica Ranger, Lakshay Raj Siwach, Liz van der Krabben and Jagir Turna.

My sincere thanks to cohort members of Lincoln and Otago University for their never-ending support in the field of administration, logistical support, technical support and analysis to fulfil this research project: AGLS Department Lincoln University – Dr Andrew Greer, Robyn Wilson, Andrea Hogan, Dr Shuang Jiang, Rosy Tung, Jenny Zhao, Professor Jon Hickford; Otago University – Bettina Poller, Sumit Dadhwal, Niki Hazelton.

I would like to thank my colleague and office roommate, Gayani Priyadarshani for her support, motivation, and ideas with the layout of the thesis. It was nice to get her input as she is freshly graduated PhD student.

I would like to thank my friends and others who I have missed mentioning above who have supported and helped me throughout this journey.

Finally, I am so thankful to my husband and son for encouraging me to get into this career phase and to follow my passion and dream. If not for them this endeavour would not have been possible, thanks heaps to my loving husband and son. I cannot forget to thank my daughter-in-law who has been a great support and motivator to complete this research work. Last but not the least, I am also extremely grateful to my mother and extended family members (sisters, brother-in-laws, sister-in-laws, mother-in-law, nephews, nieces, and little grandchildren) for their love and emotional support during this journey.

Abstract

The eye is a complex visual aid (for human and animals) which gathers visual information from the surrounding physical environment. The more common vision threatening diseases that affect both anterior/posterior segment (age related macular degeneration, cataract, keratitis, glaucoma, diabetic retinopathy, retinoblastoma, allergic conjunctivitis, and ocular trauma) is a massive social and economic burden especially for less developed countries. Drug delivery to any tissue is a challenge, eye is not an exception. Barriers to ocular drug delivery are both physiological, anatomical, static, and dynamic. The current cost-effective cataract treatment option involves surgical removal of opaque or cataractous lens and replicated with artificial intraocular lens followed with topical application of corticosteroid eye drops as post-operative management. Whilst current topical drugs are easy to apply their bioavailability is impeded due to various barriers prevailing in the eye which put a strain on the cost and the duration of recovery. This has led researchers to the path of finding alternative methods of ocular drug delivery which more recently has led to the use of nanotechnology.

Nanotechnology research that can transport and deliver active ingredient (AI) safely to site of action has gained importance in recent years. Ocular drug delivery with nanotechnology though can overcome some of the challenges but does have some limitations, like patient compliance and irritation. These limitations have been addressed by researchers across the globe by reducing drug particle size, using less irritable polymers and excipients, but with limited success.

The research presented in this thesis approached this problem using nanofiber technology to develop solid ocular insert that would allow sustained drug delivery. Caffeine, a model drug, was

vi

used to determine the kinetics of bioactive release. Nanofiber membranes fabricated as mono-, two- or three-layered using two polymers, poly (ethylene) oxide (PEO) and poly ε-caprolactone (PCL) and analysed for physical characteristics of fiber (mat thickness, water contact angle, tensile properties, SEM) and drug release.

Results from this study shows that the thickness of mat can be increased by having additional layer (average of 46% for two- and 54% for three-layered) compared to monolayer but it is not proportionate to the extra amount of polymer. For water contact angle the results achieved for various iterations were on par with the property of the polymer, hydrophobicity (>80°) and hydrophilicity (<50°). The tensile properties (only for mono- and three-layered formulation), puncture strength and elongation at break there was no differences between the formulations for elongation at break but for puncture strength, the force required was almost double for three-layered formulation compared to control monolayer. However, it was a challenge to measure the tensile property for monolayer formulation with PEO polymer. Mucoadhesion evaluated for only three-layered nanofiber formulations containing PEO and PCL polymer shows that the force required to detach the mat from mucin tablet (used as test material) was almost double compared to the monolayer control formulations. Surface morphology (SEM) of the nanofiber mat shows heterogenous fiber diameter distribution irrespective of the polymer and number of layers.

The caffeine release from monolayer was almost immediate (within 5 min) for the formulations with PEO polymer (>50%) compared to PCL polymer wherein the same release % was noticed 1h after the initiation of the experiment. The drug release from two-layered formulation was reduced by 50% when the drug was incorporated in the first layer and the second layer acted as a barrier. Unlike the two-layered formulation, same results could not be achieved from a three-layered formulation when the drug was incorporated in the third layer, there was average >70%

drug released after 1h. Surface morphology of mono- and three-layered formulations exhibited the presence of caffeine crystalline structures on the surface of the fiber which probably has attributed to immediate burst release of the drug when in contact with the aqueous solution.

The results from this study elucidate that mucoadhesion onto the cornea surface can be enhanced by incorporating a hydrophilic polymer into the formulation which would probably help in the retention and increase the bioavailability of the drug to the target site in the eye. The results also shows that burst release can be mitigated and sustained release achieved when there is a barrier layer to the drug as shown in the two-layered formulation where the drug release was reduced by 50% by having a barrier layer with only the hydrophobic polymer. This formulation show promise for bioactive delivery but will require further exploration and refining.

Keywords: ocular drug delivery, cataract, nanotechnology, topical, active ingredient, bioactive

Table of Contents

x

xi

List of abreviations

List of abbreviations commonly used in the text.

AMD	Age-related macular degeneration
BCOP	Bovine Corneal Opacity and Permeability
BRB	Blood retinal barrier
DCM	Dichloromethane
DR	Diabetic retinopathy
FDA	Food and Drug Administration
FESEM	Field Emission Scanning Electron Microscopy
HCF	International Classification of Functioning, Disability and Health
HET-CAM	Hen's egg-chorioallantoic membrane
IC	Intracameral injection
IDF	International Diabetic Federation
LVET	Low-volume eye irritation test
NODS	Novel Ophthalmic Delivery System
NRU	Neutral red uptake
NSAID	Non-steroidal anti-inflammatory drugs
OECD	Organization for Economic Co-operation and Development
PCL	Poly(ε-caprolactone)
PEO	Poly(ethylene) oxide
RBC	Red blood cell
RPE	Retinal pigmented epithelium
SEM	Scanning Electron Microscopy
SEM	Standard error of mean
SODI	Soluble Ophthalmic Drug Insert
SRB	Sulforhodamine B
VEGF	Vascular endothelial growth factor
WHO	World Health Organization

List of Tables

List of Figures

Preface

This thesis consists of five chapters and appendix.

Chapter 1 is review of literature to the topic and outlines the research aims.

Chapter 2 describes the methodology used for polymer preparation, nanofiber membrane fabrication, nanofiber mat thickness, tensile properties (puncture strength and mucoadhesion), water contact angle, surface morphology (SEM), and in-vitro release studies.

Chapter 3 provides the results and discussion for various formulation iterations.

Chapter 4 provides conclusions of the various analysis

Chapter 5 is a general discussion and conclusions, some challenges encountered with the research project, limitation, and future direction.

Appendix contains SEM images for mono- and three-layered formulations.

CHAPTER 1   LITERATURE REVIEW

1.1   Gross anatomy of the eye

The human eyes are complex sensory organs, they act as a gateway to capture external images and transmit to the brain through the optic nerve, The eyes sit in the bony cavities called the orbits, in the skull, six extraocular muscles control eye movements. Anteriorly (toward the front) the eye is protected by the eyelids. Posteriorly (toward the back), the optic nerve, the main neural output of the eye travels from the eye towards the brain.

The eye has a slightly asymmetrical spherical shape with an approximate sagittal diameter or length of 24 to 25 mm and a transverse diameter of 24 mm. It has a volume of about 6.5 ml. The wall of the eye is made up of three primary layers enclosing various anatomical structures, an outer, middle, and inner layer. The outer layer has a tough, white, opaque membrane called sclera (the white of the eye). Clear, thin-dome shaped tissue called cornea is the slight bulge in the sclera in the front of the eye. In the middle layer choroid, the front is the coloured part of the eye called iris, while the pupil is a circular hole or opening in the centre of the iris. The inner layer is the retina, which lines the back two-thirds of the inner eyeball. The retina consists of two layers, the sensory retina which contains the nerve cells that process visual information and transmits to the brain; and the retinal pigment epithelium (RPE) which lies between the sensory retina and the wall of the eye.

The hollow eyeball (Figure 1.1) consists of three fused chambers. The anterior and posterior chamber are filled with aqueous humour and are essentially in front of the lens. The vitreous

1

chamber (behind the lens) contains a gelatinous vitreous material composed of jelly like vitreous humour and contains aqueous humour.

The anterior segment which occupies about one-third portion of the front of the eye and is comprised of tissues in front of the vitreous humour. These include the lid, cornea, conjunctiva, aqueous humour, trabecular meshwork, iris, ciliary body and crystalline lens. Sclera, choroid, Bruch's membrane, retinal pigment epithelium (RPE), neural retina and vitreous humour makes up the posterior segment.

Image removed for Copyright compliance

Figure 1-1 Anatomy of the eye (Chen, 2015).

Anterior ocular anatomy

The parts of the eye that constitutes the anterior portion are the cornea, iris, pupil, conjunctiva, ciliary body, and anterior chamber. Anterior chamber is an aqueous humour filled space inside the eye between the iris and the cornea's inner most layer, the endothelium and occupies one third of the eye from back surface of the cornea to the crystalline lens. Aqueous humour, trabecular meshwork and crystalline lens makes up the anterior chamber of the eye. Anterior segments contain both the fibrous and vascular layers. Fibrous layer is the outermost layer of the eye and consist of sclera and the cornea. The vascular layer is the pigmented region that includes iris, ciliary body, and choroid.

Majority portion of the ocular surface is covered by sclera or white of the eye which maintains the shape of the eye. Sclera acts as a protective layer and functions as an attachment site for extraocular muscles (Malhotra et al., 2011). The shape and thickness constantly change during the lifespan, it is thick and flexible during early childhood. As the intraocular pressure increases with age it becomes rigid. Sclera is made up of highly innervated dense fibrous connective tissues containing both collagen and elastic fibres. The layer is thinnest over the anterior surface and thickest at the posterior surface of the eye near the optic nerve exit.

Transparent convex cornea is continuous with sclera and is the most anterior part of the eye in front of the iris and pupil. It is highly innervated with organised layers of collagen and elastic fibres, most corneal nerves are sensory nerves, derived from the ophthalmic branch of trigeminal nerve (Müller et al., 2003). The cornea of adult human eye has an average horizontal diameter of about 11.5 mm and a vertical diameter of 10.5 mm, and a curvature that remains constant throughout life (Rüfer et al., 2005). The outer transparent layer of the cornea is the tear film. An inner proteinaceous layer aids the tear film to adhere to the cornea. Tear film is composed of three layers, the outer an oily or lipophilic, middle aqueous and the inner mucus layer. High lipid content in the outer layer mitigates the tear evaporation. The inner mucus layer of tear film is in direct contact with the epithelial cells of the cornea. One of the primary functions of tear film is to provide continuous lubrication. Average tear film thickness is 6.0 μm ± 2.4 μm. Cornea is made up of 5 layers (Figure 1.2), epithelium, Bowman's membrane, the lamellar stroma, Descemet's membrane and the endothelium (Farjo et al., 2009). Thickness of cornea gradually increases from centre to periphery (DelMonte & Kim, 2011). The corneal epithelium is composed of two to three layers of superficial, two to three layers of wing and one layer of basal stratified and squamous non-keratinised epithelial cells (Farjo et al., 2009). Multi-layered corneal epithelial cells are made up of cuboidal basal cells with tight junction complexes, which prevent

3

tears from entering intercellular spaces. The corneal epithelium is about 50 μm in thickness. The lifespan of corneal epithelial cells is about 7-10 days undergoing constant involution, apoptosis, and desquamation. Bowman's layer is present just below the basal corneal epithelial cells and is about 8-15 μm thick. This amorphous band of fibrillary material is non-regenerative and forms a boundary between corneal stroma and epithelial cells and maintains the corneal shape. Corneal stroma lies between Bowman's anteriorly and Descement layer posteriorly and contributes to 90% of the corneal thickness and provides structural integrity to the cornea. This layer is primarily composed of water and collagen. Descement layer is a thin layer that separates the stroma from the endothelial layer of the cornea. The layer gradually thickens with age, 5 to 15μ. Endothelium layer of cornea is a monolayer of cells with a thickness of about 5μ. Endothelial cell numbers decrease with age. This layer has limited permeability to ion flux, which is necessary to maintain an osmotic gradient. Endothelium of cornea is in direct contact with aqueous humour. A new layer of cornea (6th layer), Dua's layer was discovered in 2013 (Dua et al., 2013). Dua's layer 15 μ thick is located at the back of cornea between cornea stroma and Descemet's membrane. This layer is incredibly tough, can withstand 11/2 to 2 bars pressure and less prone to cornea tearing.

Image removed for Copyright compliance

Figure 1-2 Cornea layers (Murphy, 2013).

Iris is a thin contractile layer located between the cornea and the crystalline lens. It contains pigmented sheet of cells and separate the anterior segment into anterior and posterior chambers,

with a pupil in the central aperture. Iris regulates the amount of light that enters the eye through pupil by dilation and contraction of pupillary muscles.

Aqueous humour is present between the cornea and the lens. This layer is constantly replenished, as it flows through the pupil and fills the anterior chamber. This layer is formed by the epithelial cells of the ciliary body that is in the posterior chamber.

The conjunctiva is a thin, highly vascularized, transparent, mucous-secreting tissue that forms the inner lining of the upper and lower eyelids (Wolff, 1976). It is reflected onto the eye as a thin transparent tissue on sclera and extends up to the corneal limbus. The total surface are of conjunctiva is approximately 17 times larger relative to cornea (Watsky et al., 1988). Elastic nature of conjunctiva facilitates motion of the eyeball and eyelids. Conjunctiva tissue can be further divided into three types based on location, thickness, and vascularization, palpebral, forniceal and bulbar. Palpebral conjunctiva is the internal lining of upper and lower eyelid, bulbar conjunctiva is present near to the sclera and forniceal conjunctiva is the small portion of connected tissue between palpebral and bulbar conjunctiva. A unique feature of conjunctiva is presence of goblet cells in the stratified epithelium. These goblet cells are specialised apocrine cells which provide mucin layer to the tear film (Cher, 2013).

The ciliary body extends from the posterior insertion of the iris to merge with the choroid at the ora serrata, which is also the site of fusion of the retinal sensory and pigment epithelium. The ciliary body runs around the inside of the anterior sclera and forms a complete ring. It connects to the lens via the zonules, also known as the suspensory ligaments. The inner layer of the ciliary epithelium is not pigmented and is continuous with neural tissue, whereas the outer layer is highly pigmented and is continuous with the retinal pigmented epithelium (RPE). The backside

5

of the ciliary body secretes the fluid (aqueous fluid) that fills up the anterior chamber of the eye when it is drained out through the trabecular meshwork. Too much production of the fluid or little outflow of the fluid can increase the pressure in the eye. High pressure is a significant risk factor for developing glaucoma. Several conventional glaucoma eye-drop medications target the ciliary body and alleviate secretion of the aqueous fluid.

1.2 Ocular diseases

Vision is the most significant sense of the five senses for humans to manoeuvre the world and survive. With the life expectancy higher these days there is more chances for most of the surviving human being to experience at least one eye condition in their lifetime that would require appropriate care. Globally, at least 2.2 billion people have a vision impairment or blindness, of whom at least 1 billion have a vision impairment that could have been prevented or has yet to be addressed (World Health Organization, 2019). In 2020, an estimated 596 million people (predicted to increase to 895 million by 2050) had distance vision impairment worldwide, of whom 43 million were blind and it may lead to 61 million by 2050 (Burton et al., 2021). Visual impairment is a major global issue as the population growth increases with a massive burden especially for less-developed countries. The significant risk factor to progression of eye conditions and treatment outcomes are lack of access to quality eye care (Arun et al., 2009; Lindfield, 2014; Ramke et al., 2017). "Impairment" is a term used to describe a problem in the function or structure of a person's body due to health condition, according to the International Classification of Functioning, Disability and Health (HCF) (World Health Organization, 2001). Ophthalmic diseases can affect both the anterior and the posterior segments of the eye. Anterior segment consists of front one-third of the eye that mainly includes pupil, cornea, iris, ciliary body, aqueous humour, and crystalline lens while the posterior segment consists of the back two-

thirds of the eye that includes sclera, choroid, Bruch's membrane, retina and vitreous humour (Cholkar et al., 2012). The major ocular diseases include age-related macular degeneration(AMD), diabetic retinopathy (DR), cataract, uveitis, and glaucoma, which can lead to blindness unless treated (Pascolini & Mariotti, 2012). In the anterior, common diseases include ocular inflammation and pain, allergic conjunctivitis, anterior uveitis, keratitis, dry eye, blepharitis, meibomian gland disease and glaucoma. Further details of these anterior diseases is covered below in the sub-section.

Posterior ocular diseases.

The most common posterior ocular infections are age-related macular degeneration (AMD) and diabetic retinopathy (DR). AMD involves the progressive dysfunction and degeneration of macula's photoreceptor cells that leads to loss of central vision. Globally 8.7% of the world population has age-related macular degeneration, the projected number of people with this disease is around w196 million in 2020, increasing to 288 million in 2040 (Wong et al., 2014). AMD can be managed by lifestyle interventions (cessation of smoking, control of blood pressure, micronutrient supplementation, healthy weight management) and Vascular endothelial growth factor (VEGF)-targeted therapies which can prevent vision impairment (Apte, 2021; Borooah et al., 2012). Diabetic retinopathy (DR) develops in many individuals with an endocrine disorder (diabetes mellitus) that interferes with glucose metabolism. The disease eventuates due to blockage of small retinal blood vessels followed by excessive growth of abnormal blood vessels that invade the retina and extend into the space between the pigment and inner neural layers. The International Diabetic Federation (IDF) estimated global population with diabetic mellitus (endocrine disorder) in 2021 to be 537 million and to increase to 783 million in 2045 (International Diabetic Federation., 2021). Management of DR varies depending on the severity

of the disease. The ideal management is prevention which is achieved by glycaemic control and blood pressure monitoring. Proliferative DR with haemorrhage is cleared by a procedure called vitrectomy and diabetic macular oedema is treated by very low-power laser to the areas of oedema (Borooah et al., 2012).

Anterior ocular diseases

The common diseases of the anterior segments are ocular inflammation and pain, allergic conjunctivitis, anterior uveitis, keratitis, dry eye, blepharitis, meibomian gland disease and glaucoma.

Ocular inflammation can eventuate because of multiple pathologies. Ocular inflammation and pain generally result from ophthalmic surgery, such as cataract, vitreoretinal, cornea and glaucoma procedures. Some of these symptomatic conditions can lead to acute inflammation. Corticosteroids or NSAID eye drops are used to mitigate the pain and inflammation (Chen, 2015).

Conjunctivitis is inflammation of conjunctiva and for most patients it is usually a transitory irritation. This condition is contagious and very common, more so with children who can rapidly spread to other children in school or nursery. The body immune response results in inflammation which leads to the hyperaemia and discharge (Borooah et al., 2012). Mild symptoms are dealt with following hygiene procedures like washing hands after touching the infected eye, severe conditions are mitigated with antibiotics.

Anterior uveitis is the inflammation of the anterior uveal tract, including the iris, ciliary body or both. This condition is relatively uncommon, and the exact pathogenesis is still unknown. It is presumed an unknown antigen is thought to provoke an inflammatory response that results in the breakdown of the eye-blood barrier (Borooah et al., 2012).

Keratitis is the inflammation of cornea caused frequently by infection (Ansari et al., 2013). The infection is treated with antibacterial, antifungal, or antiviral therapy, depending on the etiology of the infection. Commonly prescribed antibiotics for topical application can be used to alleviate bacterial keratitis (Austin et al., 2017).

Dry eyes is an ocular surface disease that can result in irritation and blurred vision. The signs and symptoms eventuate from inadequate tear production and imperfect coating of the cornea by the tear film (Foulks, 2007). Dry eye disease is also known as keratoconjunctivitis. Artificial tear substitutes are used to overcome the inadequate tear production.

Blepharitis is inflammation due to clogged oil glands of eyelids near the base of the eyelashes characterised by redness and irritation of the eye and eyelid (World Health Organization, 2019). This condition results from build-up of bacteria on either the lash follicles or meibomian orifices which leads to burning sensation and watering from the eyes. Chronic blepharitis conditions need further investigations followed by topical antibiotic application. Meibomian gland disease also known as anterior blepharitis is known to be a major component for some of the patients suffering from dry eye (Nichols et al., 2011).

Glaucoma has become the most frequent cause of irreversible blindness worldwide (Tham et al., 2014). Glaucoma results in vision loss due to build of intraocular pressure which ultimately leads

to damage of the optic nerve and often without exhibiting any symptoms. If the disease exhibits symptoms, initially it is darkening peripheral vision, if left undetected and untreated can lead to severe damage and result in blindness. Glaucoma is relatively a common condition, it is estimated that 76 million people (aged 40-80 years) suffer from this disease during 2020 which is projected to increase to 111.8 million (aged 40-80 years) by 2040 globally (Tham et al., 2014). Primary open angle glaucoma was more common than primary angle closed glaucoma, globally the prevalence of the disease was highest in the African region. Glaucoma can be treated either by topical application to alleviate the stress on aqueous humour or by surgical correction, perforating the wall of the anterior chamber to encourage drainage.

Cataract develops when the crystalline lens loses its transparency and leads to blurred vision due to lack of light passage through the lens. It continues to be a major disease of blindness particularly in developed countries (Lee & Afshari, 2017). WHO, estimates that population growth and aging will escalate the risk with more people (65.2 million) suffering from vision impairment (World Health Organization, 2019). Surgical intervention can aid in the sight improvement by replacing the damaged lens with artificial substitute and fine-tuned with glasses and contact lenses.

1.3 Ocular drug delivery

Ocular drug delivery is hampered by the barriers protecting the eye. The bioavailability of the active drug substance is often the major hurdle to overcome. Anatomically, the human eye includes unique physiological barriers, including the tear film, cornea, and conjunctival barriers constituting the anterior segment barriers (Cholkar et al., 2012; Maurice, 1980), and the inner limiting membrane and blood retina barrier (BRB), which forms the posterior segment barriers

(Peyman & Ganiban, 1995; Thrimawithana et al., 2011). The tight ocular barriers whilst having protective function, they also pose major obstacles for efficient drug delivery as they limit the diffusion and penetration of ophthalmic active ingredients. Overcoming these barriers and improving the ocular drug bioavailability is a major challenge for researchers working in this domain. Commercially available conventional ophthalmic medication are eye drops, suspensions, emulsions, and ointments. Most (>60%) of the ophthalmic formulation marketed are in the form of solution and ointments (Kuno & Fujii, 2011; Lang, 1995) which is not desirable for treating vision-threatening ocular diseases. Ophthalmic solution will continue to dominate the market and forecasted to continue to do so until the end of 2031 (Report, 2022). These formulations are mostly applied as topical application targeting anterior segment (Lang, 1995; Lee & Robinson, 1986b; Neervannan, 2021) and are not successful in reaching the posterior segment of the eye (Urtti, 2006).

Invasive administration is often preferred for the treatment of posterior segment disorders. Treatment followed to treat posterior segment ocular diseases are with high drug dosage regimen given intravenously or by intravitreal administration or implants or by periocular injections. Drug penetration into the posterior ocular tissues is mainly controlled by the blood retinal barrier (BRB). BRB is composed of two types of cells, retinal capillary endothelial cells and the retinal pigment epithelium cells (RPE) known as the inner and outer blood-retinal barrier, respectively. Tight junctions of RPE efficiently restrict intercellular permeation. Following treatment, oral or intravenous dosing, drugs can easily enter into the choroid due to its high vasculature compared to retinal capillaries. This layer is selectively permeable to highly hydrophobic drug molecules. To maintain high drug concentration, frequent invasive dosing is necessary intravitreally, which often leads to systemic adverse effects (Duvvuri et al., 2003; Ghasemi Falavarjani & Nguyen, 2013).

11

The major challenges for effective ophthalmic drug delivery is due to the complex nature of various eye diseases and the presence of ocular barriers to achieve a therapeutic effect of the drug. To circumvent such challenges and barriers and improve the bioavailability of the drug in the ocular tissue, the focus of rational design of the ocular therapeutic system has to be to enhance the ocular residence duration and for deeper permeation of the active ingredient. Ocular treatments can be improved by better understanding the basic ocular and corneal pharmacokinetics (Chun et al., 2008; Ghate & Edelhauser, 2006; Urtti, 2006; Urtti & Salminen, 1993). Hence, fundamental research is indispensable and essential for applied sciences.

The emphasis of this research work is on the anterior ocular drug delivery; hence the further section will detail regarding the anterior ocular delivery, its challenges and the formulations targeting the anterior segment.

Anterior ocular drug delivery

Ocular infection/diseases are intervened by treating the site of infection with drugs. Systemic drugs can be used but more so often only topical applications are preferred or suggested for anterior segment. Topical application remains the most preferred route due to ease of administration, low cost, and patient compliance. The other drug delivery options for anterior segment are subconjunctival and intracameral injection (IC). Despite the topical application being the preferred choice, ocular drug delivery still remains challenging due to barriers in the anterior segment, only 1-7% of the instilled drug reaches the aqueous humour (Ghate & Edelhauser, 2006).

Barriers that pose a challenge to anterior segment drug delivery are either be static, or dynamic++ barriers (Duvvuri et al., 2004; Gaudana et al., 2010). Precorneal factors, such as dosage spill-over, nasolacrimal drainage, blinking, tear film and tear mucin, and low corneal permeability are the main factors to impediment of drug absorption and bioavailability in anterior segment (Patel et al., 2010).

A typical eye dropper tip delivers 35-50 µl per drop, significantly exceeding the normal tear volume of 7-10 µl with a turn-over rate of 0.5 -2.2 µL/min (Singh et al., 2011). Under normal conditions, human palpebral tissues can hold 30 µL without overflowing. Sudden increase in the volume due to topical instillation causes reflex blinking (5-7 blinks/min) and dilution of the tear film which results in rapid drainage from ocular surface. Topically applied eye drops are washed away within 15-30 s due to new tear fluid which eventuates due to tear production and tear film renewal post application.

Majority of the applied drug is drained from the surface though the nasolacrimal duct and eventually cleared via systemic circulation. These factors contribute to short contact time with the ocular surface and reduces the bioavailability of the applied drug to reach the infected intraocular tissues (Gaudana et al., 2010). Tear film is the first protective layer of the cornea and conjunctiva and also the first barrier for topical drug penetration (Morrison & Khutoryanskiy, 2014). The drug concentration is quickly diluted by tears post application and removed from ocular surface though blinking and turnover of the tears (Agarwal et al., 2016) and washed away from the corneal surface in <3 min (Molokhia et al., 2013). Tear film is 6-7 µm thick and composed of three layer, outer lipid, middle aqueous and inner layer mucin (Morrison & Khutoryanskiy, 2014) (Figure 1.3).The aqueous layer makes up 90% of the total tear volume

(Gan et al., 2013), composed of dissolved oxygen, aqueous nutrients, electrolytes, large variety of proteins, peptides and glycoproteins (Ohashi et al., 2006). Drug non-specific binding with tear enzyme, mucin layer, and proteins may result in the drug to reach the cornea, anterior chamber, due to enhance clearance with each blink (Gaudana et al., 2010; Wels et al., 2021).

The cornea, the anterior most layer of the eye, is a mechanical barrier which limits the entry of exogenous substance into the eye and protects the ocular tissues. Physiochemical drug properties, such as lipophilicity, solubility, molecular size and shape, charge and degree of ionization affect the route and rate of permeation through the corneal membrane. Cornea consists of six layers, epithelium, Bowman's membrane, stroma, Dua's layer, Descemet membrane, and endothelium (Figure 1.3). Epithelium, stroma and endothelium are cellular layers, Dua's layer acellular, whilst Bowman's and Descemet's membrane and two interface layers. The critical barrier to drug penetration in the anterior segment of the eye is the epithelium. Drug absorption through cornea may occur via transcellular (for lipophilic drugs) or paracellular (for hydrophilic drugs) pathway or by active transport. The superficial corneal epithelium consists of stratified squamous non-keratinized cells, which limits the permeation of hydrophilic drug though the cornea due to the hydrophobicity of the epithelium and the presence of tight junctional proteins between the corneal epithelial cells (Downie et al., 2021; Gaudana et al., 2010). Stroma, is a lamellar structure compromised of glycosaminoglycan and collagen fibrils and it has a hydrophilic environment which restricts the penetration of lipophilic drug (Gaudana et al., 2010). The inner most layer of the cornea, the endothelium is composed of hexagonal-shaped endothelial cells which allows the passage of macromolecules into the aqueous humour (Gaudana et al., 2010). Cornea acts a physical barrier to hydrophilic drugs due to the superficial corneal epithelial layers, and to the lipophilic drugs due to the hydrophilic stroma. The Bowman's layer do not provide any significance resistance to drug penetration (Holowka & Bhatia, 2014). Whereas, the Descemets

membrane might not serve as a barrier to the diffusion of molecules due to the larger pore sizes, but drugs administered directly to stroma could be prevented from reaching the endothelium (Wels et al., 2021).

Figure 1-3 Cross-sectional view of tear film: a high tear turnover rate and gel-like mucin layer make a tear film as a major barrier in topical ocular drug delivery before drug penetration into cornea and corneal barrier (Mofidfar et al., 2021).

Topically administered drugs can be absorbed into the anterior segment through conjunctiva or sclera pathway (Ghate & Edelhauser, 2006), the alternative pathway for drug to enter the eye. Conjunctival pathway, is a rate-limiting barrier for water-soluble drugs due to rapid drug elimination by conjunctival blood and lymphatic flow (Ahmed et al., 1987).

Poor bioavailability and low delivery efficiency from topical application also led to the adoption of invasive measures, intracameral injection (IC) to the anterior segment of the eye. Advantage in use of IC injection is to provide higher drug levels in the anterior chamber which is a challenge to achieve by topical application. It is a cost-effective and efficient method of delivering antibiotics compared with topical antibiotics and antifungal agents. IC route is the preferred route to prevent the occurrence of endophthalmitis after cataract surgery (Chang et al., 2009). Administration of IC injection can lead to complications, like toxic anterior segment syndrome and toxic endothelial cell destruction syndrome due to incorrect antibiotic dosing, formulation, and preparation (Mamalis et al., 2006). Other constraints of IC injection must be administered

by experienced ophthalmologist which is a logistic constraint and burden to patients and caregivers.

Sustained anterior ocular drug delivery remains a challenge due to human eye's distinctive anatomical structures, physiology, and several other barriers in the anterior segment. Many researchers are attempting to address the paradigm of novel drug delivery systems across the globe over the past decades to overcome the inherent shortcomings of existing therapies. It is essential that the formulation designed for targeting the structurally complex cornea should be able to enhance precorneal retention, precorneal elimination, increase corneal bioavailability and improve the bioavailability of the drug. Topical application remains the most preferred route for instillation of drug to the anterior segment, >95% of products available in the market are conventional dosage forms of topical applications, like eye-drops, ointment. Various modern approaches like *in situ* gel, ocuserts, nanosuspensions, nanoparticles, liposomes, noisomes, and implants are being tested to improve the ophthalmic bioavailability of the drugs and controlled release of the ophthalmic drugs to the anterior segment of the eye (Chen et al., 2018).

Topical applications, eye drops and gel, hybrid ocular formulations (micro and nanoparticles) and solid ocular inserts are briefly discussed below which is within the scope of this research project.

Eye drops and gels

Topical drug delivery was first used about >3500 years ago, when ancient Egyptians used compressed ox liver juice on ocular surface to treat night blindness (Maumenee, 1993; Wolf, 1996). Ophthalmology as a specialist science area can be traced back to 17 and 18th centuries (Grossniklaus, 2015) whilst it is difficult to pin point the first "modern" eye medication. Electron

microscopy aided in elucidating additional information into the topical ocular drug delivery which enabled studies on the structure and different layers of normal cornea which led to major development of technologies and therapeutic drug (Crawford et al., 2013; Teng, 1962).

Topical administration, mostly in the form of eye drops, is used to treat anterior segment diseases. Eye drops are more often formulated using saline solution with medication and used for treating many ocular diseases such as infection, inflammation, glaucoma, dry eye and allergy, representing >90% of the commercialised products in the global ophthalmic drug market (Awwad et al., 2017). The site of action for topically applied eye drops is usually different layers of the cornea, conjunctiva, sclera, and the other tissues of the anterior segments such as the iris and ciliary body. The advantages of using eye drops are high patient compliance, self-administered and non-invasive. However, there are several challenges as previously elaborated under, "Anterior ocular drug delivery" (1.4.1) which leads to relatively low efficacy. In addition, preservatives and thickening agents in the eye drops can cause irritation, hence for frequent dosing to the anterior ocular surface it is best to use eye drops without any preservatives. To achieve a therapeutic efficiency, high concentration of dosage and repeated instillation are often required to achieve the therapeutic effects (Urtti, 2006). This can cause side effects such as toxicity and low tolerability, which are often associated with poor compliance by the patient, an important limiting factor for many topical ophthalmic medications (Gholizadeh et al., 2021).

Precorneal retention time and enhancing corneal, scleral and/or conjunctival drug permeability are strategies followed to improve the ocular bioavailability (Patel et al., 2013). Viscosity enhancers like hydroxy methyl cellulose, hydroxy ethyl cellulose, sodium carboxy methyl cellulose, hydroxypropyl methyl cellulose and polyalcohol are used to improve precorneal residence time and bioavailability (Gebhardt et al., 1995; Vulovic et al., 1990). Drug molecule

weight is also a limiting factor for topical delivery as only small molecules (less than 1kDa) can readily pass though the cornea (Barar et al., 2008).

Conventional ocular delivery systems, like eye drops show poor bioavailability and lesser therapeutic response because of high tear turnover and thus rapid precorneal elimination of drug. Due to this, high frequency of eye drops instillation is required which results in patients' incompliance. To overcome the drawbacks associated with conventional drug delivery, ophthalmic gels are used for topical application as an alternative drug delivery system. Ophthalmic gels are divided into two categories: classical gel eye drops and in situ gel (Dubald et al., 2018). Classical gel eye drops are readily available viscous solution that do not change their viscosity on instillation and are normally used to treat dry eyes as a tear substitute (Pal Kaur & Kanwar, 2002). The limitations with classical gel eye drops, do not allow accurate and reproducible drug administration and can cause blurred vision, crusting on the eyelids, and tearing (Jumelle et al., 2020; Kurniawansyah et al., 2018). The concept of producing a gel in situ was suggested for the first time in the early 1980s. The main advantage of in situ forming gels is sustained and controlled drug delivery and less or no blurred vision as in the case with ointments. Instillation of low viscosity solution as topical application, undergo a phase transition in the conjunctival ocular cul-de-sac to form a viscoelastic gel due to conformational changes of polymer in response to physiological environment. This process helps to slight prolonged precorneal residence time, decreased nasolacrimal drainage, less blurred vision, and increased bioavailability. Use of swellable water insoluble polymers, like hydrogel which swells in the aqueous medium and give controlled drug delivery systems. Temperature (Miller & Donovan, 1982), pH (Ibrahim et al., 1990), and ionic strength (Rozier et al., 1989) are stimuli-responsive excipients used in the formulations that can change and trigger the phase transition and most widely used for development of in situ gelling systems for ocular drug delivery. A wide variety

18

of drug molecules and materials of therapeutic advantages such as antibiotics (Ofloxacin, Ciprofloxacin, Gatifloxacin), beta blockers (Timolol, Carteolol), NSAIDs (Ketorolac Tromethamine, Indomethacin), Pilocarpine hydrochloride, Peurarin, Recombinant rHEGF, Antivirals (Acyclovir) has been delivered through in situ gelling systems (Balasubramaniam et al., 2003; Balasubramaniam & Pandit, 2003; Cao et al., 2007; Cohen et al., 1997; El-Kamel, 2002; Kim et al., 2002; Lin et al., 2004; Liu et al., 2006; Ma et al., 2008; Miyazaki et al., 2001; Qi et al., 2007; Séchoy et al., 2000; Srividya et al., 2001). An in situ forming gel Timoptic-XE®, containing timolol maleate in Gelrile® manufactured by Merck and Co. Inc. has been commercially available since 1994. The other marketed products are AzaSite Plus™ (marketed by InSite Vision), and Pilopine HS (marketed by Alcon Laboratories Inc.) (Kute et al., 2015).

The advantage of gel formation results in reduced systemic exposure, however the end results is only a limited improvement in the bioavailability, blurred vision and matted eyelids which reduces patient acceptability. For topical application to be effective, it requires the patients to be compliant with the dosing schedule. Due to poor compliance with adhering to dosing schedule, patients do not achieve the full therapeutic effect of the medication. This has led researchers to develop novel formulations (micro and nanoparticles) to circumvent the current drawbacks (corneal static and dynamic barriers) with eye drops and gels.

Hybrid ocular formulations such as micro and nanoparticles

Primary reason for the low bioavailability of the drug after topical administration is the short retention time due to rapid clearance of the ocular surface via tear film renewal, nasolacrimal drainage, biologic and enzymatic drug degradation. Therefore, micro-, and nanoparticle-based

system have been used to increase the retention time of drugs on the ocular surface. Due to their functional groups and the surface charge, microparticles and nanoparticles can closely interact with the mucin layer of the tear film on the ocular surface to prolong the retention of the therapeutic drug on the cornea (Janagam et al., 2017), requiring lower dosage and preventing side effects. Numerous lipid and polymeric materials, singly or in combination have been used to develop micro-/nanoparticle that are able to deliver a variety of drugs to the anterior segment. Nanoparticle based systems have shown their ability to increase the permeation through ocular layers with limited increase of the formulation viscosity and allows modification of the pharmacokinetics of drug release by prevention of a burst release effect of the drug.

The advantages of using nanocarriers are, controlled therapeutic release over time, protects the drug from enzymatic degradation, ample choice of materials and increase drug bioavailability. The drawback of nanocarriers, possibility of particle aggregation, possible toxicity from polymers and excipients used, low drug loading capacity for some formulations, additional manufacturing steps, and possible discomfort and blurred vision.

Solid ocular inserts

Ocular inserts are flexible polymeric materials, solid or semi-solid sterile preparations to be placed in the cul-de-sac of the eye or the cornea, to prolong the residence time (Gurtler & Gurny, 1995; Saettone & Salminen, 1995). Solid ocular inserts can be used for sustained single dose drug delivery that contains preservative-free drug that can be delivered to the target ocular tissue(s) at the intended therapeutic concentration for a sustained extended period of time. Drug release from ocular inserts takes places by three mechanisms: diffusion, osmosis, and erosion. The size and shape of the inserts are tailored for ophthalmic application. Advantages of using

20

inserts over eye drops are, reduce dosing, avoid/minimise drug-induced systemic toxicity, outflow through nasolacrimal duct and blurring of vision occurrence.

Early forms of ocular inserts have been used since the Middle Ages and were given the Arabic term al-kohl. By 19 century, paper patches soaked with drug solutions were used and in the early 20th century glycerinated gelatin systems were used (Saettone & Salminen, 1995). The inserts based on the solubility behaviour can be classified into three groups, insoluble, soluble or bio-erodible (Rathore & Nema, 2009).

Insoluble inserts have been further classified into three groups: Diffusion system, Osmotic system, and Hydrophilic contact lenses. Diffusional and osmotic systems, include a reservoir in contact with the inner surface of the drug rate controller and supplying drug thereto. The reservoir contains a liquid, a gel, a colloid, a semi-solid matrix or a carrier-containing drug homogeneously or heterogeneously dispersed or dissolved therein (Di Colo et al., 2001). Carriers can be made of hydrophobic, hydrophilic, organic, inorganic, naturally occurring or synthetic material (Shell & Gale, 1984). The pilocarpine Ocusert® (ALZA Corp.) was the first commercially (1974) marketed device in USA to achieve zero-order kinetics. The drug is contained in a reservoir enclosed by two release-controlling membranes made of ethylene vinyl acetate copolymer and surrounded by a ring to aid in the positioning and placement. It has been shown to maintain a therapeutic effect with a smaller amount of drug and, thus, lesser side effects (Macoul & Pavan-Langston, 1975). The origin of the Ocusert® can be traced back to two fundamental research papers, published by Lerman in 1970 and by Lerman and Reininger in 1971 (Lerman, 1970; Lerman & Reininger, 1971). These authors demonstrated for the first time in glaucoma patients that a sustained release of pilocarpine (simulated by continuous instillation of microdrops)

provided good intraocular pressure control with a fraction of the drug dose administered by conventional eyedrop therapy. Some disadvantages of this system were unreliable control of intraocular pressure, leakage, folding, and difficulty inserting the devices and ejection or irritation (Kuno & Fujii, 2011; Saettone & Salminen, 1995). The osmotic inserts are generally composed of a central part surrounded by a peripheral part (Bloomfield et al., 1978). The first central part can be composed of a single reservoir or of two distinct compartments. In the first case, it is composed of a drug with or without an additional osmotic solute dispersed through a polymeric matrix, so that the drug is surrounded by the polymer as discrete small deposits (Ahmed et al., 1987). In the second case, the drug and the osmotic solutes are placed in two separate compartments, the drug reservoir being surrounded by an elastic impermeable membrane and the osmotic solute reservoir by a semi-permeable membrane. The second peripheral part of these osmotic inserts comprises in all cases a covering film made of an insoluble semi permeable polymer (Eller et al., 1985). The tear fluid diffuse into peripheral deposits through the semi permeable polymeric membrane, wets them and induces their dissolution. The solubilised deposits generate a hydrostatic pressure against the polymer matrix causing its rupture under the form of apertures. Drug is then released through these apertures from the deposits near the surface of the device which is against the eye, by the sole hydrostatic pressure (Lach et al., 1983). Hydrophilic contact lenses are made up of a covalently cross-linked hydrophilic or hydrophobic polymer that forms a three-dimensional network or matrix capable of retaining water, aqueous solution or solid components (Lee & Robinson, 1986a). Hydrophilic contact lens when soaked in a drug solution, it absorbs the drug, but does not give a delivery as precise as that provided by other non-soluble ophthalmic systems. The drug release from this system is generally rapid at the beginning and then declines exponentially with time and is related to the soaking time of the contact lens and the drug concentration in the soaking solution (Shell et al., 1974). The release rate can be decreased by incorporating the drug homogeneously during

the manufacture (Grass & Robinson, 1988) or by adding a hydrophobic component. Contact lenses have certainly good prospects as ophthalmic drug delivery systems (Alvarez-Lorenzo et al., 2002). However, the downside to this group of ophthalmic devices is a high rate of patient incompliance, due to presence of foreign body sensation and insolubility of these devices (Rathore & Nema, 2009).

Soluble inserts correspond to the oldest class of ophthalmic inserts. They offer the great advantage of being entirely soluble so that they do not need to be removed from their site of application thus, limiting the interventions to insertion only (Patton & Robinson, 1976). Soluble inserts are broadly divided into two types, the first one being based on natural polymers (e.g. Collagen, cellulose derivatives) and the other on synthetic or on semi-synthetic polymers (Gurtler & Gurny, 1995). The therapeutic agent is preferably absorbed by soaking the insert in a solution containing the drug, drying and re-hydrating in before use on the eye. The amount of drug loaded will depend upon the amount of binding agent, upon the concentration of the drug solution into which the composite is soaked, as well as the duration of soaking (Himmelstein et al., 1978). The release of drug from such system is by penetration of tears into the inserts which includes release of the drug by diffusion and form a gel layer around the core of the insert, this external gel layer induces the further release, but still controlled by diffusion. The pioneer in this research is Dr. Svyatoslav Fyodorov of Soviet Union. Dr. Fyodorov was able to extract collagen from porcine sclera and shape it in the form of a contact lens that can be easily placed on the surface of the eye (Fyodorov et al., 1985). This was able to protect the ocular surface and that it was dissolvable. It seemed that naturally occurring enzymes in the tear film caused the collagen contact lens to dissolve over a period. The "Soluble Ophthalmic Drug Insert" (SODI) are the results of a vast collaborative effort from eminent Russian chemist and ophthalmologists, and led eventually (in 1976) to the development of a new soluble copolymer of acrylamide,

designated as ABE (Khromov et al., 1976). A single SODI application has been reported to replace 4-12 drop instillations or 3-6 applications of ointment, and to constitute a valid once-a-day therapy, even for long-term treatment of glaucoma (Maichuk, 1967, 1975a, 1975b; Maichuk & Erichev, 1981). Drawbacks with collagen shield, the cornea is anaesthetised while the physician uses a blunt forceps to insert the hydrated or unhydrated shields. Nevertheless, the concept of administering ophthalmic drugs in collagen shield-type insert appears to be better accepted by ophthalmologist compared to the introduction of Ocusert® era (Lee, 1990). The "New ophthalmic delivery system" (NODS®), originally patented by Smith & Nephew Pharmaceuticals Ltd in 1985 (Lloyd, 1985), is a method for delivering precise amounts of drugs to the eye within a water-soluble, drug loaded film. The device consists of a medicated flay which is attached to a paper-covered handle by means of a short membrane. The membrane proceeds to dissolve rapidly releasing the flag which swells and dissolves in the lacrimal fluid, delivering the drug. This system has a possibility of releasing the drug at a slow, pre-determined rate (Richardson & Bentley, 1993). NODS when evaluated in humans, produced 8-fold increase in bioavailability for pilocarpine compared to a standard eyedrop formulation (Kelly et al., 1989). The bioerodible inserts are composed of homogenous dispersion of a drug which can be included in or not included in the hydrophobic coat made of bioerodible polymers, which is impermeable to the drug. Successfully used bioerodible materials are the poly (orthoesters) and poly (orthocarbonates) (Di Colo & Zambito, 2002). Drug release from such a system is due to the contact of the device with the tear fluid, inducing a superficial bioerosion of the matrix (Sieg & Robinson, 1977). The advantage of bioerodible polymers is the possibility of modulating their erosion rate by modifying their final structure during the synthesis, and elimination of device removal from the cornea. The different promising devices for erodible drug inserts are Lacrisert®

(Merch & Co., Inc. (Lamberts et al., 1978)), SODI (Maichuk, 1967) and Minidisc (Bawa et al., 1988).

Solid inserts using nanotechnology, electrospinning was attempted by researchers to achieve sustained release of the bioactive. PCL nanofiber loaded with tetracycline hydrochloride was attempted by Karuppuswamy et. al. (2015). In vitro studies of the drug analyzed by UV-Visible Spectrophotometer indicated the burst release of drug within the first hour observed minimum followed by sustained control release for a period of eight days. This promising results for sustained control release of tetracycline chloride loaded in PCL nanofiber showed potential for delivery option in biomedicine and healthcare. Erodible inserts based on PEO have been investigated for the delivery of ofloxacin by Di Colo et. al. (2001). The research results showed that the residence time in rabbit eyes was shown to be dependant on the molecular weight of PEO, and the bioavailability was 3-4 times and the Cmax 11-12 times the values obtained by commercial eye drops. Nanotechnolgy-based drug delivery systems so far have been useful in reducing toxicities, multiple dosing, dose-related undesired effects, and fluctuations in dru plasma concentration, associated with a traditional drug delivery system. However, research on ocular therapeutic systems still suffer a large gap, and the design process of novel carrier that could be non-toxic, biodegradable, biocompatible, and efficacious in mitigating both the posterior and anterior segments of the eye is underway by researchers across the globe.

Solid-drug releasing devices, in spite of the advantages demonstrated by extensive investigation and clinical tests, have not gained wide acceptance by ophthalmologist (Saettone, 1993, 2019). Commercial failure of inserts has been attributed to psychological factors, such as the reluctance of ophthalmologists and patients to abandon the traditional liquid and semi-solid medications, price factors and to occasional therapeutic failures. In future, the use of solid ophthalmic devices

will certainly increase owing to the development of new polymers, the emergence of new drugs having short biological half-lives or systemic side effects and the need to improve the efficacy of ophthalmic treatments by ensuring an effective drug concentration in the eye over an extended period.

Novel ocular drug delivery systems

New ophthalmic drug delivery approaches are explored to overcome the ocular drug delivery barriers and improve the ocular bioavailability of the existing therapies, such as short ocular contact time, high dosing frequency and limited drug penetration. The therapies explored but not limited to are drug eluting punctal plugs, implants, contact lens, iontophoresis, gene therapy and particular systems (Chen, 2015). Therapeutic ultrasound, sonophoresis, has emerged as an option recently to treat glaucoma by cyclocoagulation (Aptel & Lafon, 2015) or enhance ocular uptake of molecules such a low molecular weight drug, genes and proteins (Cheung et al., 2010; Nabili et al., 2013; Yamashita et al., 2007). Nanotechnology based novel drug carrier system with micelle, liposome, microemulsion, nanosuspension, microneedle, nanofiber, mesoporus silica nanoparticles, solid lipid nanoparticle, nanospore, nanocapsule and gold nanoparticle are being explored as a favourable delivery system to treat ocular disorders (Akhter et al., 2022).

Punctal plugs are made with polymers (silicone, collagen, hydrophobic polymer, polydioxanone or hydrogel) and commonly used to treat dry eye disease. Punctal plug, which is also called punctum plug, lacrimal plug of occluders, is a very tiny (size of a rice grain) biocompatible insert. It is inserted into either the punctum or canaliculi of the lacrimal duct of sustained ocular delivery. As the punctal plugs are designed to stay in the tear duct for an extended period of time, they are now being evaluated by several companies as a potential for sustained delivery of drugs to the eye (Gupta & Chauhan, 2011; Kompella et al., 2010). The drawback with punctum plug

26

is limited drug loading due to their small size and , although it has been effective for drug delivery for up to six weeks (Torkildsen et al., 2017) Mati Therapeutics (Austin Texas, USA) and Ocular Therapeutic Inc. (Bedford, Massachusetts, USA) trialled punctum plugs in Phase IIb and Phase III trial hoping to commercialise them eventually but to date none has been commercialised so far (Bertens et al., 2018).

Implants are drug-eluting devices specially designed for local sustained drug release over longer periods (Lee et al., 2010). The device is placed intravitreally with a minor incision at pars plana situated between the crystalline lens and the retina. Many devices to implant in the ocular cavity have been designed and formulated as ocular therapeutic systems for vitreoretinal chronic therapy.

Contact lenses have been around for decades and present an attractive platform for ocular drug delivery that are non-invasive and non-degradable. Patient acceptance improved ocular bioavailability due to reduced tear mixing between the lens and the cornea and extended drug release are some of the potential advantages with this delivery system (Kompella et al., 2010; Patel et al., 2013). However, the success of this drug delivery platform has been limited due to low drug loading and difficulty in controlling drug release over extended period of time (Kompella et al., 2010; Patel et al., 2013).

Iontophoresis is a method to deliver drugs across biological membranes with low-level of electrical current (Dixit et al., 2007). Generally, this technique has been used for transdermal drug delivery, but recently it has also generated interest in ocular drug delivery (Eljarrat-Binstock & Domb, 2006) due to its ease of application and minimum or non-invasive nature of delivery. Ocular iontophoresis was first investigated in 1908 by the German researcher Wirtz, who passed

electric current through electrolyte-saturated cotton sponges placed over the globe for the treatment of corneal ulcers, keratitis and episcleritis (Wirtz, 1908). The basic design of ocular iontophoretic devices consists of power source and two electrodes: the donor electrode (ocular applicator) and the return electrode. The drug is filled into the applicator and the return electrode is placed at a distal site on the body, generally on the forehead, to form an electrical circuit (Kalia et al., 2004). The mechanism of delivery by iontophoresis is by opening the tight junctions without significantly affecting the barrier properties of the eye (Ali & Byrne, 2008). Despite its widespread use during the first 6 decades of the twentieth century, the delivery system was not adopted as a standard procedure due to some drawbacks, like the lack of carefully controlled trials and the paucity of toxicity data. The procedure can produce complications, and damage to the cornea surface immediately affects the vision and comfort of the patient which is less pronounced when applied to the sclera. The clarity of cornea is essential for interaction with light while the sclera is not relevant for light interaction. However, during the first decade of 21st century researchers have explored the development and optimization of the technology of ocular iontophoresis for fast and safe delivery of small molecule, macromolecules and nanocarriers to the eye (Chopra et al., 2010, 2012; Souza et al., 2015). The safety of prolonged and frequent application of iontophoretic drug delivery have yet to be established. Future research goals and innovations in this area of drug delivery is to make this approach user-friendly with disposable component in a system designed for home use without professional training.

1.4   Assays of ocular irritation

Ocular irritation is a general term to describe a sensation that bothers the eyes like dryness, itchiness, burning or grittiness. Accidental exposure to things like dust particles, smoke or chemical vapours can cause eye irritation. In many cases, thoroughly rinsing the eyes with

ambient temperature water can relieve the symptoms in 15 to 20 minutes. However, exposure to some irritants have the potential to cause permanent damage or burn to your eyes. Irritation may be associated to several factors, for example like blepharitis, glaucoma, blocked tear duct, corneal abrasion, rheumatoid arthritis, brain tumour, and multiple sclerosis can cause eye irritation. Researchers testing ocular dosage forms have recorded toxicological signs of ocular tissues exposed to topically applied cosmetics and pharmaceuticals. Ocular tissues, such as cornea and conjunctiva, are susceptible to injuries and adverse ocular effects, either from the administered drug or from pharmaceutical ingredients (excipients) used in the formulating ophthalmic products (Basu, 1983; Li et al., 2008).

Testing ocular tolerability of ocular pharmaceuticals is an essential regulatory requirement. A preliminary requirement of any ocular formulation is lack of local adverse effects, like burning, stinging, and tearing. Since ancient times, animals have been used as surrogates for humans (Maehle, 1987). One of the earliest recorded animal experiments occurred 2500+ years ago when the function of the optic nerve was deduced by noting a living animal's blindness after the nerve was cut (Hirschberg, 1921). Evaluating potentially harmful products on the eyes of laboratory animals has been done since the 18th century (Jackson, 1992).

Ocular toxicology developed during the 20th century as the pharmaceutical industry grew (Green, 1992) and as drugs were found to have effects on the eye. The use of animals for understanding the eye's responses to external stimuli grew out of the experimental methods of Claude Bernard (1813-1878) (Olmsted & Olmsted, 1952). The initial rationale for creating models of ophthalmic toxicity was not to screen medication by rather to find chemicals that could harass, harm, and blind. Quantitative scoring of the severity of ocular irritancy was first developed by Jonas S. Friedenwald (1897-1955) to deliver a research contact into the effect of chemical agents on the

eye (Friedenwald & Hughes, 1948). Friedenwald proposed grading the severity of different components of ocular toxicity on numerical scales, 0, 1, or 2 for conjunctival redness, and 0 to 4 for corneal oedema. This grading scheme was soon adapted by others (Seifried, 1986). The method was further refined in the 1940s to include the recovery time and residual corneal scarring as additional outcome measures. John Draize, a pharmacologist at the FDA adapted Friedenwald's procedure from a way of assessing hazardous substance to a method for assuring the safety of products intended for topical application. The current approved reference model for ocular irritation testing is the Draize test (Draize, 1944). "Draize rabbit eye irritation test" is the oldest eye irritation test that was developed by two Food and Drug Administration (FDA) toxicologist, John H. Draize and Jacob M. Spines in 1944 (Draize, 1944) and is still widely used for 7+ decades and approved by the Organisation for Economic Co-operation and Development (OECD) and the FDA to evaluate potential ocular irritation (Bartok et al., 2015; TG236, 2013). The first reported experimental animal procedure was devised to investigate the effects of acids and basis on the eye and for the first time the effects on cornea, conjunctiva and iris were separately recorded (Friedenwald et al., 1944).

The protocol followed for Draize test, is to instil 0.1 ml or liquid or 0.1 mg of solid in the conjunctival sac of a rabbit eye, with the upper and lower eyelids being kept closed for a few seconds. The other eye (contralateral eye) is used as a control. Any irritation and/or corrosion effects are then observed on the conjunctiva, iris, and cornea, and scored at regular interval up to 72h to observe any lesions and up to 21 days to evaluate the persistence and resolution of those lesions.

The albino rabbits have historically been the animal of choice for testing potential eye irritants, primarily because its large eyes make it easy to observe damage. There are few advantages of

using rabbit as a test animal. Rabbit has a large conjunctival sac that easily accepts test material and holds it against the eyes. Conjunctival sac of rabbit is much larger that human which enables more test material placed in the rabbit's eye. Despite the advantages, rabbit is far from a perfect model for human due to striking differences. Nictitating membrane or third eyelid is present in the rabbit compared to the humans. This membrane moves laterally across the eye, likely causing the kinetics of removal of many test materials to differ from humans. Also, the conjunctival sac of the rabbit is much larger than in humans, which results in more test material placed in a rabbit's eye than would be likely to ever get into the human eye during an accidental exposure. Rabbit cornea is somewhat thinner than that of humans and there is less tear production to aid in washing out a foreign material. Hence, rabbit is generally considered an overly sensitive model for humans. By 1960, the Draize test came under criticism, due to high number of variables in the test and its reproducibility (York & Steiling, 1998), especially for moderately irritating compounds. The main shortcomings of the Draize test is its subjectivity, poor reproducibility and the differences between the rabbit and the human eye (structurally, physiologically and biochemically) (Lordo et al., 1999).

Low-volume eye irritation test (LVET) were developed in response to a recommendation from the National Research Council (National Research Council, 1977). This test is a refinement of Draize test (Griffith et al., 1980), where lower volumes of test substances (0.01 mL/0.01g) are applied to the right eye of the animal with no forced eyelid closure employed. This modified test though overcame some of the drawbacks of Draize test, still it came under criticism by animal welfare groups for the use of live animals. Another downside of this test was, if negative irritation results is obtained using the lower amount of test material, the standard protocol of the LVET required increasing the amount of the test material and thus can reach the same level as the normal Draize test.

The concept of using alternatives to animals in testing emerged around 1960 (Russell & Burch, 1959), and many methods have since been proposed (Goldberg & Silber, 1992). Initially the validation were comparison of the procedures to the Draize test rather than human exposure (Bruner et al., 1998). Over the past decade, several irritation assays were successfully developed and tested, amongst which are the isolated/enucleated organ method such as the Bovine Corneal Opacity and Permeability (BCOP) test, the non-ocular organotypic models such as Hen's test on the Chorioallantoic Membrane (HET-CAM), and the cell-based cytotoxic colorimetric methods such as Red Blood Cell (RBC) lysis and protein denaturation, Neutral Red Uptake (NRU) and Sulforhodamine B (SRB) assay (Ying et al., 2010). Classification of ocular irritants is based on United Nations Organization (UNO) system, that is, the GHS "Globally Harmonized System of Classification and Labelling of Chemical" (Luechtefeld et al., 2016). As per this international classification system, the irritants are grouped as, severe irritants (Category 1), moderate irritants (Category 2A), mild irritants (Category 2B), and non-irritants (No Category). The current alternative models for ocular irritation cannot distinguish Category 2A from 2B irritants. These irritants are usually differentiated based on the kinetics of the reversibility of damage (Bonneau et al., 2021). Over three decades of research has failed to yield an acceptable alternative to the standard Draize eye test for screening new eye products. These test assays could alleviate animal suffering by employing immortal cell lines, non-human blood or excised tissues from local abattoirs, and are more objective endpoints compared with Draize test. Using alternative in vitro test, assessment of ocular damage from cell lysis, protein denaturation, corrosion, saponification and cytotoxicity for a wide range of chemical substances have been attempted. However, none of these tests can effectively monitor corneal innervation or corneal sensitivity, nor can they discriminate between substance that cause mid to moderate irritation, or between substances that exert a delayed toxic effect at the sub-cellular level (Abdelkader et al., 2015).

1.5   Research outline

The objective of this research project to fabricate and evaluate mono and multi-layered nanofiber membrane formulation for their physical characteristics (nanofiber mat thickness, water contact angle, surface morphology and tensile properties), bioactive drug release and biocompatibility. The novelty in fiber fabrication is to either fabricate a multilayer overlapping when there are two kinds of polymer used or fabricate multilayers by stacking the eventuated fibers one layer over the other. The rationale for overlapping the layers when more than one polymer is used to fabricate a formulation is to avoid de-lamination of the layers due to lack of chain entanglement due to different chemical properties between the two polymers.
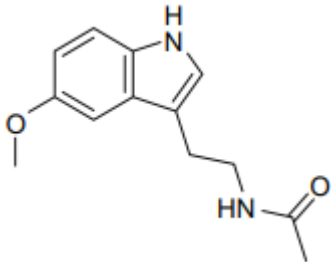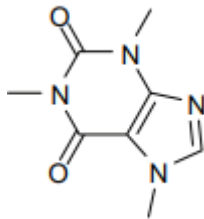
An extended-release ocular drug delivery membrane would reduce the need for multiple applications which would be of benefit to both physicians and patients. The tight ocular barriers while having protective functions, they also pose major obstacles for efficient drug delivery as they limit the diffusion and penetration of ophthalmic active ingredients.

As stated in the research proposal, the plan was to use melatonin as a model drug to study the release characteristics. Ocular disease research globally has shown that melatonin provides neuroprotective effect other than having potential benefits to cataract/glaucoma ocular disease. Melatonin molecule acts directly on ocular structures by mitigating disrupted circadian rhythms, lowers intraocular pressure, and improves retinal ganglion cells function in glaucoma. Normal ocular pressure ranges from 7-22 mm/Hg. Increased intraocular pressure, caused by obstruction of normal outflow of fluids, leadsto glaucoma as a result of neuropathy of the optic nerve and eventually blindness. Intraocular pressure exhibits diurnal variations with lowest pressure occurring in the early morning hours at the time of high melatonin levels, exogenous melatonin

has been tried as a probable agent for reducing IOP in glaucomatous patients. Melatonin was found to decrease intraocular pressure in humans (Samples, Krause et al. 1988). Eye drops have been widely used for delivering melatonin in animal experiments but their bioavailability should be further examined due to ocular barriers (Dal Monte, Cammalleri et al. 2020). Intravitreal injection has been trialled to bypass the ocular barriers with high dose melatonin which results in degeneration of retinal cells (Tao, Hu et al. 2020). We could not procure a pure form of melatonin drug in NZ hence had to look for alternative drug to be used in the research project. One of the option was to use caffeine drug molecules.

Caffeine is an alkaloid consumed worldwide in coffee. Caffeine solution in the form of eye drops is very stable and resistant to photodynamic degradation and hence tested for prevention of cataract by providing ultraviolet protection (Pinheiro, Araújo Filho et al. 2018). Melatonin and caffeine have similar molecular weight, water solubility and both are non-ionisable (Table 1) hence for this project we decided to use caffeine as a model drug.

Table 1 Melatonin and Caffeine drug molecules properties

Property	Melatonin	Caffeine
Structure		

Molecular weight	232.281 g/mol	194.194 g/mol
Melting point	117°C	235 to 238° C
Discovery	First isolated in 1958 by American physician Aaron B. Lerner and his colleagues at Yale University School of Medicine.	It was recorded as purified while crystalline substance by physician Friedlieb Ferdinand Runge in 1819.
Solubility in water	0.1 mg/mL	0.2 mg/mL
pKa	4.4	10.4
Source	Natural product from in plant and animals. It is hormone released by pineal gland in the brain at night.	Found in seeds, fruits, nuts or leaves. A psychostimulant that act as an adenosine receptor antagonist.
Biological half life	20-50 minutes	Adults 3-7h

Spectrophotometry as an analytical tool for the determination of caffeine in various kinds of samples is very simple and is an accessible technology (Ahmad Bhawani, Fong et al. 2015). Caffeine is recommended as a test substance by OECD because it has be studied extensively in vitro and in vivo. Caffeine's molecular weight is very close to that of melatonin. Caffeine is used in various research into mitigating ocular diseases due to ease of availability, highly

recommended by OECD as a model drug, cost and readily available analytical tools. In our laboratory too, caffeine was readily available to be used in this research project rather than sourcing melatonin in pure form which is only available under doctor's prescription. Melatonin (NZ$256/g) is far more expensive to procure in a pure form from Sigma chemicals compared to caffeine (NZ$0.50/g).

Mono-, two- and three-layered formulations were prepared using caffeine molecule as a model drug. Caffeine (Tsedeke Wolde 2014) is recommended as a test substance by the OECD because it has been studied extensively in vitro and in vivo (OECD 2004).

Two polymers were used in the studies, PCL and PEO. Poly (ε-caprolactone) (PCL) is one of the most important and widely used degradable polymers with a history dating back to the very first synthetic polyesters in the 1930s. It is a saturated linear aliphatic polyester hydrophobic polymer with a hexanoate repeat units (Figure 1.4), and can be classified as semi-crystalline with degrees of crystallinity up to 70% depending on average molecular weight (Mw) typically ranging from 3000 to 800,000 g/mol. In addition, PCL has a low glass transition temperature and shows elastic behaviour at room temperature. Polyethylene oxide (PEO) is a hydrophilic polymer available in a wide molecular weight range (200 to 7.0×10^6 g/mol) non-ionic with low toxicity polymer used in a variety of applications, food, pharmaceutical including clinical products such as laxatives and skin creams. The polymer is highly soluble in both aqueous and organic solvents. Structurally it has repeating units of ethylene oxide (Figure 1.4). The polymer has ability to dissolve in water in addition to other solvents such as ethanol and hence researchers use as a choice polymer in electrospinning fibres.
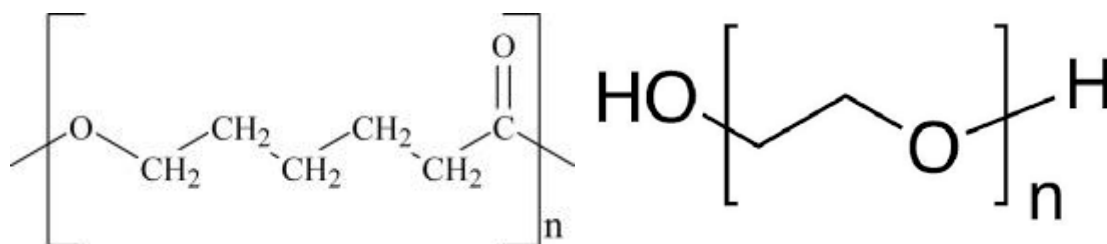
Figure 1.4 Molecular structure of PCL (left) and PEO (right)

The formulations were prepared using two of these polymers, PCL and PEO along with the model drug, caffeine and tested for various physical and drug release properties, nanofiber mat thickness, water contact angle, surface morphology, tensile properties (puncture strength and mucoadhesion) and in-vitro drug release.

CHAPTER 2   MATERIALS AND METHODS

2.1 Material

The chemicals, polymers, and solvents were sourced from various suppliers. Polycaprolactone (PCL), Sigma-Aldrich, UK (Molecular weight 80K, product code 1002495167), Poly(ethylene oxide) (PEO), Sigma-Aldrich, USA (Molecular weight 200K, product code 1002219549), Caffeine, Sigma-Aldrich, China (Molecular weight 194.19, product code 1002183388), Dichloromethane (DCM), Fisher Chemicals (HPLC grade, 99.8% pure, CAS No. 75-09-02), and Methanol, Thermo Fisher Scientific New Zealand Ltd. (Laboratory grade).

Hamilton syringe needle 23G (HAMC91023), Bio-Strategy NZ. Aluminium mono-foil (industrial grade and non-stick grade) was purchased from local supermarket.

3D printed collector devices were printed from Premium UP ABS+ using an UP Mini printer, both from 3D Printing Systems, NZ.

De-ionised water produced by reverse osmosis at the main centre in the University and delivered through a dedicated tap in the laboratory was used for all the experiments.

2.2 Fabrication of membranes

2.2.1 3D printed collectors

The components of the collectors, rotary shaped mandrel were printed using a 3D printer machine and designed using Tinkercad (https://www.tinkercad.com/). The components were assembled (Figure 2.1) to yield a final collector product which was rotary shaped collector.
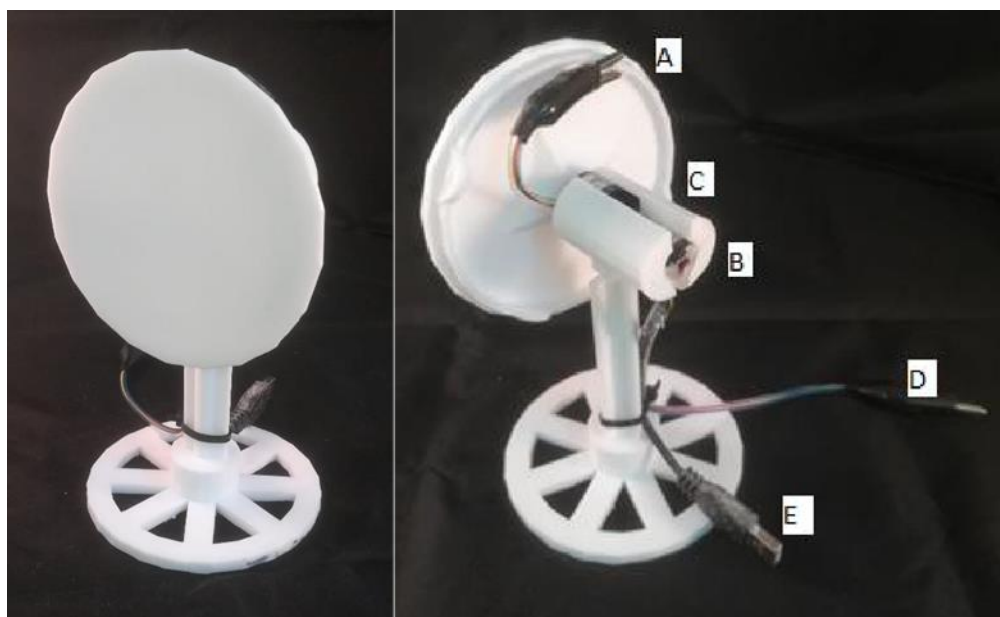
Figure 2-1 Nanofiber collection mat. Left; front view showing 10 cm diameter disk. Aluminium foil is placed covering the disc and wrapped over to the other side by approximately 2cm. Right; rear view showing earth clip attached tothe disc (A, in operation will contact the aluminium foil), geared DC motor(B), rotating pass through (C), earth clip (D), and connector for 3 V powersupply (E).

2.2.2 Polymer solution preparation

PCL polymer solutions were prepared by dissolving PCL or PCL + Caffeine in binary-solvent system of DCM and Methanol (3:1 ratio) to obtain a 5%, 10% v/w PCL concentration or combination of PCL and caffeine (5% or 10%). The formulation details are given in the result section as appropriate.

PEO polymer solution was prepared by dissolving PEO in de-ionised water (v/w) to yield 10% PEO concentration.

2.2.3 Nanofiber membranes fabrication
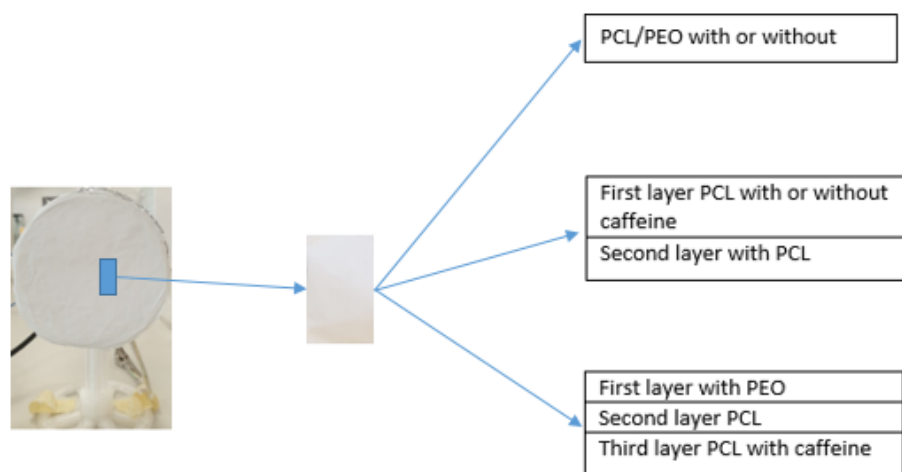
Figure 2-2 Nanofiber fabrication, mono-, two- and three-layered with details of polymer and drug in the fiber layer

40

Electrospinning process was carried out at room ambient temperature. The setup consists of a high voltage power supply, a syringe, a spinneret, positively charged needle and negatively charged collector wrapped with non-stick aluminium foil (rotating mandrel circular shaped). The basic process of electrospinning is to apply high voltage to a capillary filled fluid by means of an electrode, and then to collect the resulting fibre on a grounded plate/collector. The polymer solution is expelled at a constant rate through the syringe to produce a single droplet at the tip of the needle, which is charged and forms a Taylors cone, jet is initiated to produce nanofibers, which is drawn and collected on the negatively charged collector. The height of the needle/spinneret was adjusted to point towards the centre of the collector. The set up and spinning parameters adopted for nanofiber production were selected based on the parameters reported in the literature and feasibility of the process to be carried out in the laboratory. The process is usually carried out at 10-25 kV, spinneret inner diameter 0.21 – 0.9 mm, needle tip to collector distance 10-20 cm, flow rate 0.01 to 20 mL/h (Cipitria et al., 2011). After several iterations, the various parameters ideally suited for carrying out the process under the laboratory conditions were selected and used to produce either a mono, two layers or three layers nanofiber laminate (Figure 2-2). Three layers nanofiber laminate fabricated for experiment 1, using 5% PCL (1st layer) and 5% Caffeine (2nd layer), 5% PCL (3rd layer) each (wt./v)) in binary solvent DCM:Methanol (3:1).The other parameters selected for the process, voltage 20 kV, flow rate 4mL/h, needle tip to collector 15 cm, and spinning duration 1h per layer.

Two layers nanofiber laminate fabricated for experiment 2, 5% or 10% PCL with 5% or 10% caffeine (1st layer), 5% or 10% PCL (2nd layer) each (wt./v) in binary solvent DCM:Methanol (3:1). For this experiment a control laminate was also produced which did not contain a second layer. The other parameters selected for the process, voltage 20kV, flow rate 4 mL/h, needle tip to collector distance 10 cm, and spinning duration 1h per layer.

Three layers nanofiber laminate fabricated for experiment 3, using 10% PEO (1st layer) with de-ionised water as dissolution medium (wt./v), 5% PCL and 1% PCL (2nd layer), and 10% with 10% Caffeine (3rd layer). Second and third layer, the chemicals were dissolved (wt./v) each in binary solvents, DCM:Methanol (3:1). For the second layer, two needles (bi-axial spinning) were used, one each for the polymer to expel the solution for the electrospinning process. The treatments/formulations except the control had overlapping layers for the duration of 10- or 30-min. Voltage used during the process, 23 kV (1st and 3rd layer), 28 kV (2nd layer), and 28 kV for overlapping layer. Flow rate 0.8 mL/h (1st layer), 2 mL/h (2nd layer), and 4 mL/h (3rd layer). For production of all the three layers, needle tip to collector distance 10 cm.

2.3 Physical properties of membrance

2.3.1 Nanofiber mat thickness

Standard external micrometer was used to measure the thickness of the nanofiber mat (Flack, 2001). The device uses a graduated screw mechanism to measure the precise linear displacement of the spindle along its axis which is referenced to the fixed measuring face on the axis of the spindle.

The nanofiber mat thickness measurements were carried out at either 3 or 6 points and 3 samples/treatment or formulation, avoiding the edges.

2.3.2 Puncture resistance test

The mechanical properties was evaluated by measuring the tensile properties (puncture and elongation) using TA.XT plus Texture Analyser (Stable Micro Systems, USA) with a load capacity of 5 kg. For each run, sample, 2.5 x 2.5 cm was fixed by screws between two plates with a cylindrical hole of 2 cm diameter. Two screws/pins stabilised the plates that were placed centrically under the punch probe of the Texture Analyser. 3 samples were tested for each treatment/formulation. A probe (P/5S) attached to the equipment was driven (2mm/sec pre-test and 0.5mm/sec test speed) in downward motion with a trigger force of 1g until the test sample was ruptured, to obtain the yield point for the test sample. All the testing were carried out at room temperature (20°C). Force and distance were recorded to calculate puncture strength and elongation break. The formula used to calculate the mechanical properties are given below:

Puncture Strength $(g/mm^2) = F/A$

Elongation at Break $(\%) = (\sqrt{r^2 + d^2} - r/r) \times 100\%$

Where F is the maximum force to puncture the nanofiber mat, A is the area of mat exposed in the opening hole, r is the radius of the tested mat area in the hole and d is the maximum displacement of mat being punctured (HD, 2004; Preis et al., 2014).

2.3.3 Mucoadhesive strength

TA.HD.plus textural analyser (Stable Micro Systems, UK) with 5 kg load cell used to quantify the mucoadhesion properties. The mucoadhesive strength of the test formulations were evaluated in vitro by measuring the force required to detach the formulation from a mucin disc (Baloglu et

al., 2011; Gratieri et al., 2010). Mucin (Mucin type III Porcine from Sigma) disc were prepared by direct compression of crude mucin (200mg) using a ring press with 13 mm diameter die and a compression force of 10 tonnes, applied for 30 sec. The final disc obtained were 14 mm in diameter, 1 mm thick with a surface area of 154 mm^2.

A mucin disc was placed on the non-mobile stage of the textural analyser. A circular stainless-steel plate (diameter 100 mm, height 10 mm, weight 300g) with a hole in the centre (diameter of 8 mm) was placed on the disc to ensure the top surface of the disc was visible through the hole. Probe TA-55, 5 mm diameter and 35 mm long was attached to the upper mobile end of the equipment. Prior to mucoadhesion testing, the mucin disc was hydrated with 50 μl of deionized water, by placing the water droplet in the centre of the mucin disc. The probe was lowered slowly until the probe was in contact on the upper surface of the water droplet and the water droplet was spread on the surface of the disc with the aid of the probe. Probe drawn back to its original position and the surface of the probe cleaned with a tissue paper to remove water adhering to the surface of the probe. The water dispersed on the surface of the disc was allowed to equilibrate for 2 to 3 min. Test material was attached to probe by taping the side with an adhesive tape to ensure that the test sample is held in place whilst testing. The probe attached to the equipment (10 mm/sec pre-test speed and 0.5 mm/sec test speed) was driven in downward motion with a trigger force of 100 g and contact time with the test sample for 10 sec. The force required to detach the test sample from the surface mucin disc was determined from the resulting force-time adhesion curves using Texture analyser software, Exponent Version 6.1.16.0, Stable Micro Systems, UK. All measurements were performed at room temperature (20°C) and three replicates per test sample.

2.3.4 Water contact angle

Water contact angle measurement was carried out by using a 4 μL (de-ionised water) sessile drop sample. Double sided adhesive sellotape was stuck on a cover slip, a small strip of the sample was placed on the adhesive tape and gently pressed. A 4 μl de-ionised water and gently deposited on the strip using a 10 μl pipette (Baek et al., 2012). Subsequently, two drops were deposited as the measurement progressed. Contact angle was measured at three different points avoiding the edges and three samples were tested for each treatment/formulation or one sample if it is a replicated trial. Contact angle was measured on both the sides if the sample was a laminate, top and bottom separately or on one side if it was a monolayer sample. For each measurement two values were produced, on the left and right interface between the drop and the mat. Angle values displayed in this thesis are the average of two angle.

The measurement of contact angle of a sessile drop involves a multistep process, image acquisition, image processing, and numerical computation (Hoorfar & Neumann, 2004). The set-up of image acquisition, a USB microscope (Microscope 2MP Digital 500X8LED, Andonstar) connected to a computer, to capture the images (Leese et al., 2013; Trantidou et al., 2012). A spotlight source is used to illuminate the drop, the images captured using a camera and stored in the computer. The re-captured diagram of the set up given below (Figure 2.3). The images were analysed using the DropSnake plugin (Stalder, 2006; Williams et al., 2010).

To verify the performance of the testing method, the water contact angles of various materials including, Non-sticky Aluminium Tinfoil (mono®), microscope glass coverslips (Chance Propper®), microscope slide (Chance Propper®) and PM-992Wrap (Parafilm®) were measured three times to evaluate the accuracy and repeatability.

Figure 2-3 Measurement of Water Contact Angle set up (Liu, 2019).

2.3.5 SEM observation

The surface morphology of the nanofiber mats was evaluated using field emission scanning electron microscope (FESEM). Samples were attached to 10 mm aluminium stubs, which were covered with 10 nm carbon in an Emitech K575X Peltier-cooled high-resolution sputter coater with carbon coater attachment (EM Technologies Ltd, Kent, England) or 10 nm of gold palladium (80:20) in a Quorum Q150V ES PLUS coater (Quorum Technologies, East Sussex, UK). Samples were analysed in a 5 kV JEOL JSM-6700F field emission scanning electron microscope (JEOL Ltd, Tokyo, Japan) or in a 5kV Zeiss Sigma 300 VP FE scanning electron microscope (Carl Zeiss Inc., Oberkocken, Germany) A high-resolution image was achieved by a scanning electron detector with a working distance of 5.8 and 6.4 mm.

2.4 In-vitro release studies

Minitron: Caffeine release from the sample measured using the Minitron shaker (Infors). Sample (1 x 1 cm) was placed in 25mL McCartney bottle. 3 replicates were tested. Samples were placed in bottle containing 10 mL deionised water. Samples were kept in rotary Minitron (100 rpm) at 37°C. 100 μL aliquot were withdrawn from each bottle at 2, 15, 60, 120, 240 and 300 minutes into 96-well microtiter plate and absorbance measured at 286 nm using Spectrophotometer (Multiskan GO, Thermo Scientific®). To quantify the caffeine release, a standard curve developed using pure caffeine. Pure caffeine standard stock prepared by dissolving 0.08g

caffeine in 100 mL deionised water. Subsequently four standard dilutions prepared to give a final caffeine concentration of 10, 20, 30 and 40 µg/mL. 100 µL of each of these solutions were measured for its absorbance at 286 nm and standard graph plotted using Excel.

Ussing chamber: A two-chamber Ussing diffusion equipment was used to study the release of caffeine from laminate samples (Olsen et al., 1995). Caffeine release for each sample was measured in triplicates. Circular laminate sample, 3 cm in diameter affixed to the heavy duty aluminium adhesive foil and mounted into the perfusion cell in vertical position and the cell clamped together. The top layer of the laminate was facing the respective column, exposed surface area of each test sample 3.14 cm^2. One sample was tested for each chamber. Each column filled with 15 mL de-ionised water. The contents of each chamber were mixed by bubbling a air at the rate of three to four bubbles per second, and the temperature within each chamber was maintained at 37 ± 10°C by a circulating water bath.100 µL aliquot pipetted into 96-well microtiter plate from each column at 1, 2, 3, 4, 5 and 24h after initiation of the experiment. The absorbance of the samples was measured at 294 nm using Spectrophotometer (Multiskan GO, Thermo Scientific®). To quantify the caffeine release, a standard curve developed using pure caffeine. Pure caffeine standard stock prepared by dissolving 0.08g caffeine in 100 mL deionised water. Subsequently four standard dilutions prepared to give a final caffeine concentration of 10, 20, 30 and 40 µg/mL. 100 µL of each of these solutions were measured for its absorbance at 286 nm and standard graph plotted using Excel.

CHAPTER 3   RESULTS AND DISCUSSION

3.1 Validation UV standard curve for caffeine and contact angle measurements

The caffeine standard curve was constructed using freshly prepared standards ranging from 10 to 40 µg/ml. A typical caffeine standard curve absorbance's across the range of standards are given below in table 2 and the curve plotted in figure 3.1. For this typical caffeine standard curve, the intercept was 0.0147 and slope 0.0835 with a correlation (R^2) of 0.9892.

The standard water contact angles (n=3) were measured for aluminium foil, parafilm, glass slide and cover slip (Table 3). Aluminium foil and parafilm exhibited the property of hydrophobicity, water contact angle >90° whereas glass slide and cover slip exhibited hydrophilicity property, water contact angle <90°. The water contact angle measured was close to those published in the literature (Lui, 2019 & Cartens, Gamelas, & Schabel 2017).

Table 2 Average caffeine absorption standards (10, 20, 30 and 40 µg/ml) at 286 nm.

Concentration (µg/ml)	Average (n=3) Absorption ± SEM
10	0.245 ± 0.00
20	0.368 ± 0.01
30	0.502 ± 0.00
40	0.691 ± 0.01
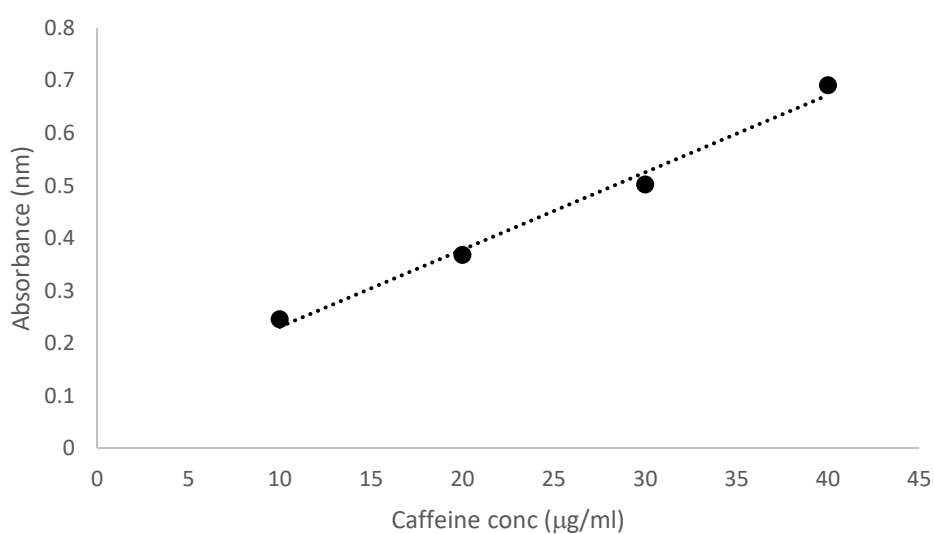
Figure 3-1 Standard curve for caffeine, mean absorbance against caffeine concentration (µg/ml).

Error bars are standard error means (n=3) and within symbols.

Table 3. Average (n=3) water contact angle (°) for control samples.

Control sample	Average Contact angle (°) ± SEM
Aluminium foil (non-stick side)	102.11 ± 17.44
Parafilm	104.08 ± 17.00
Glass slide	28.21 ± 2.74
Cover slip	53.72 ± 0.66

3.2 Two layer nanofiber formulations

Electrospun nanofiber mats prepared using PCL of 5 or 10% concentration with caffeine (5 or 10% relative to the amount of PCL) were prepared by spinning each layer for 1 hour. Single layer (5 or 10 % PCL with 5 or 10% caffeine) was prepared as controls.

3.2.1 Evaluation of nanofiber mat thickness for two layer nanofiber formulations.

A micrometre (0 to 25 mm) with graduated screw mechanism was used to measure the nanofiber mat thickness. Details of the formulations are provided above in 3.2 with further details on the protocol for nanofiber mat thickness measurement in Chapter 2, 2.1.4. The nanofiber mat thickness increased as the PCL polymer concentration increased (Figure 3.2), except for the formulation with 10% caffeine. For two layered formulations prepared with 10% caffeine (5% PCL with 10% caffeine and 10% PCL), the mat thickness achieved did not represent the amount of polymer content increased. The thickness of mat depends on the morphology, diameter and uniformity of the fibre, which are mainly determined by the fibre chemistry, processing

parameters of electrospinning, and post processing treatments. The mechanical properties of the fibre mats strongly depend on the measurement technique, processing conditions of fibre fabrication, fibre orientation, bonding between the fibres (Rashid et. al., 2021). For example, the researcher found in electrospinning of aqueous PEO dissolved in ethanol-water solvent system, too low viscosity (<1P) gave shorter and finer fibres with occasional beads because of insufficient molecular entanglement, whereas those from more viscous solutions (1-20 P) were relatively continuous. Two layers in the formulation did not produce double the thickness, however increasing PCL concentration (or number of layers) did as could be expected increase thickness (Figure 3.2) with some variations across the formulations which might have more to do with how the fibres deposit on the collector. Similar results were found by Alhusein et. al. (2012) with three layers of PCL membrane, they found the thickness of the third layer is much less than the first PCL layer; however, the diameter of the fibres in the third layer is larger than the first PCL layer. The accumulated charges of the electrospun fibres interrupt the build-up of the later deposited fibres which renders them less stretched, thus of larger diameter with reduced layer thickness.

In general, the thickness of two layered mat was higher than that of the control monolayer mat but not consistent across the formulations. There was about 2 to 20% increase for 5% PCL and 37 to 65% increase for 10% PCL compared to the monolayer formulation except for the formulation with 5 or 10% PCL and 10% caffeine. The increase for 5 and 10% PCL with 10% caffeine was 113 and 87% respectively.

Many factors can influence the thickness measurement using a micrometre, like measuring instrument, process, temperature effects etc., hence measurements are never made under perfect conditions (Flack, 2014). The deposition of the nanofiber mat is influenced by multiple factors

51

(Lee et al., 2001) and heterogenous thickness of the mat with uneven porosity and void spaces (Rashid et al., 2021).
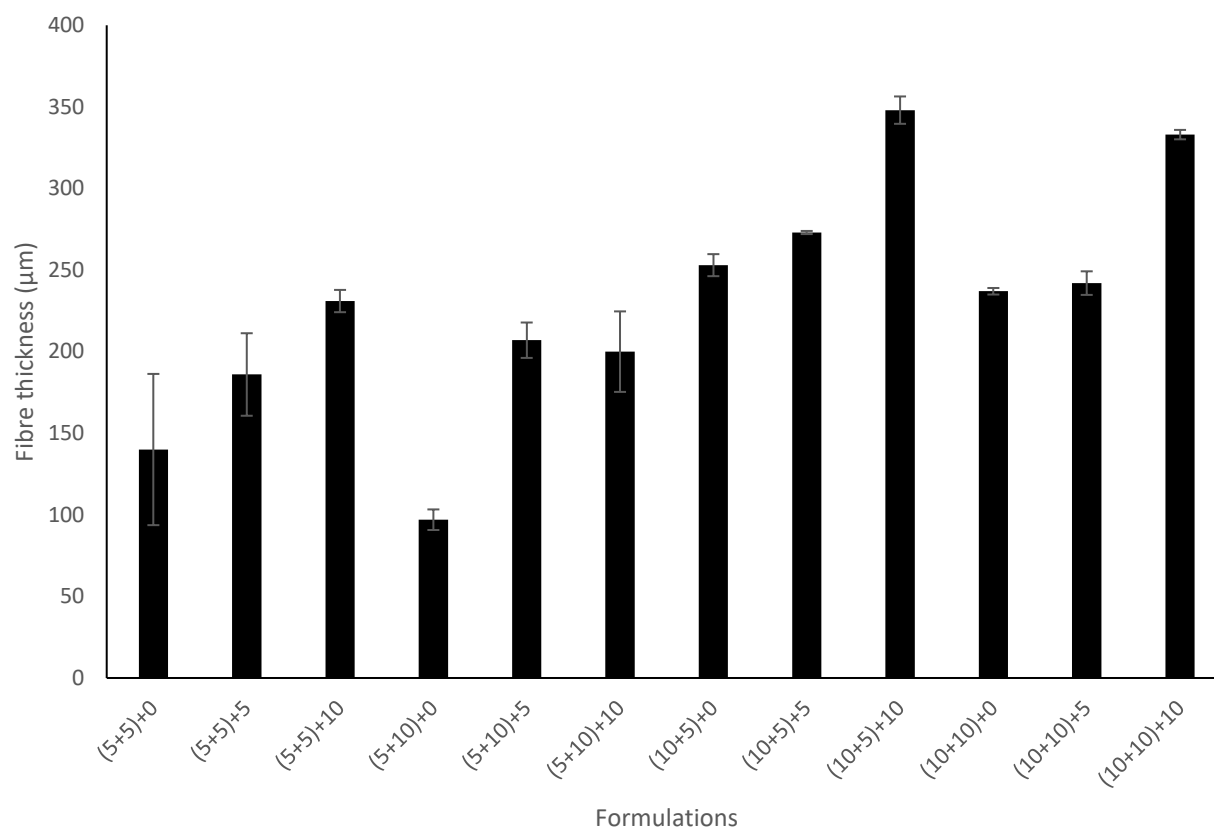
Figure 3-2 Two-layer nanofiber mat average thickness. Formulation key: (A+B)+C where A= PCL concentration (5 or 10%), B=caffeine concentration (5 or 10%) and C = second layer PCL concentration (0, 5 or 10%).

3.2.2 Evaluation of in-vitro caffeine release % for two layered nanofiber formulations

A two-chamber Ussing diffusion equipment was used to study the release of caffeine from two layered nanofiber mat formulations. Caffeine release from each sample was measured in triplicates. The details of the methodology are provided in Chapter 2, 2.1.9. As there was not much difference in the results achieved after 4h sampling (at 5 and 24h) only the % caffeine releases up to 4h are presented in the Figure 3.3. Irrespective of polymer and caffeine concentrations, 1h after the initiation of the experiment the two layered formulations had approximately 5 to 33% of caffeine released compared to the monolayer formulation which had about 40 to 52% caffeine released (Figure 3.3). The nanofibrous matrices possess a high-surface area-to-volume ratio which leads to a large initial burst of the drug, a similar results were found with the formulation PCL/poly(ethylene-co-vinyl acetate)/PCL with tetracycline hydrochloride in each layer gave a initial burst (>80%) release followed by sustained release (Alhusein et. al., 2012). The same trend was noticed after 4h too. Presence of second layer acts as a physical barrier which delays the diffusion of the buffer, similar to the results found by Alhusein et. al. (2012), when tetracycline chloride was only present in the second layer and the not the first and third layer, the sustained release improved from 6 days to 15 days, showing a barrier protection of the release by the presence of a third layer.

The % of polymer present in the first layer and second layer had an influence on the caffeine release %. Using a thicker layer, increases the restriction of caffeine release. The addition of second barrier layer first limits the core hydration process, restraining drug dissolution and diffusion because the drug has a thicker surface to cross. For formulation 5.5.10 the % of caffeine released after 1h was $17 \pm 2.2\%$ compared to formulation 5.5.5 which was $29 \pm 16.5\%$. The

presence of higher polymer concentration in the second layer probably increased the mat thickness which resulted in longer diffusion path (Alhusein et. al., 2012). Similar trend was noticed at 4h after initiation of the experiment. Similar results were noticed for other formulation as well, lower caffeine released when the polymer concentration in the second layer was 10% compared to 5%. Formulations 5.10.5, 5.10.10, 10.5.5, 10.5.10, 10.10.5, 10.10.10 had 33 ± 3.0, 22 ± 2.7, 10 ± 2.5, 5 ± 3.3, 16 ± 4.9, and $10 \pm 3.4\%$ respectively at 1h after the initiation of the experiment. At 4h, there was not much difference in the caffeine release % for the formulations which contained 10% PCL in the first layer. The plausible reason could be due to blending of hydrophilic drugs with hydrophobic carrier polymer and the release mechanism predominantly governed by diffusion process. When the water molecules attack the ester bonds in the polymer chains, the average length of the degraded chains become smaller. The process results in short fragments of chains having carboxylic end groups that render the polymer soluble in water , Armentano et. al. (2010) research results showed that the hydrolytic degradation of the PLGS matric was clearly controlled by two mismatch mechanisms: chain-scission and crosslinking. However, at 5h sampling, the formulation containing 5% PCL in the first and second layer with 10% caffeine (5.10.5) had ~40% more caffeine released compared to the formulation with 10% PCL in the second layer (5.5.10). Appears that the percentage of the polymer in the second layer acted as a barrier and had some influence on the caffeine release, similar results were found by Liu (2019) when PCL nanofibers were loaded with caffeine. Higher caffeine % in the first layer might have also contributed to a higher caffeine release %.
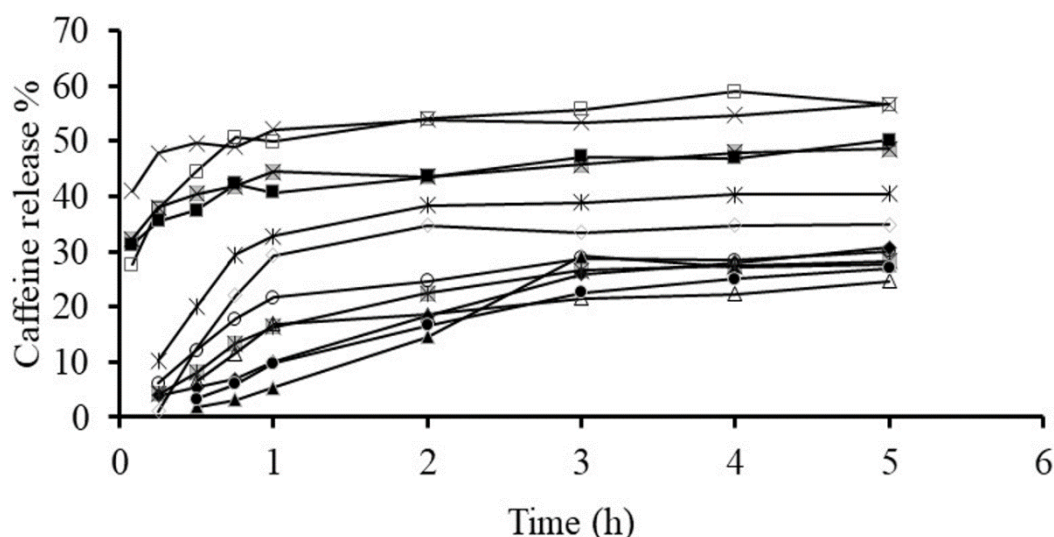
Figure 3-3 Average release of caffeine (%) from two-layer nanofiber mats into the Ussing receptor chamber containing water at 37 °C. (□) 5.5.0, (◇) 5.5.5, (△) 5.5.10, (×) 5.10.0, (✶) 5.10.5, (○) 5.10.10, (■) 10.5.0, (◆) 10.5.5, (▲) 10.5.10, (×) 10.10.0, (✳) 10.10.5, (●) 10.10.10. The caffeine containing lower layer was backed by aluminium foil. Formulation key: A.B.C where A= PCL concentration (5 or 10%), B=caffeine concentration (5 or 10%) and C = second layer PCL concentration (0, 5 or 10%). Average of n=3 replicates, error bars have been omitted for clarity.

3.3 Three layered nanofiber formulations

Three-layer formulations were prepared with first layer containing 10% PEO, second layer 5 and 1% PCL and third layer 10% PCL with 10% caffeine. Two types of formulations were prepared with the variation in the layer overlapping timing, 10 and 30 min. These formulations were compared to the control monolayer, 10% PCL with 10% caffeine. Details of the methodology for nanofiber mat fabrication are provided in Chapter 2, 2.1.3

3.3.1 Evaluation of contact angle for three layered nanofiber formulations

Measurement of water contact angle on nanofiber surface, represents an important parameter in adhesion science. It provides consistent valuable information on surface properties like surface energy, hydrophobicity or hydrophilicity, roughness, and chemical heterogeneity. Water contact angle was measured on both the surfaces, top and bottom for the formulations including the control monolayer formulation. The water contact angle of upper surface three-layered nanofiber formulation with 10 min and 30 min layer overlapping time was almost like that of control monolayer formulation, 10% PCL with 10 % caffeine (Figure 3.4). There is a direct correlation between the water contact angle and the functionality of the nanofiber mat. Higher the water contact angle higher the hydrophobicity and lesser water contact angle higher hydrophilicity. The upper layer of the three-layered formulation constitutes 10% PCL with 10 % caffeine. The upper layer exhibited hydrophobicity property with a water contact angle of $106 \pm 3.4°$ (10 min overlapping time), $111 \pm 3.6°$ (30 min overlapping time), and control monolayer upper surface $113 \pm 2.8°$ (Figure 3.4a).
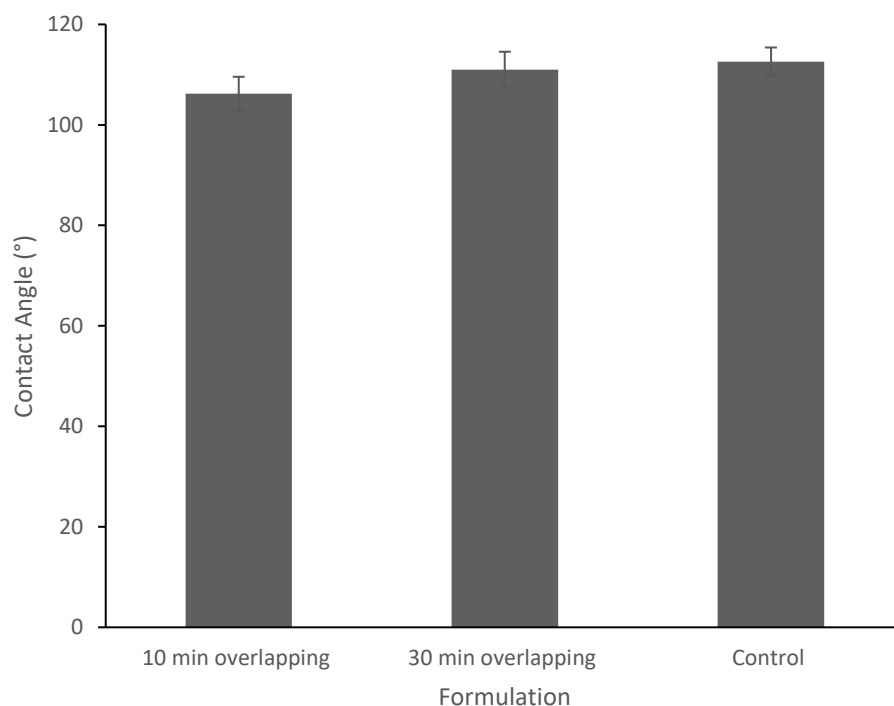
Figure 3-4 Average water contact angle (°) of the upper layer (not in contact with the collector) for 3 layer (PEO 10%, PCL (5 and 1%), PCL 10% with caffeine 10%) with 10 or 30 min overlapping between layers and control monolayer nanofiber (PCL 10% with caffeine 10%). Error bars, SEM n=3.

The water contact angle of lower surface three-layered nanofiber formulation with 10 min and 30 min layer overlapping time which was different to that of control monolayer formulation, 10% PCL with 10 % caffeine (Figure 3.4b). The water contact angle was $43 \pm 3.7°$ (10 min overlapping time), $25 \pm 4.4°$ (30 min overlapping time), and for control monolayer lower surface it was $106 \pm 4.2°$ (Figure 3.4b). The lower layer of the three-layered formulation constitutes 10% PEO polymer, a hydrophilic polymer.

The upper surface of the formulations contained the polymer PCL which is hydrophobic, and the lower surface contains a hydrophilic polymer PEO. Water contact angle <90˚ allows the water to permeate through the nanofiber mat hence it is hydrophilic, whereas water contact angle >90˚ resist the water permeation and it is hydrophobic. Hence the higher water contact angle (>90°) results were achieved from testing the upper surface containing a hydrophobic polymer compared to the lower surface wherein the water contact was less (<90°) containing a hydrophilic polymer (Figure 3.5). Dias & Bártolo, (2013) found the water contact angle to be 101 ± 0.94˚ for 17% PCL dissolved in acetone but reduced when PCL was dissolved in acetic acid with triethylamine, 83.64 ± 2.72˚. Though the overlapping time did not have any implication on the water contact angle for the upper surface the same results were not noticed for the lower surface. It is plausible, that the liquid drop is likely to be absorbed to the dried nanofiber surface, which essentially altered the surface nature by exposing more hydrophilic components. Contact angle and the wetting behaviour of solid particles are influenced by many physical and chemical factors such as surface roughness and heterogeneity as well as particle shape and size. Wenzel, the first scientist to investigate the effect of surface roughness on the static contact angle in 1936, suggested that the geometry of the surface had a greater effect on the static contact angle than did the chemistry. The water contact angle of the lower surface with 30 min layer overlapping time had about 60% less water contact angle compared to 10 min layer overlapping time. At 30 min multilayer overlapping time plausible the PEO molecules are interlocked with PCL molecules enhanced the water absorption hence the reason for lower water contact angle compared to 10 min multilayer overlapping time wherein the hydrophobic polymer PCL forms a barrier. The water droplet shape of the upper surface containing PCL polymer exhibit hydrophobic property compared to the lower surface containing hydrophilic PEO polymer where the droplet was almost flattened (Figure 3.6). Figueroa-Lopez et al. (2018) found the wettability

of multilayers PCL-GEL-PCL (83.9˚) is reduced compared to GEL layer (50.3˚) due difference

in the surface topology that could result from the multilayer formation.
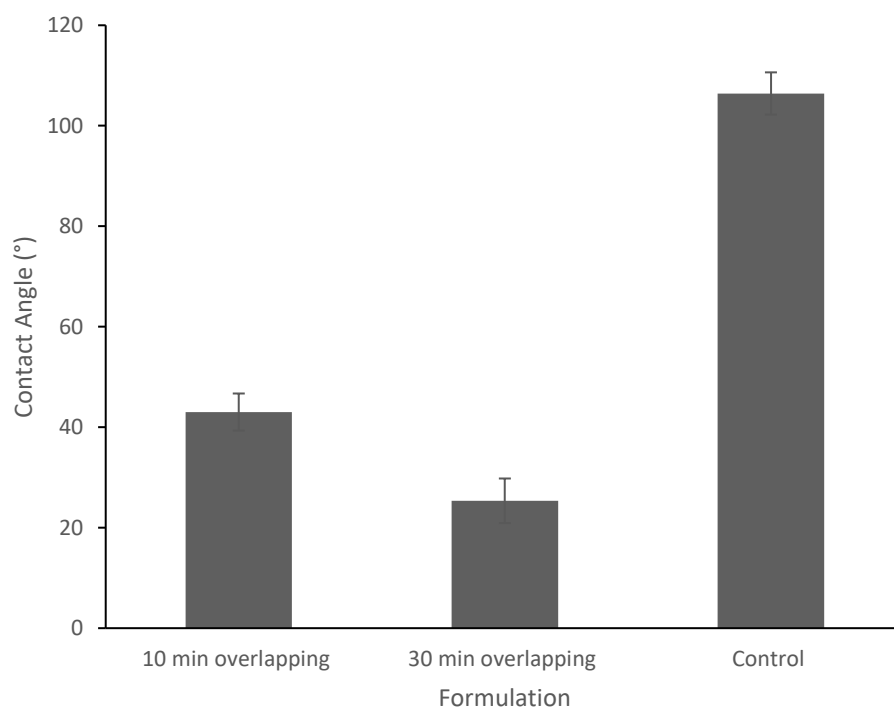
Figure 3-5 Average water contact angle (□) of the lower layer (in contact with the collector) for

3 layer (PEO 10%, PCL (5 and 1%), PCL 10% with caffeine 10%) with 10 or 30 min

overlapping between layers and control monolayer nanofiber (PCL 10% with

caffeine 10%).
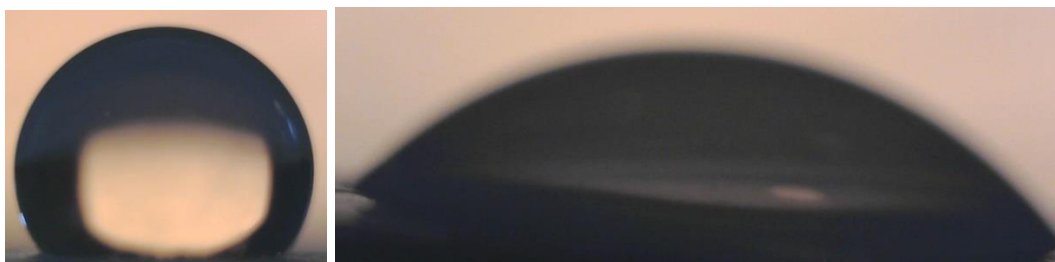
Figure 3-6 Image showing the shape of the water droplet on upper surface (left) and lower surface

(right)

3.3.2 Evaluation of nanofiber mat thickness for three layered formulations

A micrometre (0 to 25 mm) with graduated screw mechanism was used to measure the nanofiber mat thickness. Formulation details as mentioned above in 3.4 with further details of nanofiber thickness measurement protocol in the Chapter 2, 2.1.4. The nanofiber mat thickness for the three-layered formulations was higher than that of the control monolayer formulation, 120.6 ± 6.3 µm (10 min layer overlapping time), 193.9 ± 7.6 µm (30 min layer overlapping time), and 102.2 ± 9.2 µm (control monolayer). The thickness of the three-layered formulation was higher than the monolayer, 18% for 10 min layer overlapping time and 90% for 30 min layer overlapping time (Figure 3.7).

The nanofiber mat thickness did not correlate to the amount of polymer in the formulation (Flack, 2014; Ryu et al., 2020). The deposition of a well aligned fibre is possible as soon as the tangential speed of the mandrel reaches the threshold of the polymer jet speed (Huang et al., 2003) to produce aligned and random meshes. These aligned and random meshes layers can be alternated in order to design the mechanical properties of the mats. However, the system does not allow the formation of thick polymer meshes due to insulator effects caused by the first layers of fibre which prevents the adhesion of fibres (Migliaresi et al., 2012). The accumulated charges of

electrospun fibres interrupt the build-up of the later deposited fibres which renders them less stretched, thus of larger diameter and with reduced layer thickness (Alhusein et. al., 2012). Many factors can undermine thickness measurement using a micrometre, like measuring instrument, process, temperature effects etc., hence measurements are never made under perfect conditions (Flack, 2014). The deposition of the nanofiber mat is influenced by multiple factors, such as electrostatic force related to the applied voltage and charge of deposited nanofibers, initial jet velocity (Lee et al., 2001) governed by the flow rate, jetting regime and solvent evaporation governed by humidity and temperature and unpredictable bending instability due to high voltage. Ryu et al., 2020 studied the deposition behaviour of PCL nanofiber between two-parallel electrode plates at different time slots (10, 12, 30 and 32 min) and concluded that deposition behaviour of the nanofiber mat was continuously altered throughout the electrospinning process (Ryu et al., 2020). Owing to such unpredictability during the deposition of nanofibers, conventional electrospinning system often produce a nanofiber mat with non-uniform thickness.

Measurement of representative thickness of the mat with uneven porosity and void spaces still remains a challenge which further needs extensive research exploration (Rashid et al., 2021).

Figure 3-7 Average nanofiber thickness (µm) for 3 layer (PEO 10%, PCL (5 and 1%), PCL 10% with caffeine 10%) with 10 or 30 min overlapping between layers and control monolayer nanofiber (PCL 10% with caffeine 10%). Error bars, SEM n=6.

3.3.3 Evaluation of tensile properties, puncture strength and elongation at break for three layered nanofiber formulations

Details of the formulation are provided above in 3.4 and further details of methodology in Chapter 2, 2.1.5. The tensile properties, puncture strength (g/mm^2) and elongation at break (%) was measured using a TA.TXT plus Texture Analyser.

Layer overlapping time, 10 or 30 min did not have any influence on the puncture strength, it was almost similar, 0.8 ± 0.1 g/mm^2 (10 min layer overlapping time) and 0.80 ± 0.01 g/mm^2 (30 min over lapping time) (Table 4 and Figure 3.8). However, the puncture strength required to puncture a three-layered formulation was higher than that of the control monolayer formulation, $0.54 \pm$

0.03 g/mm^2. Baji, Mai, Wong, Abtahi and Chen (2010) has pointed out that only the fibres oriented along the loading direction of the tensile test provide strength, the others perpendicular to the direction of stress experience no stretch. The tensile testing of nanofiber mats provides an assessment of the average mechanical properties of the nanofibers rather than measuring an individual nanofiber. Finding a single fibre from an electrospun sample that represents the average diameter of all the fibres of a sample is challenging. The fibres collected from different positions of the mat may exhibit different mechanical properties, moreover the fibres are not necessarily uniform in structure thought the mat. Though the tensile testing for nonwoven mat is measured by researchers it is not suitable for characterising the mechanical properties of nanofiber, because the fibre orientation is changed during the tensile test and also the nanofiber mat includes friction between the fibres which influence the fibre property results which can be mitigated by measuring the tensile test on a single fibre ((Bazbouz & Stylios, 2010). The mechanical properties of the fibre mats or membranes strongly depends on the measurement technique, processing conditions of fibre fabrication, fibre orientation, bonding between the fibres, and slip of one fibre over another (Rashid et.al., 2021). When the membranes are collected on a static collector screen, there is no anisotropy in the in-plane tensile behaviour, however, it is not the same when the membranes are obtained from a rotating drum, The electrospun mats shows difference in properties in different directions as the fibre orientation depends on the linear velocity of the drum surface and other electrospinning parameters. The molecular-level orientation within fibres increases with decreasing fibre diameter and increasing spinning distance, resulting in better mechanical strength. Fibre diameter is also influenced by the solution viscosity used for electrospinning, a higher viscosity results in a larger fibre diameter. Other parameters that influence the fibre diameter are solution surface tension, charge density of the polymer solution and processing condition like temperature and humidity.

Table 4 Tensile properties of 3 layer and control nanofiber mat. Error bars, SEM n=3.

Sample	Overlapping time (min)	Average Force (g) ± SEM	Average Distance (mm) ± SEM	Average Time (secs) ± SEM	Average Puncture strength (F/A) ± SEM
1st layer 10% PEO, 2nd layer 5% PCL + 1% PCL, 3rd layer 10% PCL + 10% Caffeine	10	468 ± 83	12.4 ± 0.46	24.9 ± 0.92	0.8 ± 0.1
1st layer 10% PEO, 2nd layer 5% PCL + 1% PCL, 3rd layer 10% PCL + 10% Caffeine	30	502.7 ± 5.69	12.9 ± 0.17	25.8 ± 0.34	0.8 ± 0.01
10% PCL + 10% Caffeine		337.1 ± 20.25	13 ± 0.14	26 ± 0.28	0.54 ± 0.03
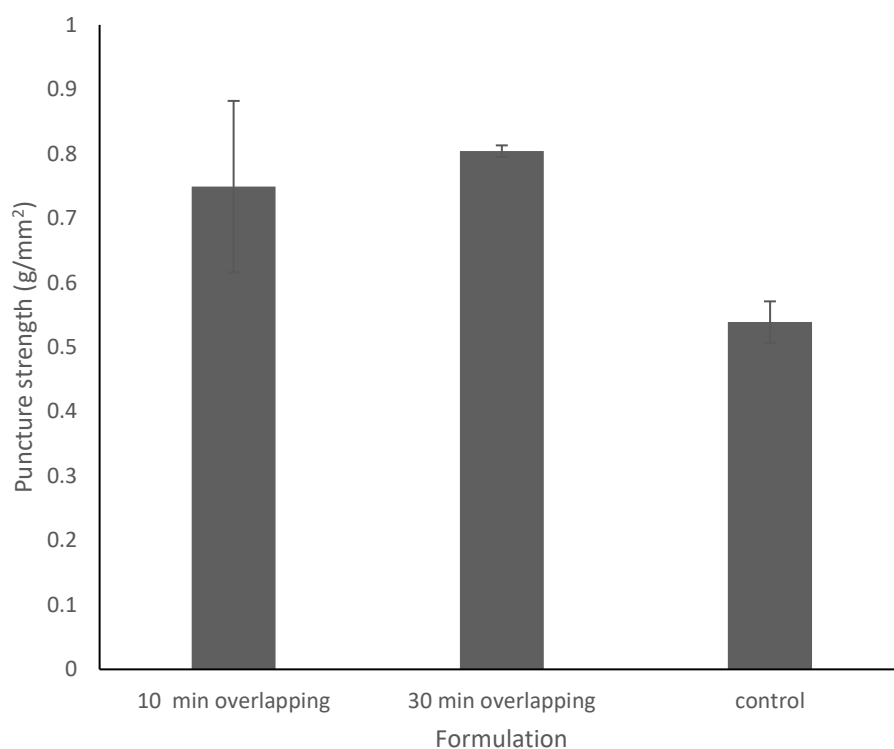
Figure 3-8 Average puncture strength (g/mm^2) for 3 layer (PEO 10%, PCL (5 and 1%), PCL 10% with caffeine 10%) with 10 or 30 min overlapping between layers and control monolayer nanofiber (PCL 10% with caffeine 10%). Error bars, SEM n=3.

Elongation at break (%) was almost similar for all the formulations including the control. 41.1 ± 2.6% (10 min layer overlapping time), 45.6 ± 1.0% (30 min layer overlapping time), and 44.3 ± 0.8% (control monolayer) (Figure 3.9).
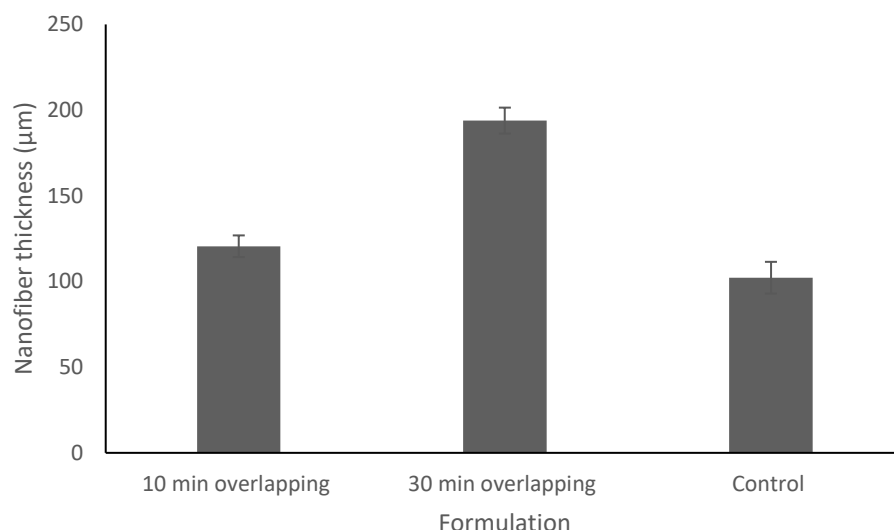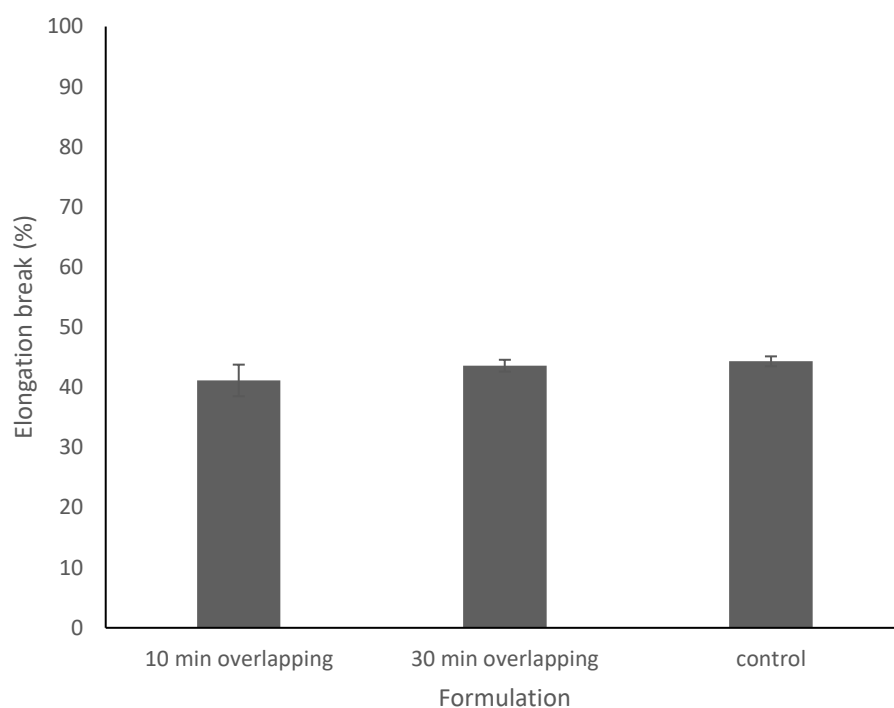

Figure 3-9 Average elongation at break (%) for 3 layer (PEO 10%, PCL (5 and 1%), PCL 10% with caffeine 10%) with 10 or 30 min overlapping between layers and control monolayer nanofiber (PCL 10% with caffeine 10%). Error bars, SEM n=3.

3.3.4 Evaluation of mucoadhesion for three layered nanofiber formulations

Details of the formulations are provided above in 3.4 and methodology details in Chapter 2, 2.1.6. TA.HD plus textural analyser with 5 kg load cell used to quantify the mucoadhesion properties. Detailed protocol used for analysing the samples provided in Chapter 2.1.6.

The average force required for detachment of three-layered formulation from mucin tablet was almost double when compared to the monolayer PEO or PCL formulation and the TA-55 probe. Synthetic polymers like PCL are generally not mucoadhesive, limiting the bioavailability on the corneal surface. In order to overcome this limitation, several formulations of synthetic polymers have been combined with mucoadhesive polymer which has enhanced mucoadhesive properties. The force required for detaching the lower surface of the formulation (the layer next to the collector) with 10 min overlapping time was 50.7 ± 13.2 (F_{max}) compared to 60.0 ± 5.5 (F_{max}) for top layer (Figure 3.10). For 30 min overlapping time formulation it was 66.7 ± 5.5 (F_{max}) for lower surface and 63.5 ± 3.2 (F_{max}) for top layer. The force required to detach the control formulation and TA-55 probe were, 26.5 ± 2.9 F_{max} (10% PCL), 25.3 ± 7.4 F_{max} (10% PEO), and 30.2 ± 3.8 F_{max} (TA=55 probe). Three layered formulations with two types of polymers exhibiting increase in mechanical integrity compared to having only one polymer either PEO or PCL (Alghamdi et al., 2016). The lower mechanical integrity for control one polymer PEO or PCL nanofiber mat is not due to weak mucoadhesive bond but to the over hydration of the polymer and its rapid disintegration (Grabovac et. al., 2005).
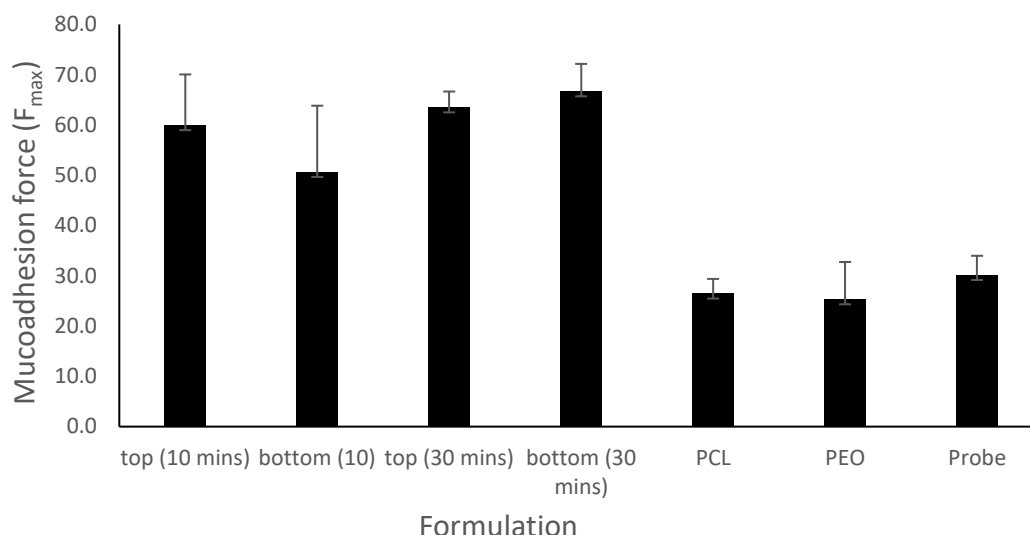
Figure 3-10 Average *in vitro* mucoadhesion (F_{max}) for 3 layer (PEO 10%, PCL (5 and 1%), PCL

10% with caffeine 10%) with 10 or 30 min overlapping between layers and controls

(PCL 10%, PEO 10% and TA 55 probe). Error bars, SEM n=3.

3.3.5 Evaluation of surface morphology for three layered nanofiber formulations

The surface morphology for nanofiber mat was evaluated using field emission scanning electron microscopy (FESEM). Details of protocol used are provided in Chapter 2, 2.1.8. Irrespective of the formulation overlapping time the images showed evidence of heterogenous fibre diameter distribution within a formulation (Figure 3.11). The fibre diameter ranged from 333 to 2452 nm for the top layer and 78 to 384 nm for the bottom layer. Images of all the formulations are provided in the appendix. The first layer of polymeric fibres deposited on the collector exerts an insulating effect that affects electrical field distribution and fibre architecture which results in bundles of aligned nonaofibres (high electric field strength), straight unaligned nanofibers (intermediate electric field) and curved unaligned fibres (Sahay et al., 2011).
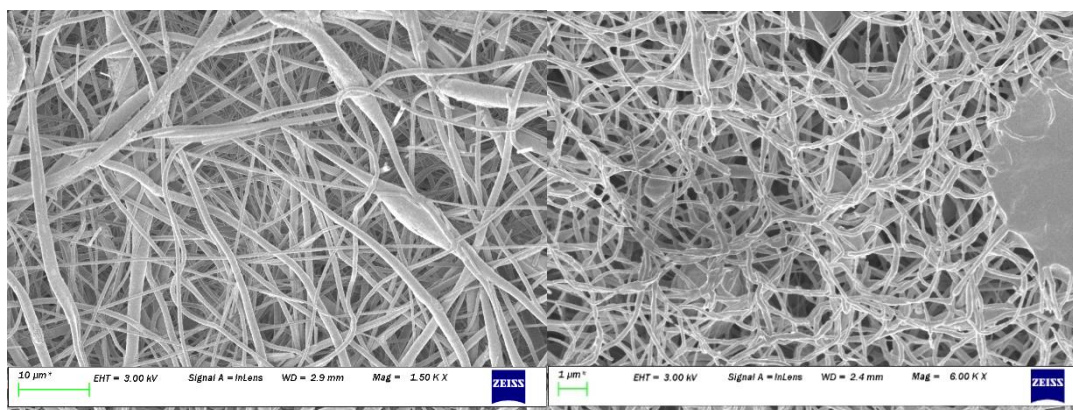
Figure 3-11 Heterogeneous fibre diameter distribution top layer containing PCL polymer (left) and bottom layer containing PEO polymer (right)

3.3.6 Evaluation of in-vitro caffeine release % for three layered nanofiber formulations

Details of the formulation provided above in 3.4 and methodology details of assay protocol in Chapter 2, 2.1.9. In-vitro caffeine release assay carried out using single Ussing chamber receptor by exposing the surface for testing to the receptor and the other surface backed to a heavy-duty aluminium foil.

At 1h after the initiation of the experiment >50% of the caffeine were released from the three-layered formulation irrespective of the layer overlapping time compared to the control monolayer formulation. For all the formulation the caffeine molecule was incorporated along with polymer in the top layer. The rapid dissolution occurred due to caffeine crystalline molecules on the

surface of the nanofibers when it came in interface with aqueous liquid. We presume it is likely as the caffeine molecules are adsorbed on the surface of the fibres, there was an immediate burst release as soon as the surface was moistened by the liquid medium. Similar results were noticed by Karruppuswamy et. al. (2015) that surface loaded PCL nanofiber with tetracycline is released instantaneously as soon as the membrane is place in the PBS, 15-20% and directly proportional to the bioactive concentration, 2 to 5%. At 1h, there was only 62 ± 6.0 % caffeine released for the formulation with 10 min layer overlapping time from the lower surface compared to 80.0 ± 15.5 % from the top surface for the same formulation (Figure 3.12). After 5h there was not many differences in the release %. Though the results were assessed for one more sampling point, 24h, results only for up to 5h are being presented as there was not many differences in the release % beyond 5h for all the formulations. Formulation with 30 min layer overlapping time the caffeine release % was almost similar from the lower and top surface, 72.7 ± 25.3 % (lower surface) and 72.7 ± 17.3 (top surface) at 1h with the similar trend noticed at 5h. However, an interesting result which needs further exploration for monolayer PCL formulation.is there is a difference in the % of caffeine released from either lower or upper surface. Lower surface had higher release % compared to top surface at 1h, 76.4 ± 3.1% (lower surface) and 42.7 ± 2.4% (top surface), similar trend was noticed at 5h (Grass & Robinson, 1988; Immich et al., 2017).
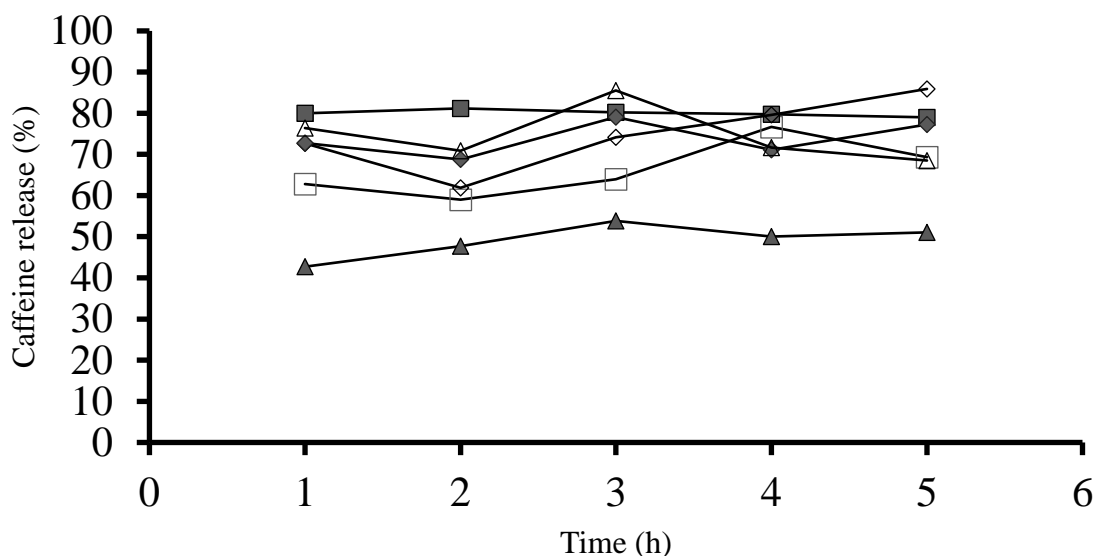
Figure 3-12 Average release of caffeine (%) from three-layer and control nanofiber mats into the Ussing receptor single chamber containing water at 37°C. (□) 10.5 and 1.10, 10, lower; (■) 10.5 and 1.10, 10, upper; (◊) 10.5 and 1.10, 30, lower; (♦) 10.5 and 1.10, 30, upper; (Δ) 10.0.0, lower; (▲) 10.0.0. upper. Mat was backed by aluminium foil exposing only one surface towards the receptor for testing. Formulation key A.B.C.D.E where A = PEO (10%) concentration except for control which is PCL (10%), B = PCL concentration (5 and 1%), C = PCL concentration (10% with 10% caffeine), D = overlapping time (10 or 30 min), and E = surface facing the Ussing receptor chamber (lower surface next to the collector or upper surface away from the collector). Average of n=3 replicates, error bars have been omitted for clarity.

3.4 Monolayer nanofiber formulations

Monolayer nanofiber formulations were prepared with 10% PCL or PEO polymer with each of the polymer having a loading of caffeine either 5 or 10 or 15% in triplicates. Details of the methodology of mat fabrication and polymer preparations are provided in Chapter 2, 2.1.2 and 2.1.3.

3.4.1 Evaluation of nanofiber mat thickness for monolayer nanofiber formulations

A micrometre (0 to 25 mm) with graduated screw mechanism was used to measure the nanofiber mat thickness. Details of the protocol used for measurements are provided in Chapter 2, 2.1.4 and formulation above in 3.5. Irrespective of polymer and caffeine loading, the mat thickness of the formulations prepared with polymer PEO was thinner than that of the formulations prepared with polymer PCL (Figure 3.13). Water was used as a solvent to dissolve the PEO polymer. The SEM images (provided in the appendix) of the formulations prepared with PEO produced beads-on-string structure that solidified, leaving a beaded nanofiber. Reneker & Yarin (2008) research showed that as the charge density on the surface of the jet decreased, the number of beads per unit length increased which resulted in the decrease of polymer in the form of nanofibers resulting in thinner fibres reducing the mat thickness. As the caffeine loading increased for the formulations prepared with PCL the mat thickness reduced. The average (n=3) for 10% PCL polymer with 5, 10 and 15% caffeine were, 126.2 ± 9.36 µm, 70.8 ± 7.86 µm, and 105.1 ± 8.50 µm, respectively. The thickness of 10% PCL polymer with 10% caffeine was thinner than that of 10% PCL polymer with 15% caffeine. Many factors undermine thickness measurements like instrument, process, temperature effects etc., hence the measurements are never undertaken

under perfect conditions (Flack, 2014). Measurement of representative thickness of the mat with uneven porosity and void spaces remains a challenge (Rashid et al., 2021).

Unlike PCL monolayer formulations which did exhibit a difference in the mat thickness as the concentration of caffeine increased from 5 to 15%, that was not the case with PEO polymer. The mat thickness for 10% PEO with 5, 10 and 15% caffeine did not show any differences, the mat thickness was 23.1 ± 0.92 µm, 24.2 ± 1.52 µm, and 25.3 ± 1.71 µm, respectively (Figure 3.12).
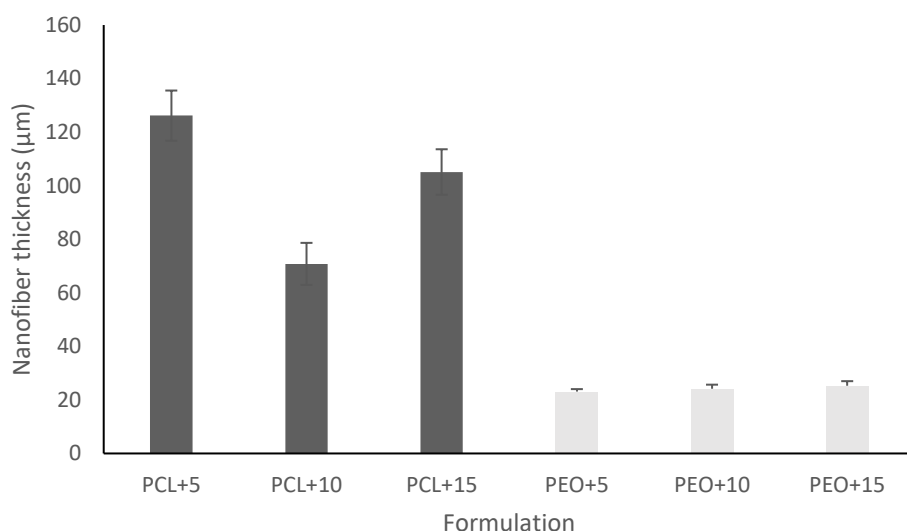
Figure 3-13 Average nanofiber mat thickness (µm) of PCL (10%) and PEO (10%) formulations with 5 or 10 or 15% caffeine. Error bars n=3.

3.4.2 Evaluation of in-vitro caffeine release % for monolayer nanofiber formulations in-vitro

In-vitro caffeine released for formulations prepared with 10% PEO or PCL polymer with 5, 10 and 15% caffeine were tested using Minitron equipment. Details of the protocol used to carry out the assay are provided in Chapter 2, 2.1.9 and formulations above in 3.5. The caffeine concentration in the collected release medium were determined measuring the UV absorbance and the % release quantified from the standard curve.

The caffeine release was almost immediate (5 min) for the formulations prepared with PEO polymer compared to PCL polymer, 1h (Figure 3.14). The initial burst release may be attributed to the enormous surface area of the nanofibers in contact with the liquid. Caffeine has high solubility in aqueous media, the fast release of caffeine is due to the immediate adsorption of the fluid phase by the polymeric membrane, which takes place in the first stage of the releasing process. When there is high rate of drug release in the first stage of the releasing process, the internal structure of the polymer matrix changes considerably, becoming more porous and less restrictive for the diffusion of any compound. Hydrophilic drugs are released at a faster rate than hydrophobic ones and particles with higher drug loading leads to more significant burst release and smaller particles exhibit higher surface area leading to higher degradation of the matrix with consequently faster release. The caffeine release after 5 min for formulations with PEO polymer with 5, 10 and 15 caffeine were, $132.4 \pm 64.74\%$ (not shown in the graph), $48.4 \pm 1.10\%$ and $45.5 \pm 21.99\%$, respectively. After 4h there was >90% caffeine release from the formulation and the caffeine loading did not have any impact on the release. Formulations with PCL polymer with 5, 10 and 15% caffeine the % caffeine released after 1h with 5, 10 and 15% caffeine loading were, $69.5 \pm 7.32\%$, $69.3 \pm 12.72\%$, and $50.5 \pm 15.6\%$, respectively. At 4h, the caffeine loading

73

had some impact on the release %, 73.5 ± 9.06% (5% caffeine loading), 68.0 ± 15.70 (10% caffeine loading), and 53.5 ± 13.00% (15% caffeine loading). Probably the wetting behaviour (Liu, 2019) and the air trapped in the fibre (Yohe et al., 2012) has an influence on the drug release. The results obtained with our study is similar to many studies that revealed that the initial burst release was inevitable for the membranes prepared by single-needle electrospinning blend form, which caused by the presence of large amounts of drug on the nanofiber surface. Despite significant progress in using electrospun fibres for drug delivery, still some challenges are to be mitigated or solved. Firstly, there is a challenge to ensure uniform nanofibers to be fabricated repeatedly and massively with the desired morphological, mechanical and chemical properties especially at industrial level. Secondly, up to now most of the studies on the release of antibacterial agents or anticancer drugs from electrospun fibres have been conducted in vitro, and in vivo studies have been rarely seen. Drug delivery with polymer nanofibers is based on the principle that dissolution rate of a particulate drug increases with increasing surface area of both the drug and the corresponding carrier (Huang et. al., 2003). Nanofiber alignment is another parameter known to affect drug release and in general randomised pattern is associated with faster drug release because of increased tendency of water uptake (Cui et al., 2006). Higher drug loading is associated with faster release. The crystalline form of the drug deposited on nanofiber surface results in burst release, as noticed with the monolayer formulation formulated with PEO polymer. The mechanism of drug release from nanofibers involves diffusion, osmosis or bio-erosion and affected by the type of polymers used in the formulation. The solubility of the polymer, the fibre diameter and the fibre structure are the primary parameters affecting drug release.
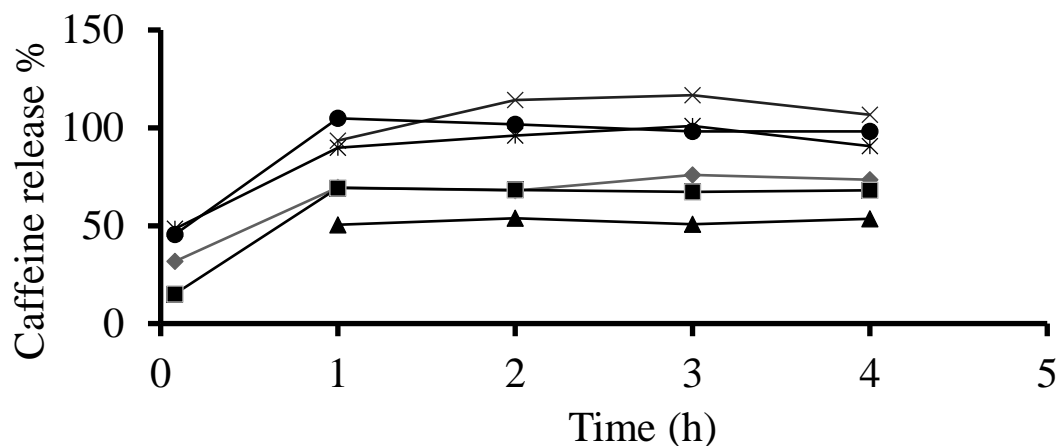
Figure 3-14 Average release of caffeine (%) for monolayer nanofiber mat PCL or PEO 10% with 5, 10 or 15% caffeine using Minitron. (♦) PCL.5, (■) PCL.10, (▲) PCL.15, (✗) PEO.5, (∗) PEO.10, (●) PEO.15. Average of n=3 replication, error bars have been omitted for clarity.

3.4.3 Evaluation of formulations tensile properties, puncture strength (g/mm^2) and elongation at break (%) for monolayer nanofiber formulations

The tensile properties, puncture strength (g/mm^2) and elongation at break (%) was measured using a TA.TXT plus Texture Analyser. Details of the protocol used to measure the tensile properties are provided in Chapter 2, 2.1.5, and formulations above in 3.5.

Tensile properties were measured (n=3) only for the formulations prepared with 10% PCL polymer with 5, 10 or 15% caffeine loading. It was a challenge to measure the tensile properties for the formulations prepared with PEO polymer. The moment the probe was in contact with the

surface of the nanofiber mat the mat started splitting even before the initiation of the downward movement of the probe (Figure 3.15). It is a possibility that due to the entanglement of certain solvent species (such as water) with PEO, the usual network of intermolecular bonds is either deformed or ruptured, resulting in a weaker interaction and fragile structure.
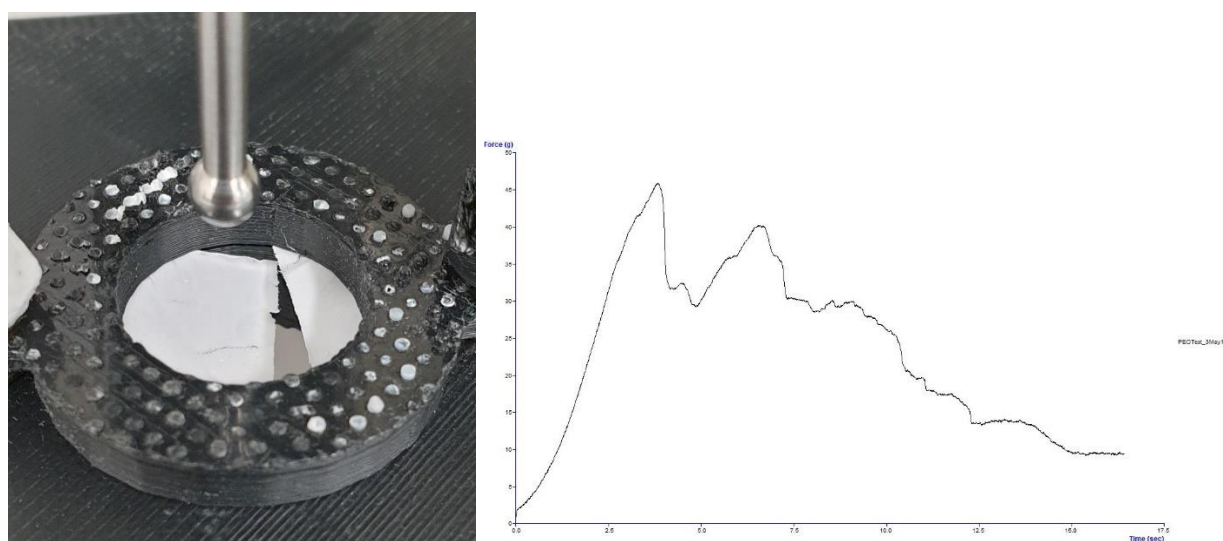
Figure 3-15 Splitting of PEO nanofiber mat (left) and corresponding graph (right) showing the data on the impact of nanofiber mat splitting

Monolayer formulations prepared with 10% PCL polymer, the puncture strength (g/mm^2) was almost similar for 5 and 15% caffeine loading, 0.565 ± 0.29 g/mm^2 and 0.601 ± 0.16 g/mm^2 (Figure 3.16). However, for formulation with 10% caffeine loading the force required to puncture the mat was less compared to 5 and 15% loading. 0.288 ± 0.06 g/mm^2. This is probably related to thickness of the mat as mentioned in the previous section (3.10) that the mat thickness of formulation with 10% loading was thinner (70.8 µm) compared to the other two formulations

126.2 and 105.1 µm. Only the fibres oriented along the loading direction of the tensile test provide the strength, the others perpendicular to the direction of stress experience no stretch (Baji et al., 2010). The data obtained is displacement of the spring over time, hence the applied load and the nanofiber elongation. The nanofiber goes through a linear elastic deformation followed by a linearly strain-plastic deformation till the final breakage point is reached at the ultimate strain. The mechanical properties of electrospun fibres depends on the morphology, diameter and uniformity of the fibres, which are mainly determined by the fibre chemistry, processing parameters of electrospinning, and post processing treatments (Rashid et. Al., 2021).
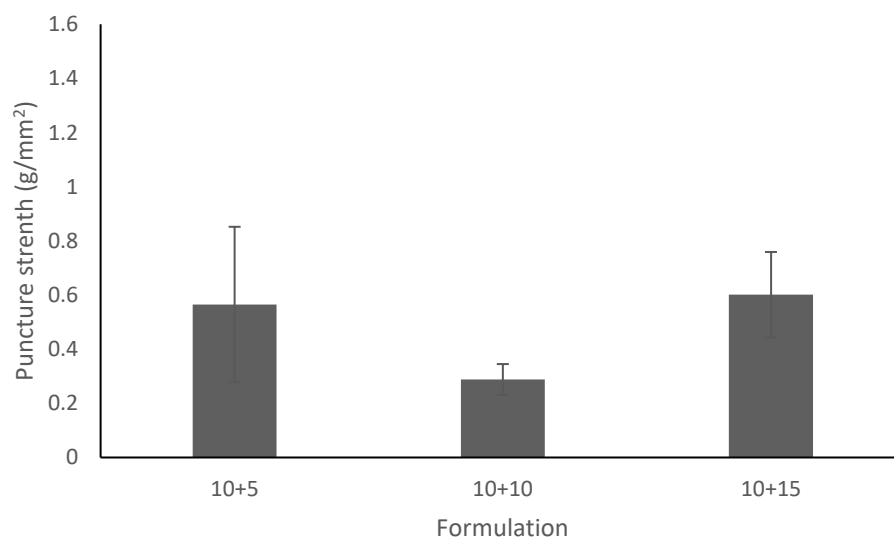
Figure 3-16 Average puncture strength (g/mm^2) for PCL 10% nanofiber mat with 5 or 10 or 15% caffeine. Error bars n=3.

Caffeine loading did not have much impact for elongation at break (%) for formulations prepared with PCL polymer. The results obtained was almost similar between the three caffeine loadings, 29.2 ± 6.58% (5% caffeine loading), 32.8 ± 4.36% (10% caffeine loading), and 38.4 ± 1.08% (15% caffeine loading) (Figure 3.17).
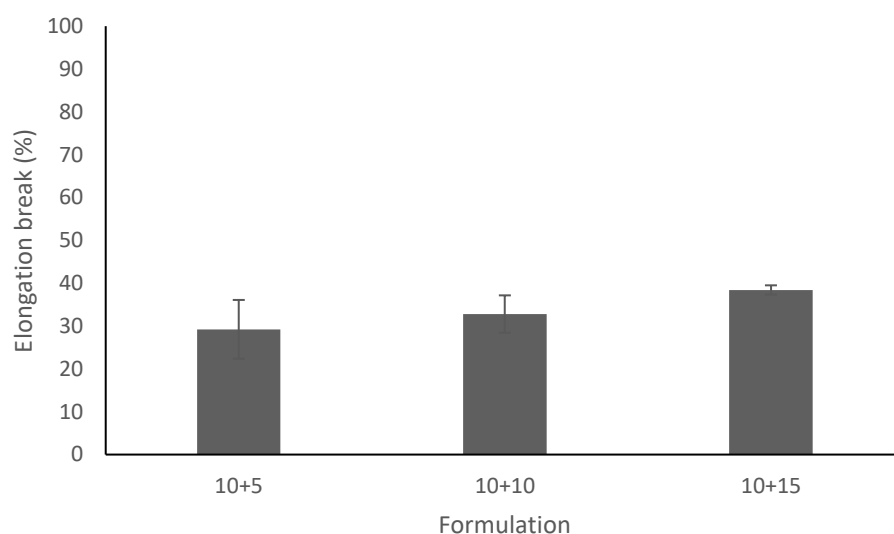
Figure 3-17 Average elongation at break (%) for PCL 10% nanofiber mat with 5 or 10 or 15% caffeine. Error bars n=3.

3.4.4 Evaluation of water contact angle for monolayer nanofiber formulations

The protocol details for measuring the water contact angle for the formulations are provided in Chapter 2, 2.1.7, and formulation details above in 3.5. Water contact angle was measured only for the formulations prepared with PCL polymer. Water contact angle could not be measured for

the formulations with PEO polymer, the polymer being hydrophilic the deionised water droplet was immediately absorbed by the polymer the moment it was placed on the surface of the mat. Caffeine particles with hydrophilicity property, the loading had an impact on the water contact angle of the formulations prepared with PCL polymer. The water contact angle reduced as the caffeine loading increased (Table 5, Figure 3.18). The plausible reason could be as the concentration of caffeine molecule increased, the permeation of water through the monolayer mat enhanced which influenced the water contact angle (Dias & Bártolo, 2013). The liquid drop is likely absorbed to the dried nanofiber surface, which essentially altered the surface nature by exposing more hydrophilic components, in this case the caffeine molecules. This transition is due to blending of hydrophilic drugs with hydrophobic carrier polymers, The reduction of contact angle was probably due to the continuous spreading on the fibre surface. Surface wetting behaviour depends on not only the surface texture (roughness and particle shape), and surface chemistry (heterogeneity) but also on hydrodynamic conditions in the preparation route.

Table 5 Average (n=3) water contact angle for PCL 10% monolayer nanofiber mat with 5 or 10 or 15 % caffeine.

Formulation	Average Water Contact Angle (°) $\pm$ SEM
PCL 10% + Caffeine 5%	106.1 $\pm$ 4.17
PCL 10% + Caffeine 10%	91.6 $\pm$ 4.14
PCL 10% + Caffeine 15%	86.4 $\pm$ 0.0
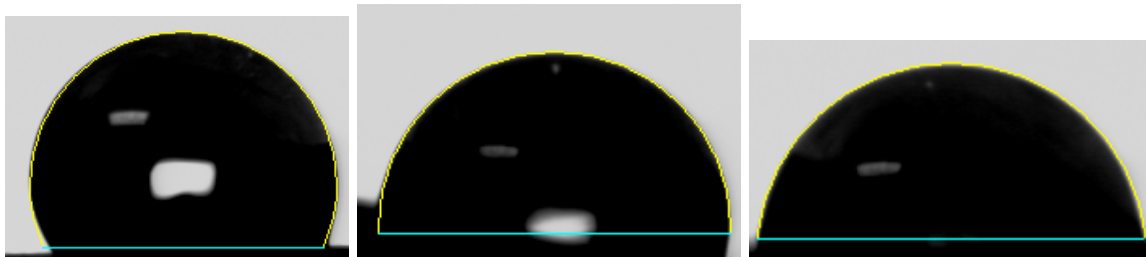
Figure 3-18 Image of water contact angle droplet for 10% PCL polymer with 5% (left), 10% (middle) and 15% (left) caffeine loading

3.4.5 Evaluation of surface morphology for monolayer nanofiber formulations

The surface morphology for nanofiber mat was evaluated using field emission scanning electron microscopy (FESEM). Details of protocol used are provided in Chapter 2, 2.1.8, and formulation details above in 3.5. Fibre diameter distribution was heterogenous within a formulation irrespective of the polymer PCL/PEO or caffeine loading 5, 10 or 15%. In general, the fibre diameter for the formulations with PEO polymer was smaller (55 to 167 nm) compared to formulations with PCL polymer (187 to 3819 nm) (Figure 3.19). Electrospun fibres often beads as "by products". The formation of beads has been observed for all most all the samples tested. Generally, beads are produced when the spinning solution has lower polymer concentration, high surface tension, low viscosity, and low electrical conductivity (Patel et al., 2012). Images of all the formulations are provided in the appendix.
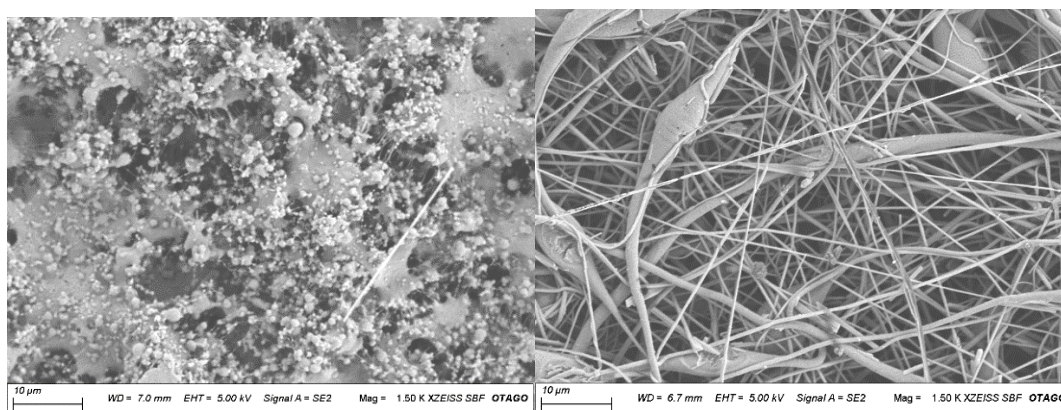
Figure 3-19 Image showing the smaller diameter for formulation with PEO polymer (left) and with heterogeneous diameter for PCL polymer (right).

Like fibre diameter the bead size of PEO polymer was smaller (83 to 820 nm) compared to PCL formulation (2527 to 8278 nm) (Figure 3.20). The narrow fibres of PEO polymer formulation coalesced together to form a mat as seen in Figure 26 which also shows the caffeine molecule crystals adhered onto the surface of the nanofiber. Jaeger et. al. (1996) and Jaeger et. al. (1998) reported beaded fibres spun from aqueous solution of PEO. He found that the bead diameter and spacing were related to the fibre diameter: the thinner the fibre, the shorter the distance between the beads and the smaller the diameter of the beads. We found similar observation with the formulations containing PEO polymer. The formation of the beaded nanofibers can be considered as the capillary breakup of electrospinning jets by surface tension, altered by the presence of electrical forces (Fong et al., 1999). More research needs to be carried out to explore whether there are variations from fibre to fibre within the same mat and from mat to mat. Based on that, a standard method should be maintained to measure the fibre diameters as well because it affects the measurement of mechanical properties to a great extent. In electrospinning, rapid solvent evaporation and phase separation occurs due to jet thinning, solvent vapour pressure plays a critical role in determining the evaporation rate and the drying time. Solvent volatility

also plays a significant role in the formulation of nanostructures as in influences the phase separation process. Images for all the formulations are provided in the appendix.
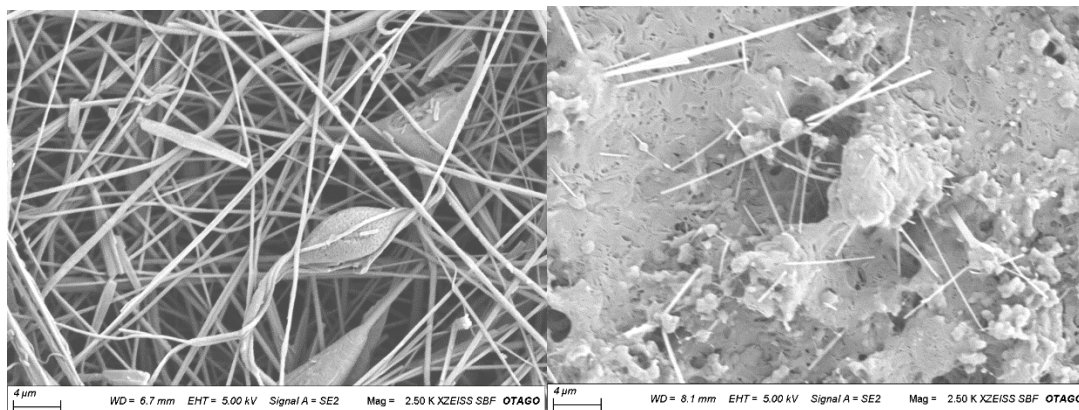
Figure 3-20 Image showing the heterogeneous bead size, PCL polymer (left) and PEO polymer (right). The image on the right showing caffeine crystals adhered onto the nanofiber.

CHAPTER 4   CONCLUSION

Ocular drug delivery has always been a challenge for ophthalmologists and drug-delivery researchers due to the complex anatomy of eye and its physiological barriers like precorneal loss and the presence of biological barriers. Ocular diseases can be treated by conventional ophthalmic dosage forms and currently >60% of the commercially available dosage forms are in the form of eye drops (Kuno & Fujii, 2011; Lang, 1995). Although topical administration is usually preferred to treat disorders of anterior segment, the static barrier layers lead to low ocular absorption and achieve poor availability of only 1-7% (Ghate & Edelhauser, 2006). Hence, there is a need for innovative drug delivery systems for the ocular route that prolong the contact time between the cornea and the drug and to have enhanced ocular tolerance (mitigate or eliminate evidence of irritation, reduce inflammatory reaction or corrosion). Nanotechnology has and continue to being investigated as an option to overcome the challenges with liquid eye drops. Nanotechnology is the engineering of functional system by design, characterization, production and application of structures, device and systems by controlled manipulation of size and shape at an atomic and molecular scale (Bawa, 2007). Drug delivery at nanoscale level can be achieved using the process, electrospinning, a cutting-edge process which combines electrospraying with spinning (Agarwal et al., 2008).

The scope and emphasis for this research project was to develop a solid insert using the electrospinning process with sustained drug delivery to treat cataract, anterior ocular anterior disease. Caffeine was used a model drug and was incorporated into three types of solid nanofiber formulations were prepared (details of the methodology provided in Chapter 2.1.3), mono-, two- and three-layered nanofiber formulations and evaluated for various properties. Nanofiber mat thickness, water contact angle, fibre morphology (SEM), tensile properties and in-vitro caffeine

release for mono- and three-layered nanofiber formulations. Only nanofiber thickness and in-vitro caffeine release was determined for two-layered nanofiber formulations. Mucoadhesion property was measured only for three-layered nanofiber formulation, only these formulations were prepared using the polymer PEO which is a useful tool since it exhibits the property of hydrophilicity.

The results obtained from this research shows that the thickness of the mat can be increased by having an additional layer. However, the thickness is not proportionate to the extra amount of polymer used to develop two- or three- layered. Plausible reasons could be, either due to the insulation effects caused by the first layer (Migliaresi et al., 2012), or effect of external environmental condition whilst performing the measurement (Flack, 2014), or electrospinning process variables like electrostatic forces related to applied voltage and fibre deposition (Lee et al., 2001). Measurement of representative thickness of the mat with uneven porosity and void spaces still remains a challenge which needs further research exploration (Rashid et al., 2021). It was challenging to measure the water contact angle for monolayer nanofiber formulations with PEO polymer. However, the water contact angle could be measured when PEO was formulated as one of the layer in three-layered nanofiber formulation. The results achieved for various formulations was on par with the property of the polymer, hydrophobic or hydrophilic exhibiting hydrophobicity (>80°) or hydrophilicity (<50°). Mucoadhesion evaluated for only three-layered nanofiber formulations containing PEO and PCL polymer shows that the force required to detach the mat from mucin tablet (used as a test material) was almost double compared to the controls, monolayer PEO/PCL and the probe. Surface morphology of the nanofiber mat shows a heterogeneous fibre diameter distribution irrespective of the polymer and the number of layers. Evidence of fibres was more apparent with PCL compared to PEO polymer. For PEO polymer, there was more elliptical beads on string whereas for PCL it was spindle shaped bead with fibre.

The caffeine drug was deposited as crystalline structures on the surface of fibres which is more prominent with PEO monolayer formulation (with caffeine) due to lack of fibre production with this polymer. Similarly, water contact angle tensile properties could not be measured for monolayer formulation with PEO polymer, the test mat started to split the moment the probe touched the surface of the mat. For PCL formulations there was no differences between the tensile properties either for mono- or three-layered mat and overlapping time. However, the tensile property for 10% PCL monolayer mats with 10% caffeine was less compared to 15% caffeine which is related to the thickness of the mat. The formulation of nanofiber is extremely complex and subject to numerous variables, while also assisting in the achievement of optimal drug release kinetic (Adepu et al., 2021). In-vitro caffeine release for monolayer, >50% of the caffeine from released from PEO formulation within 5 min from the initiation of the experiment but it took about 1h for PCL formulations. Irrespective of the polymer, the results shows that there is significant burst release, after 4h, >90% of caffeine released from PEO formulations but only 53-73% released for PCL formulations. Two layered formulations, presence or absence of second layer had an impact on the release %. At 1h after the initiation of the experiment, the % of caffeine released from the formulations with the presence of a second layer was almost half compared to the formulation with no second layer (used as a control). The same trend continued at 4h sampling too. It appears, that the presence of second layer act as a barrier for drug release due to thickness and longer diffusion path (Alhusein et. al., 2012). For three-layered nanofiber mat the testing surface had an impact on the caffeine release % initially but at 4h there was no difference either on the overlapping time or the surface (Figure 3.11). At 1h, the caffeine % released from the lower surface containing PEO polymer was less compared to the top surface containing PCL and caffeine. During the investigation of the caffeine release from three-layered mat we also tested a monolayer PCL with caffeine on both the surfaces, lower adjacent to the collector and the upper surface. The interesting observation was, there was almost 72% caffeine

released from the lower surface compared to only 50% from the upper surface. Probably the wetting behaviour (Liu, 2019) and the air trapped in the fibre (Yohe et al., 2012) has an influence on the drug release.

Based on the results we achieved within the scope of this research project we conclude that it is possible to reduce the burst release and achieve sustained release of the drug of anterior ocular drug delivery to treat cataract with further tweaking of the two layered formulation. We suggest preparing a three-layered formulation using electrospinning (first and third layer) and electrospraying (second layer), using PEO polymer for first layer, swellable nanocarriers with the drug for second layer and a hydrophobic layer (5+1% PCL) for third layer. Using a swellable nanocarrier with the drug would take time to hydrate and swell when in contact with liquid which would mitigate the burst release and enhance the sustain release.

CHAPTER 5   GENERAL DISCUSSION, CONCLUSION, FUTURE DIRECTION

5.1 General Discussion

The eye is a sensory organ that converts light to an electric signal that is treated and interpreted by the brain. The eye possesses efficient protective mechanisms like reflex blinking, lachrymation, and drainage, while lid closure protects the eye from external aggression. All the protective mechanisms are responsible for the rapid and extensive precorneal loss of topically applied ophthalmic drugs due to ocular residence time limited to a few minutes and other barriers, anatomical and physiological (Mofidfar et al., 2021). Anterior ocular diseases treatment is mostly prescribed with conventional ophthalmic dosage forms such as eye drops and currently >90% of the commercially available medication is in the form of eye drops (Neervannan, 2021).

Researchers world-wide are carrying out extensive research to develop innovative drug delivery systems for ocular route that prolong the contact time between the cornea and the drug, enhance the pharmacokinetics characteristics of the drug. For past few decades nanotechnology has been identified as an innovative technology that helps to break through the eye barriers to drug delivery. Nanotechnology based systems with an appropriate particle size <10 μm can be designed to ensure low irritation, adequate bioavailability and ocular tissue compatibility (Mitra, 2013). To achieve this electrospinning process is a cutting-edge technique which shows numerous merits over conventional polymer processing methods. The objective of this research project was to develop a formulation using electrospinning technique to achieve sustained drug release over time. Caffeine was used as model drug. Nanofiber mats either single, two or three-layered laminate was produced and tested for various properties. The properties tested were,

nanofiber mat thickness, water contact angle, mucoadhesion, surface morphology using SEM, tensile analysis, and in-vitro release. The results achieved are given below.

5.1.1 Nanofiber mat thickness

A micrometre (0 to 25 mm) with graduated screw mechanism was used to measure the nanofiber mat thickness. The average thickness for monolayer 10% PEO and 10% PCL with range of caffeine concentration (5, 10 and 15%) was around 25 and 126 µm respectively. Caffeine concentration did not have much of impact on the thickness for 10% PEO polymer whereas there was some noise in the data for 10% PCL polymer. The thickness of formulation with 10% caffeine was 70.8 ± 7.86 µm compared to the formulation with 15% caffeine, 105.1 ± 8.50 µm. Two-layer nanofiber mat (details of preparation and formulation are provided in the method section) the mat thickness increased by 50% as the percentage of the PCL polymer concentration increased in the second layer. The first layer containing 5% caffeine drug in addition to the polymer (5% PCL), the thickness of the mat increased from 169 ± 25.3 µm to 231 ± 6.8 µm when the concentration of the polymer in the second layer increased from 5 to 10%. The formulation containing 10 % caffeine in addition to the 5% PCL in the first layer the mat thickness decreased when the concentration of PCL polymer in the second layer increased from 5 to 10%, 207 ± 10.8 to 182 ± 24.7 µm, respectively. Whereas for the formulations with 10% PCL along with caffeine drug in the first layer the mat thickness increased as the concentration of the PCL polymer in the second layer increased from 5 to 10%, 273 ± 1.0 µm to 348 ± 8.4 µm and 242 ± 7.2 µm to 333 ± 2.9 µm, respectively. Three-layered nanofiber mat, the mat thickness increased for the laminates compared to the control formulation, a monolayer. When the layers were overlapped for longer duration 30 min the thickness was increased by 60% compared to 10 min overlapping

duration, The mat thickness for formulation with 10 min overlapping time between the layers was $120.6 \pm 6.3\ \mu m$ compared to $193.9 \pm 7.6\ \mu m$ for 30 min overlapping time between the layers. For control formulation with a monolayer the thickness was $102.2 \pm 9.2\ \mu m$ the thickness of monolayer mat was thinner than either two- or three-layered mat. The type of polymer used had an implication on the thickness of the mat, mat was thicker when PCL polymer was used compared to PEO polymer. However, the thickness did not correlate to the amount of polymer added for second and third layer (Flack, 2014; Ryu et al., 2020). Good Practice Guide No. 40 by David Flack, 2014, states that many things/factors can undermine a measurement made with a micrometer as no measurement is made under perfect conditions and there might be various factors attributing to variations, like the measuring instrument, sample measured, and measuring process and temperature effects. It is plausible that similar scenario has occurred whilst performing the measurement in our laboratory, though the laboratory was in controlled environment it was always a challenge to maintain a constant temperature of 20°C. Caffeine concentration did not have an impact on the thickness for the formulation with PEO polymer but did so when PCL polymer was used. Though the formulation were prepared under controlled conditions yet there was some noise in the data for formulation with 10% PCL polymer which indicates that there are conditions which impact the production of nanofiber mat during the process. Ryu et al., 2020 carried out research study using PCL polymer where they developed a uniform-thickness electrospun nanofiber mat production system with a movable collector based on real-time thickness measurement and thickness feedback control, micrometer measurement are never carried out in real time. They study found that light transmittance and production method influenced the mat thickness. The thickness of the nanofiber mat monotonically decreased with an increase in the light transmittance of the nanofiber mat. The variations in the light transmittance was noticeable along the horizontal axis compared to it being insignificant

along the vertical axis. Along the horizontal axis, the nanofiber mat was deposited randomly, and thus they observed a large variation in the mat thickness. Similar to their study all our nanofiber fabrication was carried out in horizontal axis wherein the fibers randomly deposited on the rotating drum, though our study we did not measure the thickness in real time we presume that those factors, light transmittance and production method has attributed to non-homogenous thickness of the mat. The study carried out by Ryu et al. characterised the fibers only upto 32 min after production but all our production was for a minimum of 1h. The resarchers achieved a uniform thickness by moving the production system, this was feasible as the measurements were carried out in real-time.

5.1.2 Water contact angle

Monolayer nanofiber mat, water contact angle could not be measured for the formulation with PEO polymer. The deionised water droplet was immediately absorbed by the polymer the moment it was placed on the mat. Water contact angle was only measured for the formulation containing PCL polymer. The contact angle reduced as the caffeine concentration increased from 5 to 15 % with PCL concentration remaining constant for all the formulation, 10%. The water contact was 106. 1 $\pm$ 4.17°, 91.6 $\pm$ 4.1°, and 86.4 $\pm$ 0.0° for formulations with 5, 10 and 15% caffeine concentration in addition to 10% PCL polymer. Water contact angle was not measured for two-layered nanofiber mat. For three-layered nanofiber mat formulation, water contact was measured both on the 1st layer (the layer adhered next to the collector) and the 3rd layer (the upper most layer). The 1st layer (lower surface) was always spun using PEO polymer whereas the 3rd layer (upper layer) spun using PCL and caffeine. The contact angle of the first layer was low compared to the 3rd layer reflecting the property of the polymer, PEO being hydrophilic and PCL hydrophobic. This result is similar to the research study carried out by Figueroa-Lopez et al.,

2018, barrier properties of gelatin coated by electrospun polycaprolactone ultrathin fibers containing black pepper oleoresin. The study concluded that the contact angle was 50° for a gel film prepared with gelatin which is characteristic of hydrophilic material similar to the results we obtained with PEO polymer. The water contact angle of the 1st layer wherein the layers were overlapped for 10 min it was 43.0 ± 3.7° compared to 25.4 ± 4.4° where the overlapping time was 30 min. The researchers also found that the wettability of multilayers is reduced compared to only gelatin or PCL. It is assumed that surface topology might have contributed to this, it is plausible that surface topology attributed to the difference in the water contact angle of the 1st layer with PEO with 10 and 30 min overlapping time, 25.4° versus 43°. The 1st layer was fabricated using a hydrophilic polymer PEO, and the 2nd layer using hydrophobic polymer, PCL. Layer overlapping time did not have much impact on the contact angle for the 3rd layer, 106.2 ± 3.4° for 10 min overlapping compared to 111 ± 3.6° for 30 min overlapping time. Water contact angle for the monolayer nanofiber mat containing 10% PCL with 10% caffeine there was not much variation between the bottom layer (layer adhered next to the collector) or top layer, 112 ± 2.8° (bottom layer) and 106.4 ± 4.2° (top layer). This is the first time this type of measurement is carried out. The rationale behind doing so, was to evaluate if surface morphology in the top and bottom surface attributed to any variations in the water contact angle for nanofiber mat fabricated using hydrophobic polymer PCL and we conclude that the water contact angle is similar on both the surfaces.

Water contact angle could not be measured for formulations with PEO polymer formulated as monolayer, as the water spread and quickly absorbed into the mat the moment it was in contact with the surface of the mat. A study carried out by Kupka and his co-workers in 2020 with single and well blended PCL and PEO electrospun nanofibers for enhancing the functional properties

by plasma processing, tried to measure the hydrolytic stability of PEO nanofibrous mat in water but could not do so, as the PEO polymer easily dissolved in water due to hydrophilic property, we found similar results when we tried to measure the water contact angle of nanofiber mat fabricated only with PEO polymer wherein the water droplet immediately dissipated when it came into contact with the mat surface. There was no surprises with the results, the hydrophilic polymer PEO (in the three-layered nanofiber mat) having lower contact angle compared to the hydrophobic polymer PCL (in monolayer, two- or three-layered mat) having higher contact angle exhibiting the property, hydrophilicity and hydrophobicity which was on par with the results achieved by Baek et al., 2012, where they measured the hydrophilicity of RO membranes contact angle using sessile drop technique similar the technique used in this study. They concluded that the reduction in contact angle can be attributed to the liquid drop likely to absorbed to the dried membrane surface exposing more hydrophilic components and reducing the contact angle eventually by continuous spreading of the water droplet on the membrane.

5.1.3 Mucoadhesion

Mucoadhesion was measured only for three-layered nanofiber mat formulations. The average force required for detachment of three-layered nanofiber formulation containing PEO and PCL polymer with caffeine from mucin tablet was almost double when compared to monolayer PEO or PCL formulation and the TA-55 probe. The force for detaching the bottom layer (layer next to the collector) with 10 min overlapping time was 50.7 ± 13.2 (F_{max}) compared to 60.0 ± 10.1 (F_{max}) for top layer. For 30 min layer overlapping formulation it was 66.7 ± 5.5 (F_{max}) for bottom layer and 63.5 ± 3.2 (F_{max}) for top layer. Control formulation and probe the mucoadhesion force

of detachment were 26.5 ± 2.9, 25.3 ± 7.4 and 30.2 ± 3.8 (F_{max}) for 10% PCL, 10% PEO and TA-55 probe, respectively.

Three-layered nanofiber formulation with PEO and PCL exhibits mechanical integrity and adhesion compared to only either having PEO or PCL polymer. The amount of force required to detach the formulation from the mucin tablet was almost double for three-layered formulation containing the polymer compared to controls containing only one polymer. The results obtained in this project were different to that achieved by Hajer et al., 2016, where they tested the ex-vivo bioadhesion for β-glucan and hydropropyl methycellulose (HPMC) as a laminate film formulated individually or in mixture. The researchers found the mixture films, containing β-glucan and HPMC polymers, inclusion of HPMC (a hydrophilic polymer) had no significant effect on the bioadhesive forces on β-glucan side, β-glucan requires hot water to form a solution and swell. However, the researchers found that HPMC (6%) and laminate films (HPMC side) the bioadhesive forces observed were two to three-fold higher. It appears that the type of polymer used to prepare laminate films have influence on the bioadhesive forces. β-glucan requires hot water for swelling which is not feasible on cornea surface unlike PCL polymer which can swell under lower temperature.

5.1.4 Nanofiber morphology

The nanofiber surface morphology and fibre diameter of the formulations (monolayer and three-layered mats) were evaluated using field emission scanning electron microscopy (FESEM). Irrespective of the polymer concentration, number of layers or caffeine concentration, the SEM images shows evidence of the heterogeneous fibre diameter distribution within a formulation (Figure 5.1). It has been reported that using DCM as the solvent produce microstructures that

93

mainly consists of micro-beads (Nguyen-Vu, Tran, & Huynh 2017), two structures supplied by two needles were able to mix together and form a joint mat by using a mobile collector (Kidoakill, Kwon, & Matsuda, 2005). The morphology of the mat achieved in this object confirms the published rationale given above. Monolayer mat the fibres were of smaller diameter with PEO polymer compared to PCL polymer. The fibre diameter distribution was within a shorter range for PEO polymer (55 to 167 nm) compared to PCL polymer (187 to 3819 nm). Extended detail surface morphology images for mono- and three-layered formulations are provided in the appendix.
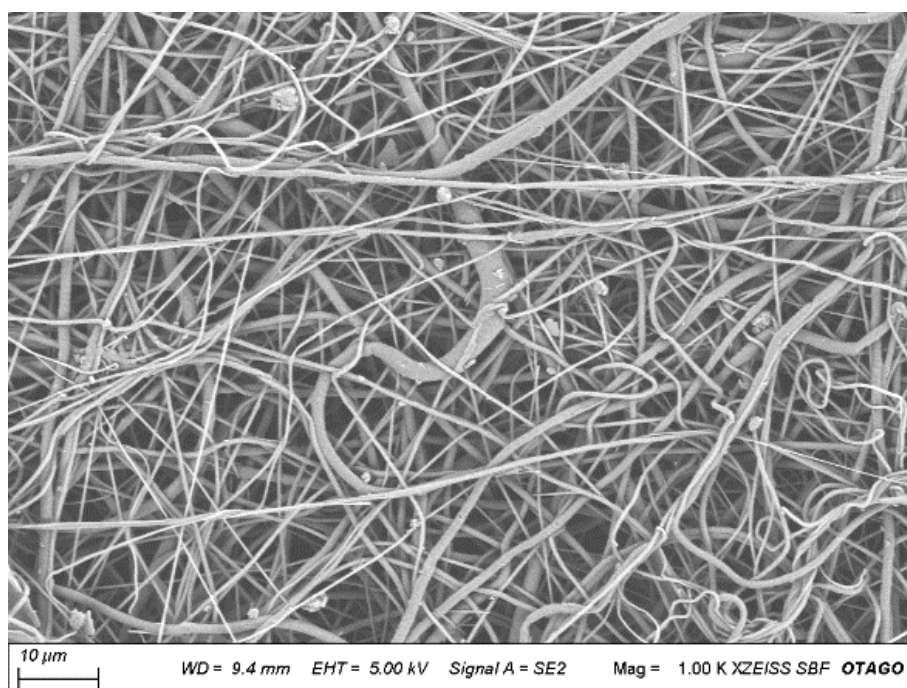
Figure 5-1 SEM image showing heterogeneous distribution of fibre diameter for the formulation 10% PCL polymer with 5% Caffeine.

Three-layered nanofiber mat the range of fibre diameter was 78 to 384 nm for bottom layer (layer next to the collector) and 333 to 2452 nm for top layer. For PEO polymer there was more

evidence of beads than fibre (Figure 5.2). The concentration and molecular weight of the aqueous PEO solution has shown to influence the fiber diameter and structural morphology of electrospun nanofibers (Jacobs et al., 2010). The researchers reported that fibers from 5% aqueous solution of PEO (molecular weight 300K) indicates fibers with almost spherical beads which is similar to what we noticed using 10% aqueous solution of PEO (molecular weight 200K). The published data also elucidate that nanofiber with aqueous PEO solution with a molecular weight of 900K produced spindle-like beads. Viscosity, chain entanglement and stretching of the polymer has influenced the structure and morphology of the beads whilst spinning aqueous PEO solution.
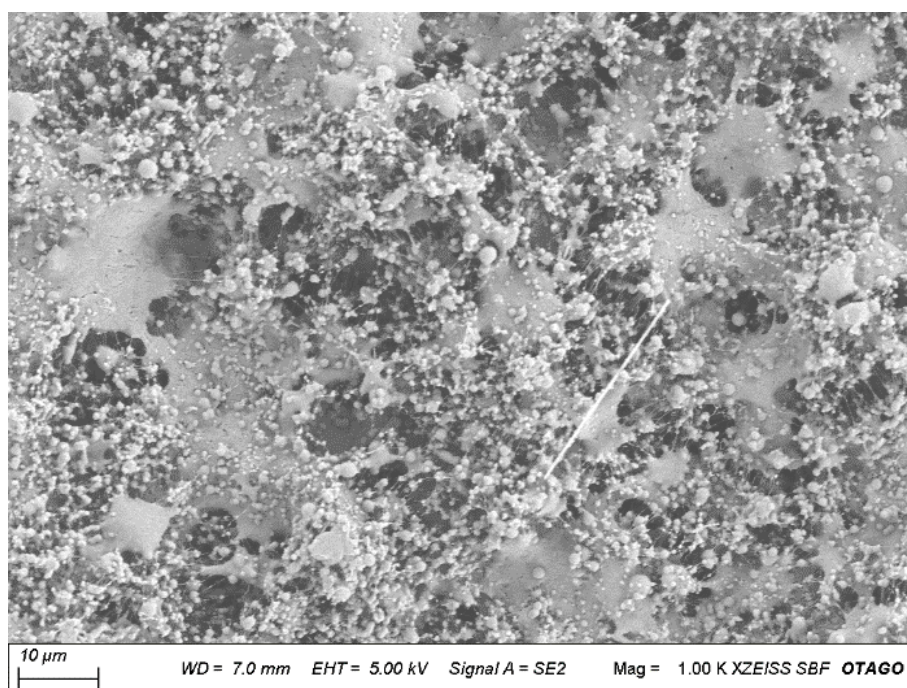
Figure 5-2 SEM image of 10% PEO polymer with 5% caffeine exhibiting more beads than fibre.

Like fibre diameter for monolayer distribution the bead size in the PEO polymer (83 to 820 nm) formulation was smaller compared to PCL formulation (2527 to 8278 nm). The beads were of elliptical shaped in PEO formulation compared to spindle shaped in PCL formulation. SEM

95

images depicts the shape of the caffeine drug as crystals which is more evident with PEO polymer due to lack of fibre production, the number of the crystalline structures increased as the caffeine concentration increased (Figure 5.3).
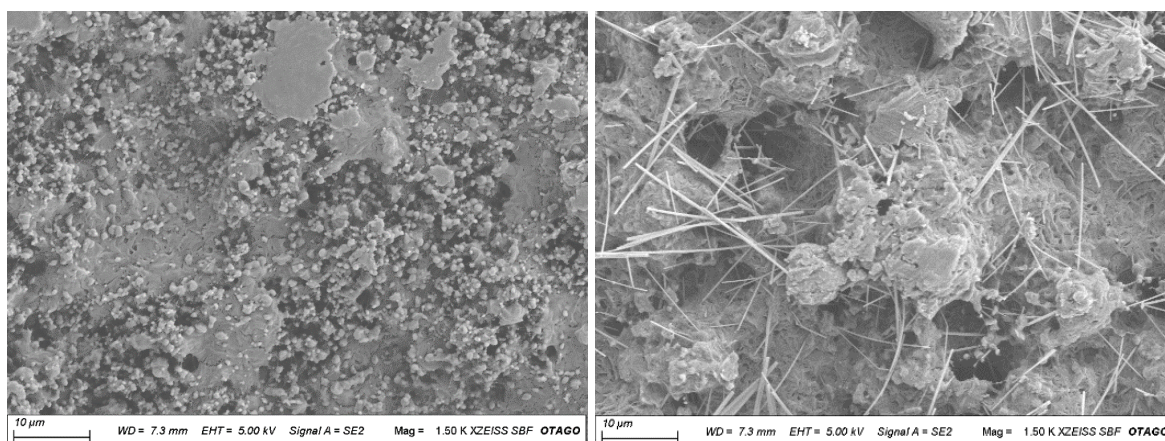
Figure 5-3 SEM image with and without crystalline structure of caffeine, on the left is the control formulation 10% PEO with no caffeine and on the right is 10% PEO with 15% caffeine concentration.

5.1.5 Tensile properties

The mechanical properties, puncture strength (g/mm^2) and elongation at break (%) was measured using a TA.XT plus Texture Analyser. The tensile properties were measured only for monolayer and three-layered formulations. Monolayer nanofiber formulation the mechanical properties was measured only for formulation containing PCL polymer. It was a challenge to measure the properties for the formulation containing PEO polymer, the moment the probe was in contact with the surface of the nanofiber mat the mat started splitting even before the initiation of downward movement of the probe. The puncture strength was almost similar for 10% PCL

formulation with either 5 (0.565 ± 0.29 g/mm^2) or 15% (0.601 ± 0.16 g/mm^2) caffeine but was lot less for the formulation with 10% (0.288 ± 0.06 g/mm^2) caffeine which probably is related to the thickness of the mat which was less compared to the other two formulations. However, there was not much variation between the three 10 % PCL formulations for elongation at break (%) irrespective of the caffeine concentration, 29.2 ± 6.58, 32.8 ± 4.36 and 38.4 ± 1.08 %, respectively. Three-layered nanofiber mat, layer overlapping time (10 or 30 min) did not have any influence on the puncture strength, 0.8 ± 0.1 (g/mm^2) for 10 min overlapping and 0.80 ± 0.01 (g/mm^2). Whereas the puncture strength for monolayer control formulation 10% PCL with 10% caffeine it was lower, 0.54 ± 0.03 (g/mm^2). Elongation at break (%) was almost similar for all the three formulations including the control, 41.1 ± 2.6 % (three-layered, 10 min overlapping), 45.6 ± 1.0 % (three-layered, 30 min overlapping), and 44.3 ± 0.8 % (control, monolayer).

Tensile analysis was a challenge to measure for monolayer formulation with PEO polymer. The moment the probe touched the surface of the PEO mat it started to split which indicated it is very fragile and lacks any plasticity. At high viscosities (>20P), the instability of flow due to high cohesiveness of the solution led to the formation of poor quality fiber. Electrospun fibers are commonly collected as nonwoven mat, therefore, measurement of the mechanical properties of single electrospun fiber is a great challenge. Testing of an electrospun mat is easier compared to that of individual fibers, however, data interpretation is more difficult due to the variation in the structure and morphology of the fibers in the mat. Factors, like polymer chemistry, fiber diameters, processing conditions, and environmental parameters influence the overall mechanical properties of the nanofiber. Rashid et al., 2021 reported that higher concentration (>40%) of polymer gives uniform fibers, decreasing the number of beads and improving the mechanical properties. A high-concentration polymer solution with higher viscosity possesses

higher molecular entanglement, requiring larger force to initiate Taylor cone formation. In our research we had limited flexibility either to increase the polymer concentration or higher voltage. The puncture strength was almost similar to for monolayer formulation with 10% PCL polymer either with 5 or 10% caffeine but was less for 10% caffeine which is related to the thickness of the mat which was thinner compared to the other two formulation 70μm compared to 126 and 105μm. This formulation needs further exploration to determine the plausible reasons for producing thinner mat, whether it is the solution parameter, processing parameter or environmental conditions. There was no difference for elongation at break, appears that the thickness did not have an implication for that property and all the formulations were relatively equally flexible. Elongation is deformation occurring to the mat after applying stress resulting in a change of shape and/or length of the film. For three-layered mat overlapping time did not have any impact on the tensile properties, puncture strength and elongation at break, it was almost similar for all the formulations similar to the results published by Hajer et al., 2016, wherein they found that laminate films required higher force to break and elongate compared to films prepared only with either β-glucan or HPMC.

5.1.6 In-vitro caffeine release

All the in-vitro release experiments were conducted using de-ionised water as a release medium, either filled in glass universals (Minitron equipment) or glass chamber (Ussing chamber equipment). Monolayer nanofiber mat formulation were tested using Minitron and two- and three-layered nanofiber formulation using Ussing chamber. The caffeine concentration in the collected release medium were determined measuring the UV absorbance at determined wavelength for over 24 h but only results up to 4 h are presented. The caffeine release

concentration (converted to percentage) determined using a validated caffeine calibrated standard curve with a correlation (R^2) 0.9996, 0.9999, and 0.9995 for monolayer, two- and three-layered nanofiber mat, respectively.

Monolayer nanofiber formulations, >50% of the caffeine was released within 5 min for the formulations with PEO polymer whereas for formulations with PCL polymer it was 1h. There is no data point for 10% PEO polymer with 5 % caffeine due to noise in the results. At 4h there was >90% of caffeine release from the sample containing PEO polymer irrespective of caffeine concentration but only there was 73%, 68% and 53% for PCL polymer with 5, 10 and 15% caffeine concentration. There is no surprise with the results achieved, as there was evidence of caffeine crystals on the surface of PEO nanofibers whilst assessing the surface morphology (SEM) of the sample (Figure 3-20). It is plausible that PEO being a hydrophilic polymer and presence of caffeine crystals on the surface of the fiber has attributed to the rapid release within 5 min and >90% release 4h after the initiation of experiment. This outcome though not fulfilling the objective of the project, sustain release of drug molecule, however, it has opened a pathway for "green" fabrication and delivery of the drug. Currently the drug being used by patients are in the form of eye drops with reduced bioavailability due to static and dynamic barriers in the cornea. Fabricating PEO with only water and without any preservative added probably can overcome the challenges, but, since the polymer is highly hygroscopic there is a need to have a delivery mechanism to alleviate the property of hygroscopicity.

Two-layered nanofiber formulations presence or absence of the second layer had an impact on the amount of caffeine release. Formulation having 5% caffeine with 5% PCL (49.8 ± 1.4% (5% PCL with 5% caffeine) in the first layer had slightly higher caffeine release than the formulations with 10% PCL (40.7 ± 3.7% (10% PCL with 5% caffeine) with no second layer, 1h after initiation

of the experiment. Similar results were achieved with 10% caffeine without the second layer, 52.1 ± 3.6% (5% PCL with 10% caffeine) and 44.54 ± 4.2% (10% PCL with 10% caffeine). The caffeine release results achieved for the formulations containing the second layer exhibited the property as a barrier layer as the caffeine released was almost 50% less than those formulations without the second layer. The concentration of PCL in the second layer did have an impact on the amount of caffeine release. These results are similar to the that published by Cortez Tornello et al., 2017, the release of embelin in multi-layered mesh using PCL polymer. The researchers conclude in published research article that the embelin release was related to the thickness and the number of additional PCL layers. They found that the entry of buffer medium, which is delayed by the presence of additional PCL hydrophobic layers, and the embelin diffusion toward the release medium, which is also slowed consequently. They found that the release was reduced by 67.3% with additional PCL layers compared to control, 88.9%. At 1h after the experiment initiation, the release % was 29.3 ± 16.5% (5% PCL with 5% caffeine and 5% PCL), 16.8 ± 2.2% (5% PCL with 5% caffeine and 10% PCL), 32.8 ± 3.0% (5% PCL with 10% caffeine and 5% PCL), 21.6 ± 2.7% (5%PCL with 10% caffeine and 10% PCL), 10.1 ± 2.5% (10% PCL with 5% caffeine and 5% PCL), 5.3 ± 3.3% (10%PCL with 5% caffeine and 10% PCL), 16.3 ± 4.9% (10% PCL with 10% caffeine and 5% PCL) and 9.7 ± 3.4% (10% PCL with 10% caffeine and 10% PCL). Almost the same result trend was noticed at 4h with the second layer providing as a barrier for caffeine release. The results indicate that it is possible to modulate the release of the drug by either increasing the thickness or having an additional only PCL layer as a barrier. As observed with monolayer formulations with PCL polymer, there only around 50% caffeine release from all the formulations without the second layer, around 20 – 30% with the second layer, similar results were by Liu (2019) when a second layer containing micro-beads and thinner fibres was added on top of the first 10% PCL layer it successfully reduced the release rate. Yohe et. al. (2012) found that superhydrophobic nanofiber fabricated with PCL and poly (glycerol monostereate-

co- ε-caprolactone) with model bioactive (SN-38) showed a release rate with a striking dependence on the apparent contact angle that can is explained by displacement of air within the electrospun meshes.

Three-layered nanofiber mat formulations only one-side was exposed to the glass chamber to assess whether the surface layer has an impact on release of caffeine. To achieve this the side that is not for evaluation was stuck onto a high duty aluminium foil and only the side to be evaluated was exposed to the release to the release medium in the glass chamber. The lower surface (next to the collector) or the first layer contained PEO polymer except the control which was a monolayer with PCL polymer. Formulations with 10 min overlapping time there was a difference in the release % after 1h from the lower (10% PEO, 5% and 1% PCL, 10% PCL with 10% caffeine, lower) compared to the upper layer (10.5 and 1.10,10, upper) which contained caffeine, $62.8 \pm 9.0\%$ compared to $80.0 \pm 15.5\%$. Whereas the release was almost similar for formulations with 30 min overlapping time, $72.7 \pm 25.3\%$ (10.5 and 1.10, 30, lower) and $72.7 \pm 17.3\%$ (10.5 and 1.10, 30, upper). After 4h, the % of caffeine released was almost similar for all the formulations >71%, the layer surface did not have any impact on the amount of caffeine release. The rationale behind this formulation is to see if the middle layer containing 5 + 1% PCL is acting as a barrier for release of the caffeine when the top layer was stuck to the foil and release assessed from the first PEO layer. The results shows that though there was some reduction in the release % for 10 min overlapping sample when the first layer was exposed to the aqueous solution but at 4h there was not much differences between the release %, either the testing side of the overlapping time influenced the release %. Usually the researchers test the release kinetics using the nanofiber mat sample loaded with drug either using Minitron or Ussing chamber where in both the surfaces are exposed to the aqueous solution, but for the three-layered formulation we tested only one side at a time. These results are similar to that published by Immich et al., 2017,

they found when poly L-lactic acid polymer (PLLA) with caffeine was tested for release kinetics, using a thicker PLLA membrane (0.1192 to 0.1655 mm) increased the restriction of caffeine release until equilibrium is reached. The extra thickness layer first limits the core hydration process, restraining drug dissolution and diffusion. Probably with 10 min overlapping there is more clear demarcation of the second layer PCL fibers which probably is creating a barrier initially similar to results achieved by Immich et al. compared to 30 min overlapping samples wherein the PEO and PCL fibers are entangled. Membrane thickness appears to be an important factor, acting as a barrier and restraining drug dissolution and diffusion but patient's compliance and safety should be give due consideration. However, we found an interesting observation which needs further exploration for monolayer PCL control nanofiber formulation. The amount of caffeine release was only $42.7 \pm 2.4\%$ from the upper surface compared to $76.4 \pm 3.1\%$ from the lower surface (next to the collector) at 1h after the initiation of the experiment. After 4h there was about 72% caffeine released from lower surface compared to 50% from the upper surface. This observation was not noticed and feasible when using Minitron or Ussing chamber where both the surfaces were exposed to the release medium.

Li et. al. (2013) published the results achieved from their research which showed that PVA/caffeine and PVA/riboflavin nanofibrous mats had almost the same dissolution time (about 1.5 s) and wetting time (about 4.5 s) but the drug released in a burst manner, 100% nanofiber containing caffeine and 40% with riboflavin within 60 s. Published results show that there was >60% caffeine released within the first 30 seconds when poly vinyl alcohol (PVA) was used as a polymer. This results are similar to what we obtained with PEO polymer but we assessed the caffeine release 5 min after the initiation of the experiment, but, however, the observation was quick dissipation of the samples with PEO polymer when it came in contact with the aqueous solution. We noticed that there is an immediate burst release and almost 50% of the caffeine is

released in almost all the formulations with PCL polymer within 1h for monolayer formulation, similar to the results achieved by Li et al. as stated earlier using PVA/caffeine and PVP/riboflavin. For monolayer formulations with PEO polymer that was achieved at around 5min from the initiation of the experiment, >50% caffeine released. Two layered nanofiber formulation the second layer acted as a barrier for the caffeine release, it was almost 50% less after 1h compared to those formulation with no second layer polymer, and similar trend was noticed at 4h too. Three-layered nanofiber formulation overlapping time and the surface tested had an impact on the amount of caffeine release after 1h. This results is similar to the published results of Cortez Tornello et al., 2017 and Ng et al., 2015 using embelin and timolol, respectively. Cortez Tornello et al., found that the embelin drug release can reduced upto 63% by having a non-drug multilayer, similarly Ng et al., found that that timolol drug in an "sandwich" structure notably reduced the burst release approximately ten times compared to monolithic structure. The formulation wherein the layers were overlapped for 10 min the caffeine release (%) after 1h was lower from the lower surface compared to the upper surface, whereas no such differences were noticed for formulation layers overlapped for 30 min. However, after 4h the release % was almost similar in all the formulations, neither the overlapping time or surface had any impact on the caffeine release. One interesting observation was the results which was achieved from the control formulation wherein the release was tested from the both the surface, lower and upper surface. Noticed that the lower surface (next to collector) had higher release % compared to the upper surface even after 4h. The interesting observation is after 4h, the amount of caffeine released from lower surface was 72% compared to 50% from the upper surface. This result was not observed when both the surfaces were exposed to the release medium.

A strategy to avoid the drawbacks of an individual technology is to combine the advantages of different technologies. Combination of technologies such as iontophoresis, microneedle delivery, and other nanosystems like magnetic nanocarriers and carbon nanotubes, hold a great potential in improving bioavailability of drugs/formulations.

5.2   Some of challenges with the research project

The following are some of challenges I encountered initially at the start of the research project. To overcome these challenges a few trial runs were carried out to optimise the protocol for our laboratory conditions. Once it was optimised, we had very minimal challenges for the rest of the project experiment journey.

1. If the small custom-made electrospinning chamber (using the fish tank) is placed in the fume hood which is located in a separate extension from the temperature-controlled laboratory, it is a challenge to get consistent fibre production during the process. More so, if the process is carried out in the morning around 7 am when the humidity is >75% and temperature <10C.

2. If the collector is not properly negatively charged there is every chance of secondary fibre formation which are deflected towards the base of the electrospinning chamber.

3. If the electrospinning duration for a single formulation is >1h, the humidity in the chamber increases over time which leads to aggregate build at the needle tip and lack of jet initiation.

4. Aluminium foil wrapped on the collector, ensure that the non-stick side of the foil faces the needle. This helps in peeling off the mat from the foil easily at the end of the process.

5. If the custom-made electrospinning chamber is placed on a glass base there is every possibility for the chamber to move due to soft surface of the glass and the friction caused during the process. To mitigate this, place the chamber on a wooden base to avoid it moving. If it moves, it leads to change in the needle tip to collector distance which ultimately leads to disturbance in the production of nanofibers and distorting the needle.

6. Similarly place the syringe pump on a small stack of tissue paper to avoid it moving from its original location placed at the start of the electrospinning process.

7. Lack of jet whipping results due to increase in relative humidity (>60%) in the electrospinning chamber which led to concentration of nanofibers in the central region of the collector which results in forming a small mound.

8. When using two polymer solution a hydrophobic (PCL) and a hydrophilic polymer (PEO) and filled in two syringes with different diameter, 13 mm, and 4.7 mm, it failed to eject the solvent from the syringe. Plausible reason could be the differences in the diameter of the syringes attributed to lack of solvent ejection from the needle.

9. Co-spinning two polymer solution simultaneously from the single positive electrode, where in the electrode is connected to one needle but both the needles are connected using a clip was not successful in producing continuous stream of fibres, more so when the polymer solution is a hydrophobic and hydrophilic. Plausible reason could be the voltage in not enough (25Kv) to sustain the continuous production of nanofibers.

10. Build-up of laminate nanofiber mat with two different polymer property, hydrophobic and hydrophilic when individually stacked one layer on the top of other led to delamination post electrospinning process. This issue was resolved when the polymer solution was co-spun for some time before disconnecting the previous polymer solution and continuing with the current polymer solution.

11. Ussing chamber, first turn "on" the airflow before adding the liquid to the columns.

12. Ussing chamber, at the end of the experiment, drain out the liquid from the columns and then turn "off" the air flow.

13. Electrospinning hydrophilic polymer from a aqueous solution for long time (around 4h) on a dry day when the relative humidity is <20% lead to formation of cracks in the dried nanofiber mat on the collector whilst the process is still in progress.

14. Ocular irritation HET-CAM assay was attempted but we had issue with the fertilisation of the eggs.

5.3   Conclusions

The scope of this research project was to develop a sustained release nanofiber formulation using the electrospinning technique to treat cataract (anterior ocular disease) using caffeine as a model drug. Two types of polymers (PEO and PCL), solvents (Methanol, DCM) and water were used as the research progressed. The formulations were characterised for various physical, surface morphology and in-vitro release properties.

The physical property, water contact angle results achieved was as expected, however there was some variations with the nanofiber mat thickness. The thickness did not relate to the number of layers build up in the formulation which was observed by other researchers too as explained in Chapter 4 and 5. Surface morphology of the nanofiber mat for the different formulations achieved was also in align with the results observed by other researchers working in the similar research area. Mucoadhesion test, we noticed that the force required for detachment of a surface (top or bottom surface) from the mucin table for a three-layered nanofiber formulations was almost double than that of the control or probe used for testing.

The drug released from the monolayer was almost immediate for the formulations with PEO compared to PCL polymer. This observation is not surprising due to the hydrophilic property of the PEO polymer, however future researchers can give some more thought to this formulation. This formulation was produced using "green" electrospinning process where only water was used to dissolve the polymer which would avoid all the ill-effects noticed with the current conventional eye drops. However, the challenge could be to find a suitable device for delivery of this formulation onto the ocular surface.

In a two-layered nanofiber formulation when the drug was incorporated in the first layer and the second layer acted as a barrier the drug release was reduced by 50% compared to the control monolayer formulation. Appears that the second layer acts as a barrier for the drug release due to thickness and longer path for the diffusion of water. There was not much an impact on the drug release from a three-layered nanofiber formulation when drug was incorporated in the third layer or the upper most layer. In this situation the thickness or testing surface did not have any influence on drug release, 60 – 80% drug released within 1h. We presume that since the drug molecules were exposed directly to aqueous solution the drug molecules are immediately dispersed into water. The middle barrier layer without the drug did not provide any protection for the drug release when the lower surface was exposed to the aqueous medium. The drug release characteristics noticed in the laminate formulation, two- or three-layered it appears that the drug molecules need a barrier layer to protect it from direct contact to aqueous media. Hence we are proposing for future researchers to test a three-layered sandwich (PEO+nanocarrier+PCL 5 and 1%) formulation using electrospinning and electrospraying technique. Using nanocarrier with a swellable property would delay the burst release and plausibly a sustain drug release could be achieved resulting in enhanced bioavailability

5.4   Limitations and future directions

The findings from this research have shed light that there is a pathway to develop a nanofiber formulation for anterior ocular delivery but some caveats. Several aspects relating to formulation and analytical tools needs further optimisation. For researchers interested in continuing this work, the following sub-sections offer some suggestions.

5.4.1 Burst release

The burst release of drugs with nanofiber mats is still unexplored. Long-lasting other slow degrading biomimetic nanofibrous materials like PLA, PLGA and PGA must be explored to overcome the rapid release of the drug from nanofiber mat. Nanofiber spun using coaxial method can be used to control the burst release of the drugs, as the shell of the polymer acts as diffusion barrier for drugs. Degree of swelling plays an important role in the drug release behaviour from the nanofiber mat, Due to smaller diameter of the fibres they may have more pockets for absorbing the liquid media and space for swelling. The initial burst release may be attributed to the enormous surface area of the nanofibers followed by controlled release of the drug from the core of the nanofibers. By using a combination of thick and thin fibres within the structure of the polymeric scaffold, it is possible to imitate the two stages of systemic drug delivery, initially a burst release from thick fibres followed by controlled release from thin fibres.

5.4.2 In vitro release models

The existing USP apparatus for in vitro drug assessment of nanofiber/nanoparticles, the set-ups were designed primarily for oral and transdermal products and as such pose many challenges during a release study. The volume of dissolution medium, as well as the hydrodynamic provided by these apparatuses, are generally not in line with the in vivo conditions at mucosal administration sites. Small volume of dissolution medium can more accurately recapitulate in vivo conditions, because the average amount of tear fluid produced in the precorneal area during a 24h period is 2 mL. Ideally, an in vitro release method should stimulate in vivo conditions, release mechanisms, and enable the establishment of an in vitro - in vivo correlation (IVIVC). Improved in vitro release testing can be carried out using PermeGear vertical glass diffusion cells that has a flexibility with a range of orifice diameter. This model would enable to use a minimal dissolution media of 5 mL which was not feasible using an Ussing chamber where the minimum aliquot used was 15 mL. Currently this model of testing in vitro drug release using PermeGear vertical glass diffusion cells is rapidly emerging as apparatus of choice for testing topically semisolid dosage forms, the same can be adapted to test nanofiber mat too.

5.4.3 Nanofiber characterisation

Nanofiber mat characterisation using SEM provides excellent spatial resolution and is informative with respect to the fibre structure and morphology. Raman microscopy could potentially be an effective complimentary technique for imaging the distribution of components within a nanofiber as the technique is non-destructive and can provide detailed structural and compositional information. However, these two tools fail to measure the void spaces/density of the fibre. A helium pycnometer can be used to determine the density of the nanofiber mat. An

inert gas, typically helium is used as a displacement medium. The pressure observed after filling the sample cell and the pressure discharged into the expansion chamber are measured, and the volume is calculated and is referred to as "helium density". Air trapped in the void spaces can act as a barrier component in porous electrospun mesh to control rate at which the drug is released.

5.4.4 Ocular irritation assays

New formulations/drugs require to be investigated for acute irritation and/or for chronic side-effects, hence there is a need for development and validation of alternative models and tests with short and/or repeated exposure. The current in-vitro and in-vivo test models pose challenge to the researchers, for e.g., suitable cell culture models and cell-lines, sourcing constant supply of fertilized eggs to test for ocular irritation using HET-CAM assay.

REFERENCES

Abdelkader, H., Pierscionek, B., Carew, M., Wu, Z., & Alany, R. G. (2015). Critical appraisal of alternative irritation models: three decades of testing ophthalmic pharmaceuticals. *British Medical Bulletin, 113*(1), 59-71. doi:10.1093/bmb/ldv002

Adepu, S., Kalyani, P., & Khandelwal, M. (2021). Bacterial cellulose-based drug delivery system for dual mode drug release. *Transactions of the Indian National Academy of Engineering, 6*(2), 265-271.

Agarwal, R., Iezhitsa, I., Agarwal, P., Abdul Nasir, N. A., Razali, N., Alyautdin, R., & Ismail, N. M. (2016). Liposomes in topical ophthalmic drug delivery: an update. *Drug Delivery, 23*(4), 1075-1091. doi:10.3109/10717544.2014.943336

Agarwal, S., Wendorff, J. H., & Greiner, A. (2008). Use of electrospinning technique for biomedical applications. *Polymer, 49*(26), 5603-5621. doi:https://doi.org/10.1016/j.polymer.2008.09.014

Ahmad Bhawani, S., Fong, S. S., & Mohamad Ibrahim, M. N. (2015). Spectrophotometric analysis of caffeine. *International journal of analytical chemistry*, *2015*.

Ahmed, I., Gokhale, R. D., Shah, M. V., & Patton, T. F. (1987). Physicochemical determinants of drug diffusion across the conjunctiva, sclera, and cornea. *Journal of pharmaceutical sciences, 76*(8), 583-586.

Akhter, M. H., Ahmad, I., Alshahrani, M. Y., Al-Harbi, A. I., Khalilullah, H., Afzal, O., . . . Karim, S. (2022). Drug Delivery Challenges and Current Progress in Nanocarrier-Based Ocular Therapeutic System. *Gels, 8*(2), 82.

Alhusein, N., Blagbrough, I. S., & De Bank, P. A. (2012). Electrospun matrices for localised controlled drug delivery: release of tetracycline hydrochloride from layers of polycaprolactoe and poly(ethylene-co-vinyl acetate. Drug Delivery and Translation Research, 2, 477-488.

Ali, M., & Byrne, M. E. (2008). Challenges and solutions in topical ocular drug-delivery systems. *Expert Review of Clinical Pharmacology, 1*(1), 145-161. doi:10.1586/17512433.1.1.145

Alghamdi, H. J., Svirskis, D., Bunt. C. R., Swift, S., & Rupenthal, I. D. (2016). Azithromycin and Dexamethasone loaded β-Glucan films for the treatement of blepharitis. *Drug Delivery Letters*, 6, 22-29.

Alvarez-Lorenzo, C., Hiratani, H., Gomez-Amoza, J. L., Martínez-Pacheco, R., Souto, C., & Concheiro, A. (2002). Soft contact lenses capable of sustained delivery of timolol. *Journal of pharmaceutical sciences, 91*(10), 2182-2192.

Ansari, Z., Miller, D., & Galor, A. (2013). Current Thoughts in Fungal Keratitis: Diagnosis and Treatment. *Current Fungal Infection Reports, 7*(3), 209-218. doi:10.1007/s12281-013-0150-1

Apte, R. S. (2021). Age-related macular degeneration. *New England Journal of Medicine, 385*(6), 539-547.

Aptel, F., & Lafon, C. (2015). Treatment of glaucoma with high intensity focused ultrasound. *International Journal of Hyperthermia, 31*(3), 292-301. doi:10.3109/02656736.2014.984777

Armentano, I., Dottori, M., Fortunati, E., Mattioli, S., and Kenny, J.M. (2010). Biodegradable polymer matric nanocomposites for tissue engineering: A review. *Polymer Degradation and Stabilty*, 95, 2126-2146.

Arun, C., Al-Bermani, A., Stannard, K., & Taylor, R. (2009). Long-term impact of retinal screening on significant diabetes-related visual impairment in the working age population. *Diabetic Medicine, 26*(5), 489-492.

Austin, A., Lietman, T., & Rose-Nussbaumer, J. (2017). Update on the Management of Infectious Keratitis. *Ophthalmology, 124*(11), 1678-1689. doi:https://doi.org/10.1016/j.ophtha.2017.05.012

Awwad, S., Mohamed Ahmed, A. H. A., Sharma, G., Heng, J. S., Khaw, P. T., Brocchini, S., & Lockwood, A. (2017). Principles of pharmacology in the eye. *British Journal of Pharmacology, 174*(23), 4205-4223. doi:https://doi.org/10.1111/bph.14024

Baek, Y., Kang, J., Theato, P., & Yoon, J. (2012). Measuring hydrophilicity of RO membranes by contact angles via sessile drop and captive bubble method: A comparative study. *Desalination, 303*, 23-28.

Baji, A., Mai, Y., Wong, S., Abtahi, M., & Chen, P. (2010). Electrospinning of polymer nanofibers: Effects on oriented morphology, structures and tensile properties. *Composites Science and Technology*, 70(5), 703-718.

Balasubramaniam, J., Kant, S., & Pandit, J. K. (2003). In vitro and in vivo evaluation of the Gelrite gellan gum-based ocular delivery system for indomethacin. *Acta Pharm, 53*(4), 251-261.

Balasubramaniam, J., & Pandit, J. K. (2003). Ion-activated in situ gelling systems for sustained ophthalmic delivery of ciprofloxacin hydrochloride. *Drug Deliv, 10*(3), 185-191. doi:10.1080/713840402

Baloglu, E., Senyıgıt, Z. A., Karavana, S. Y., Vetter, A., Metın, D. Y., Polat, S. H., . . . Bernkop-Schnurch, A. (2011). In vitro evaluation of mucoadhesive vaginal tablets of antifungal drugs prepared with thiolated polymer and development of a new dissolution technique for vaginal formulations. *Chemical and Pharmaceutical Bulletin, 59*(8), 952-958.

Barar, J., Javadzadeh, A. R., & Omidi, Y. (2008). Ocular novel drug delivery: impacts of membranes and barriers. *Expert Opinion on Drug Delivery, 5*(5), 567-581. doi:10.1517/17425247.5.5.567

Bartok, M., Gabel, D., Zorn-Kruppa, M., & Engelke, M. (2015). Development of an in vitro ocular test system for the prediction of all three GHS categories. *Toxicology in Vitro, 29*(1), 72-80. doi:https://doi.org/10.1016/j.tiv.2014.09.005

Basu, P. K. (1983). Toxic effects of drugs on the corneal epithelium: a review. *Journal of Toxicology: Cutaneous and Ocular Toxicology, 2*(4-5), 205-227.

Bawa, R. (2007). Patents and nanomedicine.

Bawa, R., Dais, M., Nandu, M., & Robinson, J. (1988). New extended release ocular drug delivery system: Design, characterization and performance testing of minidisc inserts Symposium conducted at the meeting of the Proc Int Symp Control Rel Bioact Mater

Bazbouz, M. B., & Stylios, G. K. (2010). The tensile properties of electrospun nylon 6 single nanofibers. *Journal of Polymer Science Part B: Polymer Physics, 48*(15), 1719-1731.

Bertens, C. J. F., Gijs, M., van den Biggelaar, F., & Nuijts, R. (2018). Topical drug delivery devices: A review. *Exp Eye Res, 168*, 149-160. doi:10.1016/j.exer.2018.01.010

Bloomfield, S. E., Miyata, T., Dunn, M. W., Bueser, N., Stenzel, K. H., & Rubin, A. L. (1978). Soluble gentamicin ophthalmic inserts as a drug delivery system. *Archives of Ophthalmology, 96*(5), 885-887.

Bonneau, N., Baudouin, C., Réaux-Le Goazigo, A., & Brignole-Baudouin, F. (2021). An overview of current alternative models in the context of ocular surface toxicity. *Journal of Applied Toxicology*.

Borooah, S., Wright, M., & Dhillon, B. (2012). Ophthalmology Pocket Tutor. *JP Medical Ltd: London*.

Bruner, L. H., Carr, G. J., Curren, R. D., & Chamberlain, M. (1998). Validation of alternative methods for toxicity testing. *Environ Health Perspect, 106 Suppl 2*(Suppl 2), 477-484. doi:10.1289/ehp.98106477

Burton, M. J., Ramke, J., Marques, A. P., Bourne, R. R., Congdon, N., Jones, I., . . . Bascaran, C. (2021). The lancet global health commission on global eye health: vision beyond 2020. *The Lancet Global Health, 9*(4), e489-e551.

Cao, Y., Zhang, C., Shen, W., Cheng, Z., Yu, L. L., & Ping, Q. (2007). Poly(N-isopropylacrylamide)-chitosan as thermosensitive in situ gel-forming system for ocular drug delivery. *J Control Release, 120*(3), 186-194. doi:10.1016/j.jconrel.2007.05.009

Carstens, F., Gamelas, J. A., & Schabel, S. (2017). Engineering microfluidic papers: determination of fibre source and paper sheet properties and their influence on capillary-driven fluid flow. *Cellulose*, *24*, 295-309.

Chang, D. T., Herceg, M. C., Bilonick, R. A., Camejo, L., Schuman, J. S., & Noecker, R. J. (2009). Intracameral dexamethasone reduces inflammation on the first postoperative day after cataract surgery in eyes with and without glaucoma. *Clinical Ophthalmology (Auckland, NZ), 3*, 345.

Chen, H. (2015). Recent developments in ocular drug delivery. *Journal of Drug Targeting, 23*(7-8), 597-604. doi:10.3109/1061186X.2015.1052073

Chen, H., Jin, Y., Sun, L., Li, X., Nan, K., Liu, H., . . . Wang, B. (2018). Recent Developments in Ophthalmic Drug Delivery Systems for Therapy of Both Anterior and Posterior Segment Diseases. *Colloid and Interface Science Communications, 24*, 54-61. doi:https://doi.org/10.1016/j.colcom.2018.03.008

Cher, I. (2013). Ocular surface concepts: development and citation. *The ocular surface, 12*(1), 10-13.

Cheung, A. C. Y., Yu, Y., Tay, D., Wong, H. S., Ellis-Behnke, R., & Chau, Y. (2010). Ultrasound-enhanced intrascleral delivery of protein. *International Journal of Pharmaceutics, 401*(1), 16-24. doi:https://doi.org/10.1016/j.ijpharm.2010.09.001

Cholkar, K., Patel, S. P., Vadlapudi, A. D., & Mitra, A. K. (2012). Novel Strategies for Anterior Segment Ocular Drug Delivery. *Journal of Ocular Pharmacology and Therapeutics, 29*(2), 106-123. doi:10.1089/jop.2012.0200

Chopra, P., Hao, J., & Li, S. K. (2010). Iontophoretic transport of charged macromolecules across human sclera. *International Journal of Pharmaceutics, 388*(1), 107-113. doi:https://doi.org/10.1016/j.ijpharm.2009.12.046

Chopra, P., Hao, J., & Li, S. K. (2012). Sustained release micellar carrier systems for iontophoretic transport of dexamethasone across human sclera. *Journal of Controlled Release, 160*(1), 96-104. doi:https://doi.org/10.1016/j.jconrel.2012.01.032

Chun, D. K., Shapiro, A., & Abelson, M. B. (2008). 17 Ocular Pharmacokinetics. *Principles and Practice of Ophthalmology E-Book*, 179.

Cipitria, A., Skelton, A., Dargaville, T., Dalton, P., & Hutmacher, D. (2011). Design, fabrication and characterization of PCL electrospun scaffolds—a review. *Journal of Materials Chemistry, 21*(26), 9419-9453.

Cohen, S., Lobel, E., Trevgoda, A., & Peled, Y. (1997). A novel in situ-forming ophthalmic drug delivery system from alginates undergoing gelation in the eye. *Journal of Controlled Release, 44*(2), 201-208. doi:https://doi.org/10.1016/S0168-3659(96)01523-4

Cortez Tornello, P. R., Feresin, G. E., Tapia, A., Cuadrado, T. R., & Abraham, G. A. (2017). Multilayered electrospun nanofibrous scaffolds for tailored controlled release of embelin. *Soft Materials*, null-null. doi:10.1080/1539445X.2017.1398173

Crawford, A., Patel, D., & McGhee, C. (2013). A brief history of corneal transplantation: From ancient to modern [Review Article]. *Oman Journal of Ophthalmology, 6*(4), 12-17. doi:10.4103/0974-620x.122289

Cui, W., Li, X., Zhu, X., Yu, G., Zhou, S., & Weng, J. (2006). Investigation of Drug Release and Matrix Degradation of Electrospun Poly(dl-lactide) Fibres with Paracetanol Inoculation. *Biomacromolecules, 7*(5), 1623-1629. doi:10.1021/bm060057z

Dal Monte, M., Cammalleri, M., Amato, R., Pezzino, S., Corsaro, R., Bagnoli, P., & Rusciano, D. (2020). A topical formulation of melatoninergic compounds exerts strong hypotensive and neuroprotective effects in a rat model of hypertensive glaucoma. *International Journal of Molecular Sciences*, *21*(23), 9267.

DelMonte, D. W., & Kim, T. (2011). Anatomy and physiology of the cornea. *Journal of Cataract & Refractive Surgery, 37*(3), 588-598.

Dias, J., & Bártolo, P. (2013). Morphological characteristics of electrospun PCL meshes - The influce of solvent type and concentration. *Procedia CRP*, 5, 261-221.

Di Colo, G., Burgalassi, S., Chetoni, P., Fiaschi, M., Zambito, Y., & Saettone, M. F. (2001). Gel-forming erodible inserts for ocular controlled delivery of ofloxacin. *International journal of pharmaceutics, 215*(1-2), 101-111.

Di Colo, G., & Zambito, Y. (2002). A study of release mechanisms of different ophthalmic drugs from erodible ocular inserts based on poly (ethylene oxide). *European journal of pharmaceutics and biopharmaceutics, 54*(2), 193-199.

Dixit, N., Bali, V., Baboota, S., Ahuja, A., & Ali, J. (2007). Iontophoresis - an approach for controlled drug delivery: a review. *Curr Drug Deliv, 4*(1), 1-10. doi:10.2174/156720181070401001

Downie, L. E., Bandlitz, S., Bergmanson, J. P. G., Craig, J. P., Dutta, D., Maldonado-Codina, C., . . . Wolffsohn, J. S. (2021). BCLA CLEAR - Anatomy and physiology of the anterior eye. *Contact Lens and Anterior Eye, 44*(2), 132-156. doi:https://doi.org/10.1016/j.clae.2021.02.009

Draize, J. H. (1944). Methods for the study of irritation and toxicity of substances applied topically to the skin and mucous membranes. *J. Pharmacol. Exp. Ther., 82*, 377-390.

Dua, H. S., Faraj, L. A., Said, D. G., Gray, T., & Lowe, J. (2013). Human Corneal Anatomy Redefined: A Novel Pre-Descemet's Layer (Dua's Layer). *Ophthalmology, 120*(9), 1778-1785. doi:https://doi.org/10.1016/j.ophtha.2013.01.018

Dubald, M., Bourgeois, S., Andrieu, V., & Fessi, H. (2018). Ophthalmic drug delivery systems for antibiotherapy—a review. *Pharmaceutics, 10*(1), 10.

Duvvuri, S., Majumdar, S., & Mitra, A. K. (2003). Drug delivery to the retina: challenges and opportunities. *Expert Opin Biol Ther, 3*(1), 45-56. doi:10.1517/14712598.3.1.45

Duvvuri, S., Majumdar, S., & Mitra, A. K. (2004). Role of metabolism in ocular drug delivery. *Current drug metabolism, 5*(6), 507-515.

El-Kamel, A. H. (2002). In vitro and in vivo evaluation of Pluronic F127-based ocular delivery system for timolol maleate. *Int J Pharm, 241*(1), 47-55. doi:10.1016/s0378-5173(02)00234-x

Eljarrat-Binstock, E., & Domb, A. J. (2006). Iontophoresis: A non-invasive ocular drug delivery. *Journal of Controlled Release, 110*(3), 479-489. doi:https://doi.org/10.1016/j.jconrel.2005.09.049

Eller, M., Schoenwald, R., Dixson, J., Segarra, T., & Barfknecht, C. (1985). Topical carbonic anhydrase inhibitors III: Optimization model for corneal penetration of ethoxzolamide analogues. *Journal of pharmaceutical sciences, 74*(2), 155-160.

Farjo, A. A., McDermott, M. L., & Soong, H. K. (2009). Corneal Anatomy, Physiology, and Wound Healing

Federation., I. D. (2021). IDF Diabetes Atlas, 10th edn. Brussels, Belgium: International Diabetes Federation, 2021.

Figueroa-Lopez, K., Castro-Mayorga, J., Andrade-Mahecha, M., Cabedo, L., & Lagaron, J. (2018). Antibacterial and Barrier Properties of Gelatin Coated by Electrospun Polycaprolactone Ultrathin Fibres Containing Black Pepper Oleoresin of Interest in Active Food Biopackaging Applications. *Nanomaterials, 8*(4), 199.

Flack, D. (2001). Measurement good practice guide no. 40: callipers and micrometers. *United Kingdom.*

Flack, D. (2014). Good Practice Guide No. 40, Callipers and Micrometers. *Teddington, Middlesex: National Physical Laboratory.*

Fong, G., Chun, I., & Reneker, D.H. (1999). Beaded nanofibers formed during electrospinning. *Polymer*, 40, 4585-4592.

Foulks, G. N. (2007). DEWS report: a mission completed. *The Ocular Surface, 2*(5), 65-66.

Friedenwald, J., & Hughes, J. (1948). Chemical warfare agents: effects on the eye and their treatment. *Ophthalmology in the War Years, 2*, 63-70.

Friedenwald, J., Hughes, W., & Herrmann, H. (1944). Acid-base tolerance of the cornea. *Archives of Ophthalmology, 31*(4), 279-283.

Fyodorov, S., Moroz, Z., Kramskaya, Z., Bagrov, S., Amstislavskaya, T., & Zolotarevsky, A. (1985). Comprehensive conservative treatment of dystrophia endothelialis et epithelialis cornea, using a therapeutic collagen coating. *Vestn. Oftalmol, 101*, 33-36.

Gan, L., Wang, J., Jiang, M., Bartlett, H., Ouyang, D., Eperjesi, F., . . . Gan, Y. (2013). Recent advances in topical ophthalmic drug delivery with lipid-based nanocarriers. *Drug Discovery Today, 18*(5), 290-297. doi:https://doi.org/10.1016/j.drudis.2012.10.005

Gaudana, R., Ananthula, H. K., Parenky, A., & Mitra, A. K. (2010). Ocular Drug Delivery [journal article]. *The AAPS Journal, 12*(3), 348-360. doi:10.1208/s12248-010-9183-3

Gebhardt, B. M., Varnell, E. D., & Kaufman, H. E. (1995). Cyclosporine in collagen particles: corneal penetration and suppression of allograft rejection. *Journal of ocular pharmacology and therapeutics, 11*(4), 509-517.

Ghasemi Falavarjani, K., & Nguyen, Q. D. (2013). Adverse events and complications associated with intravitreal injection of anti-VEGF agents: a review of literature. *Eye, 27*(7), 787-794. doi:10.1038/eye.2013.107

Ghate, D., & Edelhauser, H. F. (2006). Ocular drug delivery. *Expert Opinion on Drug Delivery, 3*(2), 275-287. doi:10.1517/17425247.3.2.275

Gholizadeh, S., Wang, Z., Chen, X., Dana, R., & Annabi, N. (2021). Advanced nanodelivery platforms for topical ophthalmic drug delivery. *Drug Discovery Today*.

Goldberg, A., & Silber, P. (1992). Status of in vitro ocular irritation testing. *Lens and eye toxicity research, 9*(3-4), 161-192.

Grabovac, V., Guggi, D., and Bernkop-Schnurch, A. (2005). Comparison of the mucoadhesive properties of various polymers. *Advanced Drug Delivery Reviews*, 57, 1713-1723.

Grass, G. M., & Robinson, J. R. (1988). Mechanisms of corneal drug penetration II: Ultrastructural analysis of potential pathways for drug movement. *Journal of pharmaceutical sciences, 77*(1), 15-23.

Gratieri, T., Gelfuso, G. M., Rocha, E. M., Sarmento, V. H., de Freitas, O., & Lopez, R. F. V. (2010). A poloxamer/chitosan in situ forming gel with prolonged retention time for ocular delivery. *European Journal of Pharmaceutics and Biopharmaceutics, 75*(2), 186-193. doi:https://doi.org/10.1016/j.ejpb.2010.02.011

Green, K. (1992). A brief history of ocular toxicology. *Lens and eye toxicity research, 9*(3-4), 153-159.

Griffith, J. F., Nixon, G. A., Bruce, R. D., Reer, P. J., & Bannan, E. A. (1980). Dose-response studies with chemical irritants in the albino rabbit eye as a basis for selecting optimum testing conditions for predicting hazard to the human eye. *Toxicology and Applied Pharmacology, 55*(3), 501-513.

Grossniklaus, H. E. (2015). Ophthalmic Pathology: History, Accomplishments, Challenges, and Goals. *Ophthalmology, 122*(8), 1539-1542. doi:https://doi.org/10.1016/j.ophtha.2015.04.001

Gupta, C., & Chauhan, A. (2011). Ophthalmic delivery of cyclosporine A by punctal plugs. *J Control Release, 150*(1), 70-76. doi:10.1016/j.jconrel.2010.11.009

Gurtler, F., & Gurny, R. (1995). Patent literature review of ophthalmic inserts. *Drug development and industrial pharmacy, 21*(1), 1-18.

Hajer, S. A., Darren, S., Craig, R. B., Simon, S., & Ilva, D. R. (2016). Azithromycin and Dexamethasone Loaded β-Glucan Films for the Treatment of Blepharitis. *Drug Delivery Letters, 6*(1), 22-29. doi:http://dx.doi.org/10.2174/2210303106666160506123050

HD, T. (2004). Texture Analyser Product Specification. *Vienna: Stable Micro Systems Ltd., Godalming Surrey*.

Himmelstein, K. J., Guvenir, I., & Patton, T. F. (1978). Preliminary pharmacokinetic model of pilocarpine uptake and distribution in the eye. *Journal of pharmaceutical sciences, 67*(5), 603-606.

Hirschberg, J. (1921). Alkmaion's Verdienst um die Augenkunde. *Albrecht von Graefes Archiv für Ophthalmologie, 105*(1), 129-133.

Holowka, E. P., & Bhatia, S. K. (2014). Thin-Film Materials. In *Drug Delivery* (pp. 63-116): Springer.

Hoorfar, M., & Neumann, A. (2004). Axisymmetric drop shape analysis (ADSA) for the determination of surface tension and contact angle. *The Journal of Adhesion, 80*(8), 727-743.

Huang, Z.-M., Zhang, Y. Z., Kotaki, M., & Ramakrishna, S. (2003). A review on polymer nanofibers by electrospinning and their applications in nanocomposites. *Composites Science and Technology, 63*(15), 2223-2253. doi:https://doi.org/10.1016/S0266-3538(03)00178-7

Ibrahim, H., Gurny, R., Buri, P., Grove, J., Rozier, A., & Plazonnet, B. (1990). Ocular bioavailability of pilocarpine from phase transition latex system triggered by pH. *Eur J Drug Metab Pharmacokinet, 15*, 206.

Immich, A. P. S., Tornero, J. A., Casas, F. C., & Arias, M. J. L. (2017). Electrospun PLLA Membranes for Caffeine Delivery: Diffusional Approach. *Journal of Biomedical Science and Engineering, Vol.10No.12*, 12. doi:10.4236/jbise.2017.1012042

Jackson, E. (1992). Animal testing in biomedical research. In *Manual of Oculotoxicity Testing of Drugs* (pp. 1-8): Fisher-Verlag, Stuttgart.

Jacobs, V., Anandjiwala, R. D., & Maaza, M. (2010). The influence of electrospinning parameters on the structural morphology and diameter of electrospun nanofibers. *Journal of applied polymer science, 115*(5), 3130-3136.

Jaeger, R., Schonherr, H., & Vancso, J. (1996). Chain packing in electrospun poly- (ethylene oxide) visualized by atomic force microscopy. *Macromolecules*, 29(23):7634–7636.

Jaeger, R., Bergshoef, M., Batlle, C., Schonherr, H., & Vancso, J. (1998). Electrospinning of ultra-thin polymer fibres. *Macromolecular Symposium*,127:141–150.

Janagam, D. R., Wu, L., & Lowe, T. L. (2017). Nanoparticles for drug delivery to the anterior segment of the eye. *Advanced Drug Delivery Reviews, 122*, 31-64. doi:https://doi.org/10.1016/j.addr.2017.04.001

Jumelle, C., Gholizadeh, S., Annabi, N., & Dana, R. (2020). Advances and limitations of drug delivery systems formulated as eye drops. *Journal of Controlled Release, 321*, 1-22. doi:https://doi.org/10.1016/j.jconrel.2020.01.057

Kalia, Y. N., Naik, A., Garrison, J., & Guy, R. H. (2004). Iontophoretic drug delivery. *Advanced Drug Delivery Reviews, 56*(5), 619-658. doi:https://doi.org/10.1016/j.addr.2003.10.026

Karuppuswamy, P., Venugopal, J. R., Navaneethan, B., Laiva, A. L., and Ramakrishna, S. (2015). Polycaprolactone nanofibers for the controlled release of tetracycline hydrochloride. *Materials Letters, 151, 180-186.*

Kelly, J., Molyneux, P., Smith, S., & Smith, S. (1989). Relative bioavailability of pilocarpine from a novel ophthalmic delivery system and conventional eyedrop formulations. *British journal of ophthalmology, 73*(5), 360-362.

Khromov, G. L., Davydov, A. B., Maichuk, J. F., & Tischina, I. F., &. (1976). *Base for ophthalmological medicinal preparations and on ophthalmological medicinal film*: Google Patents.

Kidoaki, S., Kwon, I. K., & Matsuda, T. (2005). Mesoscopic spatial designs of nano-and microfiber meshes for tissue-engineering matrix and scaffold based on newly devised multilayering and mixing electrospinning techniques. *Biomaterials, 26*(1), 37-46.

Kim, E. Y., Gao, Z. G., Park, J. S., Li, H., & Han, K. (2002). rhEGF/HP-beta-CD complex in poloxamer gel for ophthalmic delivery. *Int J Pharm, 233*(1-2), 159-167. doi:10.1016/s0378-5173(01)00933-4

Kompella, U. B., Kadam, R. S., & Lee, V. H. L. (2010). Recent advances in ophthalmic drug delivery. *Therapeutic delivery, 1*(3), 435-456. doi:10.4155/TDE.10.40

Kuno, N., & Fujii, S. (2011). Recent Advances in Ocular Drug Delivery Systems. *Polymers, 3*(1), 193.

Kupka, V., Dvoráková , E., Manakhov, A., Michlícek, M., Petrus, J., Vojtová, L., & Zajícková, L. (2020). Well-Blended PCL/PEO electrospun nanofibers with functional properties enchanced by plasma processing. *Polymers*, 12, 1403.

Kurniawansyah, I. S., Sopyan, I., Aditya, W., Nuraini, H., Alminda, F., & Nurlatifah, A. (2018). Preformed gel vs in situ gel: a review. *Int Res J Pharm, 9*, 1-5.

Kute, P. R., Gondkar, S., & Saudagar, R. (2015). Ophthalmic in-situ gel: an overview. *World J. Pharm. Pharm. Sci, 4*, 549-568.

Lach, J. L., Huang, H.-S., & Schoenwald, R. D. (1983). Corneal penetration behavior of β-blocking agents II: assessment of barrier contributions. *Journal of pharmaceutical sciences, 72*(11), 1272-1279.

Lamberts, D. W., Langston, D. P., & Chu, W. (1978). A clinical study of slow-releasing artificial tears. *Ophthalmology, 85*(8), 794-800.

Lang, J. C. (1995). Ocular drug delivery conventional ocular formulations. *Advanced Drug Delivery Reviews, 16*(1), 39-43. doi:https://doi.org/10.1016/0169-409X(95)00012-V

Lee, C. M., & Afshari, N. A. (2017). The global state of cataract blindness. *Current opinion in ophthalmology, 28*(1), 98-103.

Lee, S.-H., Ku, B.-C., Wang, X., Samuelson, L. A., & Kumar, J. (2001). Design, Synthesis and Electrospinning of a Novel Fluorescent Polymer for Optical Sensor Applications. *MRS Online Proceedings Library, 708*(1), 1045. doi:10.1557/PROC-708-BB10.45

Lee, S. S., Hughes, P., Ross, A. D., & Robinson, M. R. (2010). Biodegradable Implants for Sustained Drug Release in the Eye. *Pharmaceutical Research, 27*(10), 2043-2053. doi:10.1007/s11095-010-0159-x

Lee, V. H., & Robinson, J. R. (1986a). Topical ocular drug delivery: recent developments and future challenges. *Journal of ocular pharmacology and therapeutics, 2*(1), 67-108.

Lee, V. H. L. (1990). Review: New Directions in the Optimization of Ocular Drug Delivery [Article]. *Journal of Ocular Pharmacology, 6*(2), 157-164. doi:10.1089/jop.1990.6.157

Lee, V. H. L., & Robinson, J. R. (1986b). Topical Ocular Drug Delivery: Recent Developments and Future Challenges. *Journal of Ocular Pharmacology and Therapeutics, 2*(1), 67-108. doi:10.1089/jop.1986.2.67

Leese, H., Bhurtun, V., Lee, K. P., & Mattia, D. (2013). Wetting behaviour of hydrophilic and hydrophobic nanostructured porous anodic alumina. *Colloids and Surfaces A: Physicochemical and Engineering Aspects, 420*, 53-58.

Lerman, S. (1970). Simulated sustained release pilocarpine therapy. *Ann Ophthalmol, 2*, 437-439.

Lerman, S., & Reininger, B. (1971). Simulated sustained release pilocarpine therapy and aqueous humor dynamics. *Canadian journal of ophthalmology. Journal canadien d'ophtalmologie, 6*(1), 14-23.

Li, J., Tripathi, R. C., & Tripathi, B. J. (2008). Drug-induced ocular disorders. *Drug safety, 31*(2), 127-141.

Lim, J.-M., Yi, G.-R., Moon, J. H., Heo, C.-J., & Yang, S.-M. (2007). Superhydrophobic films of electrospun fibres with multiple-scale surface morphology. *Langmuir, 23*(15), 7981-7989.

Lin, H. R., Sung, K. C., & Vong, W. J. (2004). In situ gelling of alginate/pluronic solutions for ophthalmic delivery of pilocarpine. *Biomacromolecules, 5*(6), 2358-2365. doi:10.1021/bm0496965

Lindfield, R. (2014). Improving the quality of cataract surgery. *Community eye health, 27*(85), 9.

Liu, W. (2019). *Surface modification of urea granules for controlled release: A thesis submitted in partial fulfilment of the requirements for the Degree of Doctor of Philosophy at Lincoln University.* Lincoln University.

Liu, Z., Li, J., Nie, S., Liu, H., Ding, P., & Pan, W. (2006). Study of an alginate/HPMC-based in situ gelling ophthalmic delivery system for gatifloxacin. *Int J Pharm, 315*(1-2), 12-17. doi:10.1016/j.ijpharm.2006.01.029

Lloyd, R. (1985). Patent 2097680. *Smith and Nephew Research, Ltd*.

Lordo, R. A., Feder, P. I., & Gettings, S. D. (1999). Comparing and evaluating alternative (in vitro) tests on their ability to predict the Draize maximum average score. *Toxicology in Vitro, 13*(1), 45-72. doi:https://doi.org/10.1016/S0887-2333(98)00062-9

Luechtefeld, T., Maertens, A., Russo, D. P., Rovida, C., Zhu, H., & Hartung, T. (2016). Analysis of Draize eye irritation testing and its prediction by mining publicly available 2008-2014 REACH data. *Altex, 33*(2), 123-134. doi:10.14573/altex.1510053

Ma, W. D., Xu, H., Wang, C., Nie, S. F., & Pan, W. S. (2008). Pluronic F127-g-poly(acrylic acid) copolymers as in situ gelling vehicle for ophthalmic drug delivery system. *Int J Pharm, 350*(1-2), 247-256. doi:10.1016/j.ijpharm.2007.09.005

Macoul, K. L., & Pavan-Langston, D. (1975). Pilocarpine ocusert system for sustained control of ocular hypertension. *Archives of ophthalmology, 93*(8), 587-590.

Maehle, A.-H. (1987). Animal experimentation from antiquity to the end of the eighteenth century: Attitudes and arguments. *Vivisection in historical perspective*, 14-47.

Maichuk, Y. (1967). Polymeric ophthalmic inserts with antibiotics Symposium conducted at the meeting of the Proc. Conf. Ophthalmologists

Maichuk, Y. (1975a). Ophthalmic drug inserts. *Investigative Ophthalmology & Visual Science, 14*(2), 87-90.

Maichuk, Y. (1975b). Soluble ophthalmic drug inserts. *The Lancet, 305*(7899), 173.

Maichuk, Y., & Erichev, V. (1981). Soluble ophthalmic drug inserts with pilocarpine, experimental and clinical study. *Glaucoma, 3*, 239-242.

Malhotra, A., Minja, F. J., Crum, A., & Burrowes, D. (2011). Ocular Anatomy and Cross-Sectional Imaging of the Eye. *Seminars in Ultrasound, CT and MRI, 32*(1), 2-13. doi:https://doi.org/10.1053/j.sult.2010.10.009

Mamalis, N., Edelhauser, H. F., Dawson, D. G., Chew, J., LeBoyer, R. M., & Werner, L. (2006). Toxic anterior segment syndrome. *Journal of Cataract & Refractive Surgery, 32*(2), 324-333.

Maumenee, A. E. (1993). The history of vitamin A and its ophthalmic implications: a personal viewpoint. *Archives of Ophthalmology, 111*(4), 547-550.

Maurice, D. M. (1980). Structures and Fluids Involved in the Penetration of Topically Applied Drugs. *International Ophthalmology Clinics, 20*(3).

Migliaresi, C., Ruffo, G. A., Volpato, F. Z., & Zeni, D. (2012). Advanced electrospinning setups and special fibre and mesh morphologies. *Electrospinning for advanced biomedical applications and therapies. Smithersrapra, United Kingdom*, 23-68.

Miller, S. C., & Donovan, M. D. (1982). Effect of poloxamer 407 gel on the miotic activity of pilocarpine nitrate in rabbits. *International journal of pharmaceutics, 12*(2-3), 147-152.

Mitra, A. (2013). *Treatise on Ocular Drug Delivery*. Sharjah, UNITED ARAB EMIRATES: Bentham Science Publishers. Retrieved from http://ebookcentral.proquest.com/lib/lincoln-ebooks/detail.action?docID=1310827

Miyazaki, S., Suzuki, S., Kawasaki, N., Endo, K., Takahashi, A., & Attwood, D. (2001). In situ gelling xyloglucan formulations for sustained release ocular delivery of pilocarpine hydrochloride. *Int J Pharm, 229*(1-2), 29-36. doi:10.1016/s0378-5173(01)00825-0

Mofidfar, M., Abdi, B., Ahadian, S., Mostafavi, E., Desai, T. A., Abbasi, F., . . . Flowers, C. W. (2021). Drug delivery to the anterior segment of the eye: A review of current and future treatment strategies. *International Journal of Pharmaceutics, 607*, 120924.

Molokhia, S. A., Thomas, S. C., Garff, K. J., Mandell, K. J., & Wirostko, B. M. (2013). Anterior eye segment drug delivery systems: current treatments and future challenges. *Journal of ocular pharmacology and therapeutics, 29*(2), 92-105.

Morrison, P. W., & Khutoryanskiy, V. V. (2014). Advances in ophthalmic drug delivery. *Therapeutic Delivery, 5*(12), 1297-1315. doi:10.4155/tde.14.75

Müller, L. J., Marfurt, C. F., Kruse, F., & Tervo, T. M. (2003). Corneal nerves: structure, contents and function. *Experimental eye research, 76*(5), 521-542.

Murphy, J. (2013). More details on Dua's layer of the cornea: perhaps discovered two decades ago, its meaning for primary eye care is unsure. *Review of Optometry, 150*(7), 4-6.

Nabili, M., Patel, H., Mahesh, S. P., Liu, J., Geist, C., & Zderic, V. (2013). Ultrasound-Enhanced Delivery of Antibiotics and Anti-Inflammatory Drugs Into the Eye. *Ultrasound in Medicine & Biology, 39*(4), 638-646. doi:https://doi.org/10.1016/j.ultrasmedbio.2012.11.010

National Research Council, N. (1977). Principles and procedures for evaluating the toxicity of household substances. In *Principles and Procedures for evaluating the toxicity of household substances* (pp. vi, 130-vi, 130)

Neervannan, S. (2021). Introduction and History of Ophthalmic Product Development. In *Ophthalmic Product Development* (pp. 3-13): Springer.

Ng, X. W., Liu, K. L., Veluchamy, A. B., Lwin, N. C., Wong, T. T., & Venkatraman, S. S. (2015). A biodegradable ocular implant for long-term suppression of intraocular pressure. *Drug Delivery and Translational Research, 5*(5), 469-479. doi:10.1007/s13346-015-0240-4

Nguyen, V. L., Tran, N. H., & Huynh, D. P. (2017). Taylor cone - Jet mode in the fabrication of electrosprayed microspheres. *Journal of Science and Technology, 55*(1B), 216-222. doi:10.15625/2525-2518/55/1B/12112

Nichols, K. K., Foulks, G. N., Bron, A. J., Glasgow, B. J., Dogru, M., Tsubota, K., . . . Sullivan, D. A. (2011). The international workshop on meibomian gland dysfunction: executive summary. *Investigative ophthalmology & visual science, 52*(4), 1922-1929.

OECD. (2004). OECD guidelines for the testing of chemicals. Skin absorption: in vitro method No. 428, 1-8.

Ohashi, Y., Dogru, M., & Tsubota, K. (2006). Laboratory findings in tear fluid analysis. *Clinica Chimica Acta, 369*(1), 17-28. doi:https://doi.org/10.1016/j.cca.2005.12.035

Olmsted, J. M. D., & Olmsted, E. H. (1952). *Claude Bernard & the experimental method in medicine*: H. Schuman.

Olsen, T. W., Edelhauser, H. F., Lim, J. I., & Geroski, D. H. (1995). Human scleral permeability. Effects of age, cryotherapy, transscleral diode laser, and surgical thinning. *Investigative ophthalmology & visual science, 36*(9), 1893-1903.

Organization, W. H., &. (2001). *The International Classification of Functioning, Disability and Health (ICF) World Health Organization, Geneva; 2001*.

Organization, W. H. (2019). World report on vision.

Pal Kaur, I., & Kanwar, M. (2002). Ocular Preparations: The Formulation Approach. *Drug Development and Industrial Pharmacy, 28*(5), 473-493. doi:10.1081/DDC-120003445

Pascolini, D., & Mariotti, S. P. (2012). Global estimates of visual impairment: 2010. *Br J Ophthalmol, 96*(5), 614-618. doi:10.1136/bjophthalmol-2011-300539

Patel, A., Cholkar, K., Agrahari, V., & Mitra, A. K. (2013). Ocular drug delivery systems: An overview. *World J Pharmacol, 2*(2), 47-64. doi:10.5497/wjp.v2.i2.47

Patel, P., Shastri, D., Shelat, P., & Shukla, A. (2010). Ophthalmic drug delivery system: challenges and approaches. *Systematic Reviews in Pharmacy, 1*(2), 113.

Patel, S., M. Manzo, G., U. Patel, S., S. Kulkarni, P., & G. Chase, G. (2012). *Permeability of Electrospun Superhydrophobic Nanofiber Mats* (Vol. 2012). Retrieved from http://downloads.hindawi.com/journals/jnt/2012/483976.pdf. doi:10.1155/2012/483976

Patton, T. F., & Robinson, J. R. (1976). Quantitative precorneal disposition of topically applied pilocarpine nitrate in rabbit eyes. *Journal of pharmaceutical sciences, 65*(9), 1295-1301.

Peyman, G. A., & Ganiban, G. J. (1995). Delivery systems for intraocular routes. *Advanced drug delivery reviews, 16*(1), 107-123.

Pinheiro, G. K. L. D. O., Araújo Filho, I. D., Araújo Neto, I. D., Rêgo, A. C. M., Azevedo, E. P. D., Pinheiro, F. I., & Lima Filho, A. A. D. S. (2018). Nature as a source of drugs for ophthalmology. *Arquivos brasileiros de oftalmologia*, *81*, 443-454.

Preis, M., Knop, K., & Breitkreutz, J. (2014). Mechanical strength test for orodispersible and buccal films. *International Journal of Pharmaceutics, 461*(1), 22-29. doi:https://doi.org/10.1016/j.ijpharm.2013.11.033

Qi, H., Chen, W., Huang, C., Li, L., Chen, C., Li, W., & Wu, C. (2007). Development of a poloxamer analogs/carbopol-based in situ gelling and mucoadhesive ophthalmic delivery system for puerarin. *Int J Pharm, 337*(1-2), 178-187. doi:10.1016/j.ijpharm.2006.12.038

Ramke, J., Gilbert, C. E., Lee, A. C., Ackland, P., Limburg, H., & Foster, A. (2017). Effective cataract surgical coverage: An indicator for measuring quality-of-care in the context of Universal Health Coverage. *PLoS One, 12*(3), e0172342.

Rashid, T. U., Gorga, R. E., & Krause, W. E. (2021). Mechanical properties of electrospun fibres—A critical review. *Advanced Engineering Materials, 23*(9), 2100153.

Rathore, K., & Nema, R. (2009). Review on ocular inserts. *Int J PharmTech Res, 1*(2), 164-169.

Reneker, D. H., & Yarin, A.L. (2008). Electrospinning jets and polymer nanofibers. *Polymer*, 49, 2384-2425.

Report, O. D. D. S. (2022). Ocular Drug Delivery System Market by Technology (Implantable Ocular Drug Delivery Systems, Particulate Drug Delivery Systems), Dosage Form (Ophthalmic Solution, Ophthalmic Suspension, Ophthalmic Emulsion), Distribution Channel & Region - Forecast to 2021-2031. *Report - Ocular Drug DeliverySystem Market 2022*, 250 pp. doi:https://www.futuremarketinsights.com/reports/ocular-drug-delivery-system-market

Richardson, M., & Bentley, P. (1993). A new opththalmic delivery system. *Drugs and the pharmaceutical sciences, 58*, 355-367.

Rozier, A., Mazuel, C., Grove, J., & Plazonnet, B. (1989). Gelrite®: A novel, ion-activated, in-situ gelling polymer for ophthalmic vehicles. Effect on bioavailability of timolol. *International journal of pharmaceutics, 57*(2), 163-168.

Rüfer, F., Schröder, A., & Erb, C. (2005). White-to-white corneal diameter: normal values in healthy humans obtained with the Orbscan II topography system. *Cornea, 24*(3), 259-261.

Russell, W. M. S., & Burch, R. L. (1959). *The principles of humane experimental technique*: Methuen.

Ryu, H. I., Koo, M. S., Kim, S., Kim, S., Park, Y. A., & Park, S. M. (2020). Uniform-thickness electrospun nanofiber mat production system based on real-time thickness measurement. *Sci Rep, 10*(1), 20847. doi:10.1038/s41598-020-77985-0

Saettone, M. F. (1993). Solid polymeric inserts/disks as drug delivery systems.

Saettone, M. F. (2019). Solid polymeric inserts/disks as drug delivery devices. In *Biopharmaceutics of ocular drug delivery* (pp. 61-79): CRC Press.

Saettone, M. F., & Salminen, L. (1995). Ocular inserts for topical delivery. *Advanced Drug Delivery Reviews, 16*(1), 95-106. doi:https://doi.org/10.1016/0169-409X(95)00014-X

Séchoy, O., Tissié, G., Sébastian, C., Maurin, F., Driot, J. Y., & Trinquand, C. (2000). A new long acting ophthalmic formulation of carteolol containing alginic acid. *Int J Pharm, 207*(1-2), 109-116. doi:10.1016/s0378-5173(00)00539-1

Sahay, R., Thavasi, V., Ramakrishna, S. (2011). Design modications in electrospinning setup for advanced applications. *Journal of Nanomaterials*, 1-17.

Seifried, H. E. (1986). Eye irritation testing: historical perspectives and future directions. *Journal of Toxicology: Cutaneous and Ocular Toxicology, 5*(2), 89-114.

Samples, J. R., Krause, G., & Lewy, A. J. (1988). Effect of melatonin on intraocular pressure. *Current eye research*, 7(7), 649-653.

Shell, J., JW, S., & RW, B. (1974). Diffusional systems for controlled release of drugs to the eye.

Shell, J. W., & Gale, R. M., &. (1984). *Topical composition containing steroid in two forms released independently from polymeric carrier*: Google Patents.

Sieg, J. W., & Robinson, J. R. (1977). Vehicle effects on ocular drug bioavailability II: evaluation of pilocarpine. *Journal of pharmaceutical sciences, 66*(9), 1222-1228.

Singh, V., Ahmad, R., & Heming, T. (2011). The challenges of ophthalmic drug delivery: a review. *International Journal of Drug Discovery, 3*(1), 56-62.

Souza, J. G., Dias, K., Silva, S. A. M., de Rezende, L. C. D., Rocha, E. M., Emery, F. S., & Lopez, R. F. V. (2015). Transcorneal iontophoresis of dendrimers: PAMAM corneal penetration and dexamethasone delivery. *Journal of Controlled Release, 200*, 115-124. doi:https://doi.org/10.1016/j.jconrel.2014.12.037

Srividya, B., Cardoza, R. M., & Amin, P. D. (2001). Sustained ophthalmic delivery of ofloxacin from a pH triggered in situ gelling system. *J Control Release, 73*(2-3), 205-211. doi:10.1016/s0168-3659(01)00279-6

Stalder, A., &. (2006). *DropSnake and LB-ADSA user manual*: Biomedical Imaging Group, Ecole Polytechnique Federale de Lausanne.

Tan, E. P. S., & Lim, C. T. (2006). Mechanical characterization of nanofibers – A review. *Composites Science and Technology, 66*(9), 1102-1111. doi:https://doi.org/10.1016/j.compscitech.2005.10.003

Tao, Y., Hu, B., Ma, Z., Li, H., Du, E., Wang, G., ... & Song, Z. (2020). Intravitreous delivery of melatonin affects the retinal neuron survival and visual signal transmission: in vivo and ex vivo study. *Drug Delivery*, *27*(1), 1386-1396.

Teng, C. C. (1962). Fine Structure of the Human Cornea: Epithelium and Stroma* *From the laboratory of The Eye-Bank for Sight Restoration, Inc., Manhattan Eye, Ear and Throat Hospital. *American Journal of Ophthalmology, 54*(6), 969-1002. doi:https://doi.org/10.1016/0002-9394(62)94336-2

TG236, O. (2013). OECD Guidelines for the Testing of Chemicals. In *Section 2: Effects on Biotic Systems Test No. 236: Fish Embryo Acute Toxicity (FET) Test*: Organization for Economic Cooperation and Development Paris, France.

Tham, Y.-C., Li, X., Wong, T. Y., Quigley, H. A., Aung, T., & Cheng, C.-Y. (2014). Global prevalence of glaucoma and projections of glaucoma burden through 2040: a systematic review and meta-analysis. *Ophthalmology, 121*(11), 2081-2090.

Thrimawithana, T. R., Young, S., Bunt, C. R., Green, C., & Alany, R. G. (2011). Drug delivery to the posterior segment of the eye. *Drug discovery today, 16*(5-6), 270-277.

Torkildsen, G., Abelson, M. B., Gomes, P. J., McLaurin, E., Potts, S. L., & Mah, F. S. (2017). Vehicle-Controlled, Phase 2 Clinical Trial of a Sustained-Release Dexamethasone Intracanalicular Insert in a Chronic Allergen Challenge Model. *Journal of Ocular Pharmacology and Therapeutics, 33*(2), 79-90. doi:10.1089/jop.2016.0154

Trantidou, T., Prodromakis, T., & Toumazou, C. (2012). Oxygen plasma induced hydrophilicity of Parylene-C thin films. *Applied surface science, 261*, 43-51.

Tsedeke Wolde. (2014). Effects of caffeine on health and nutrition: A Review. *Food Science and Quality Management*, 30, 59-66.

Urtti, A. (2006). Challenges and obstacles of ocular pharmacokinetics and drug delivery. *Advanced Drug Delivery Reviews, 58*(11), 1131-1135. doi:https://doi.org/10.1016/j.addr.2006.07.027

Urtti, A., & Salminen, L. (1993). Minimizing systemic absorption of topically administered ophthalmic drugs. *Survey of Ophthalmology, 37*(6), 435-456. doi:https://doi.org/10.1016/0039-6257(93)90141-S

Vulovic, N., Primorac, M., Stupar, M., Brown, M., & Ford, J. (1990). Some studies on the preservation of indometacin suspensions intended for ophthalmic use. *Die Pharmazie, 45*(9), 678-679.

Watsky, M. A., Jablonski, M. M., & Edelhauser, H. F. (1988). Comparison of conjunctival and corneal surface areas in rabbit and human. *Current eye research, 7*(5), 483-486.

Wels, M., Roels, D., Raemdonck, K., De Smedt, S. C., & Sauvage, F. (2021). Challenges and strategies for the delivery of biologics to the cornea. *Journal of Controlled Release, 333*, 560-578. doi:https://doi.org/10.1016/j.jconrel.2021.04.008

Williams, D. L., Kuhn, A. T., Amann, M. A., Hausinger, M. B., Konarik, M. M., & Nesselrode, E. I. (2010). Computerised measurement of contact angles. *Galvanotechnik, 101*(11), 2502.

Wirtz, R. (1908). Die ionentherapie in der augenheilkunde [Article]. *Klin Monatsbl Augenheilkd, 46*, 543-579.

Wolf, G. (1996). A History of Vitamin A and Retinoids. *The FASEB Journal, 10*(9), 1102-1107. doi:https://doi.org/10.1096/fasebj.10.9.8801174

Wolff, E. W. R. (1976). *Eugene Wolff's Anatomy of the eye and orbit : including the central connexions, development, and comparative anatomy of the visual apparatus*. Philadelphia: Saunders. Retrieved from /z-wcorg/ database.

Wong, W. L., Su, X., Li, X., Cheung, C. M. G., Klein, R., Cheng, C.-Y., & Wong, T. Y. (2014). Global prevalence of age-related macular degeneration and disease burden projection for 2020 and 2040: a systematic review and meta-analysis. *The Lancet Global Health, 2*(2), e106-e116. doi:https://doi.org/10.1016/S2214-109X(13)70145-1

Yamashita, T., Sonoda, S., Suzuki, R., Arimura, N., Tachibana, K., Maruyama, K., & Sakamoto, T. (2007). A novel bubble liposome and ultrasound-mediated gene transfer to ocular surface: RC-1 cells in vitro and conjunctiva in vivo. *Experimental Eye Research, 85*(6), 741-748. doi:https://doi.org/10.1016/j.exer.2007.08.006

Ying, Y., Xingfen, Y., Wengai, Z., Jinheng, C., Jinyu, X., Guangyu, Y., . . . Xiang, G. (2010). Combined In Vitro Tests as an Alternative to In Vivo Eye Irritation Tests. *Alternatives to Laboratory Animals, 38*(4), 303-314. doi:10.1177/026119291003800413

Yohe, S. T., Colson, Y. L., & Grinstaff, M. W. (2012). Superhydrophobic materials for tunable drug release: using displacement of air to control delivery rates. *Journal of the American Chemical Society, 134*(4), 2016-2019.

York, M., & Steiling, W. (1998). A critical review of the assessment of eye irritation potential using the Draize rabbit eye test. *Journal of Applied Toxicology, 18*(4), 233-240.
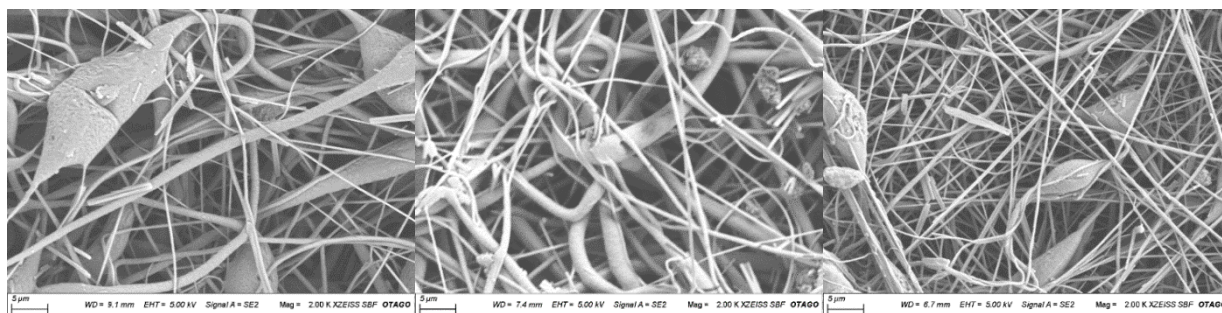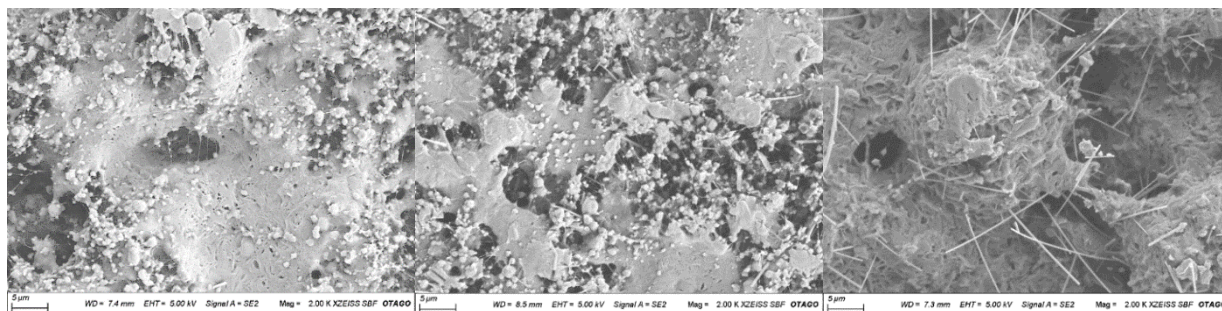
APPENDIX

Surface morphology of nanofiber formulation using FSEM

Monolayer nanofiber formulations

SEM images of 10% PCL with 5% Caffeine (left), 10% PCL with 10% Caffeine (middle) and 10% PCL with 15% Caffeine (right)
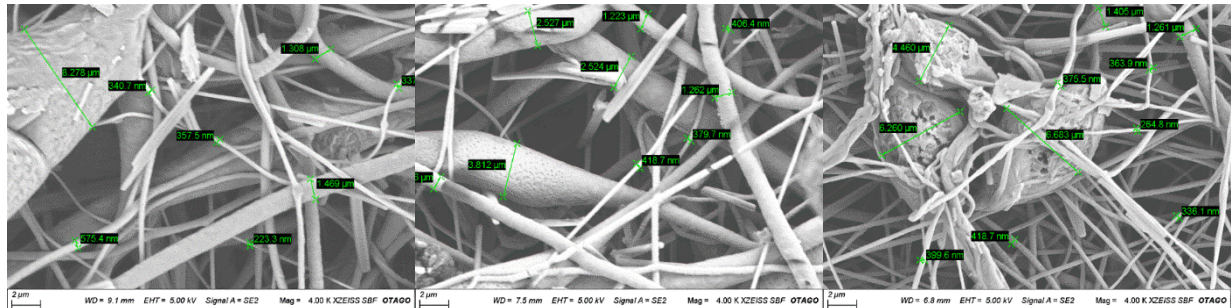

SEM images of 10% PEO with 5% Caffeine (left), 10% PEO with 10% Caffeine (middle) and 10% PEO with 15% Caffeine (right)
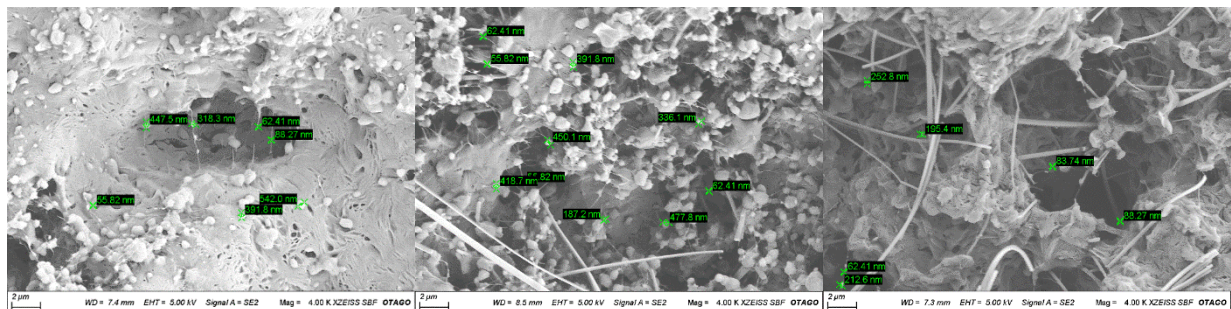
SEM images showing the fibre and bead diameter for monolayer formulations

SEM images showing the fibre and bead diameter for 10% PCL with 5% Caffeine (left), 10% PCL with 10% Caffeine (middle) and 10% PCL with 15% Caffeine (right)

SEM images showing fibre and bead diameter for 10% PEO with 5% Caffeine (left), 10% PEO with 10% Caffeine (middle) and 10% PEO with 15% Caffeine (right)

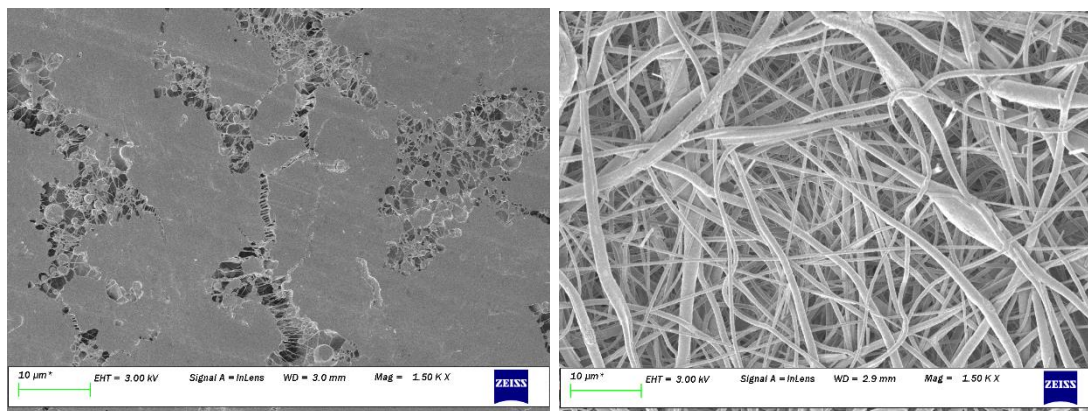SEM images of 10% PCL (left) and 10% PEO (right) monolayer formulations without the

Caffeine
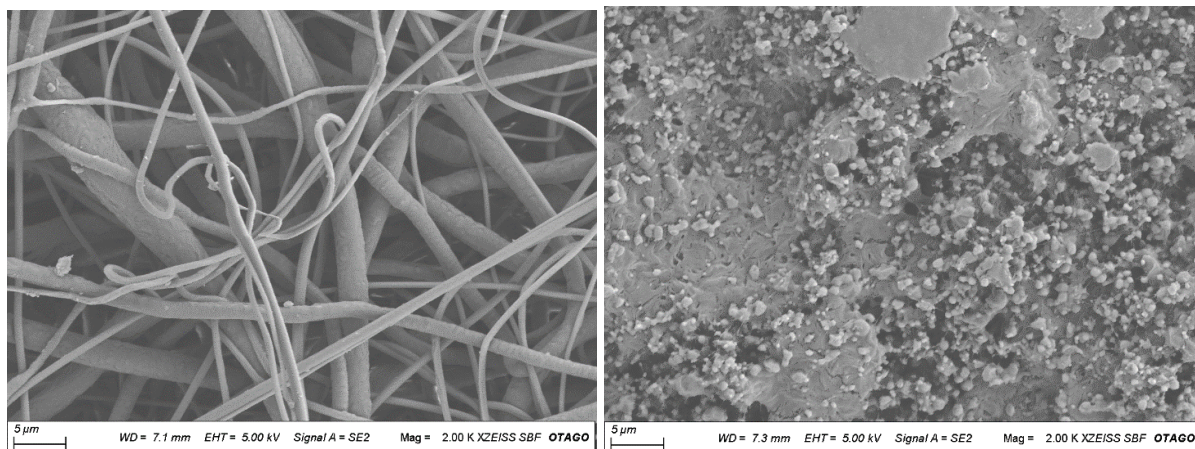
SEM images showing the fibre morphology for 10% PEO with 15% Caffeine (lower surface, on

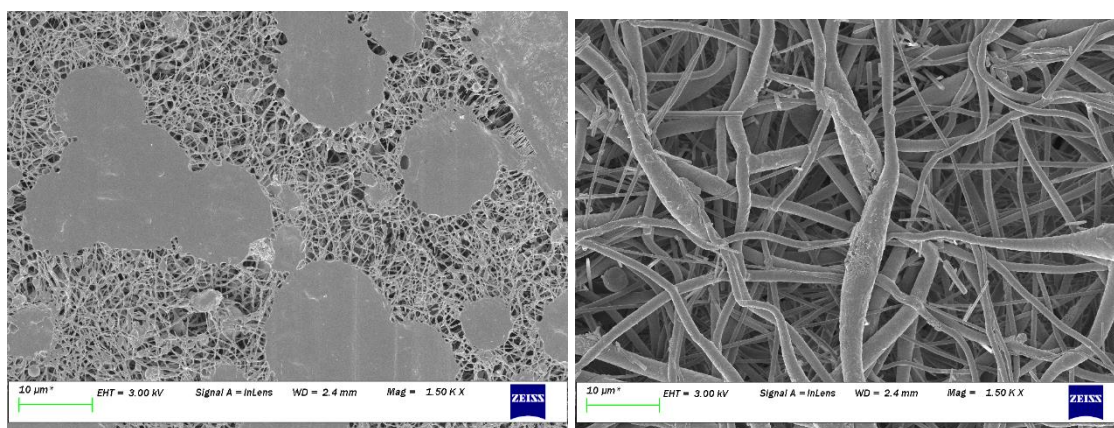the left) and 10% PEO with 15% Caffeine (upper surface, on the right)
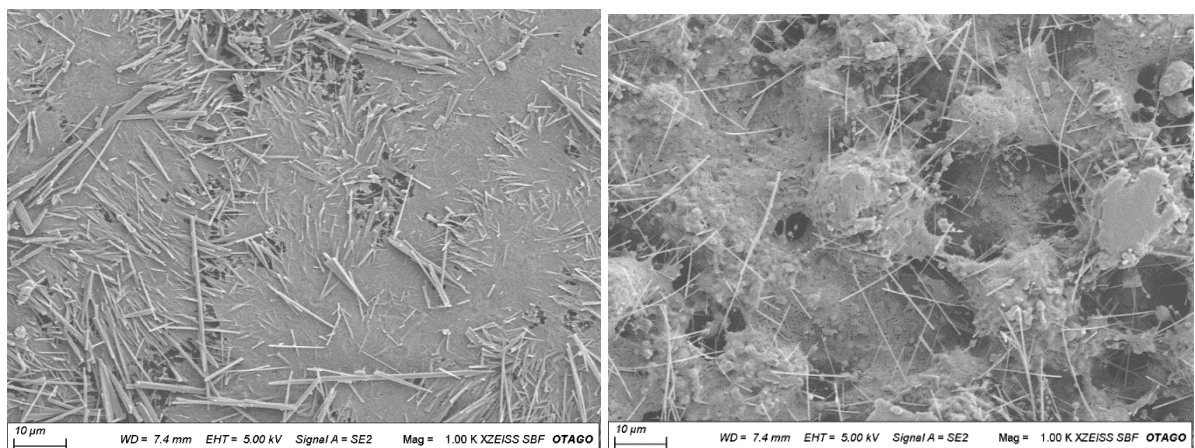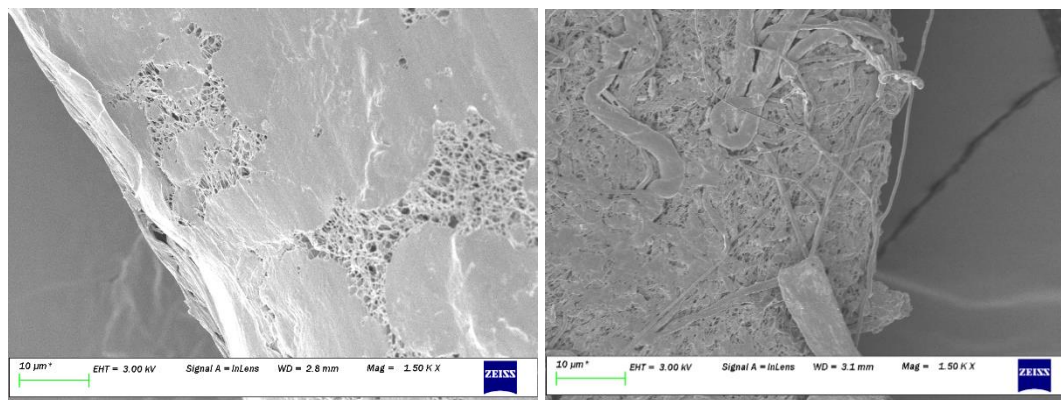
Three-layered nanofiber formulation SEM images

SEM images showing the fibre morphology for three layered nanofiber formulation 1st layer 10% PEO, 2nd layer 5 and 1% PCL and 3rd layer 10% PCL with 10% Caffeine with 10 minutes overlapping time between the layers, lower side containig PEO polymer (left) and upper side containing PCl with Caffeine (right)
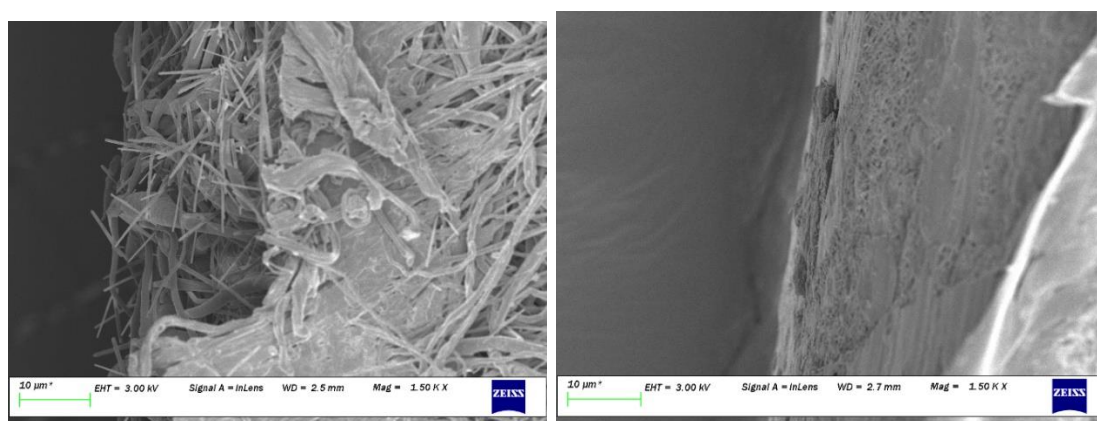

SEM images showing the fibre morphology for three layered nanofiber formulation 1st layer 10% PEO, 2nd layer 5 and 1% PCL and 3rd layer 10% PCL with 10% Caffeine with 30 minutes overlapping time between the layers, lower side containig PEO polymer (left) and upper side containing PCl with Caffeine (right)
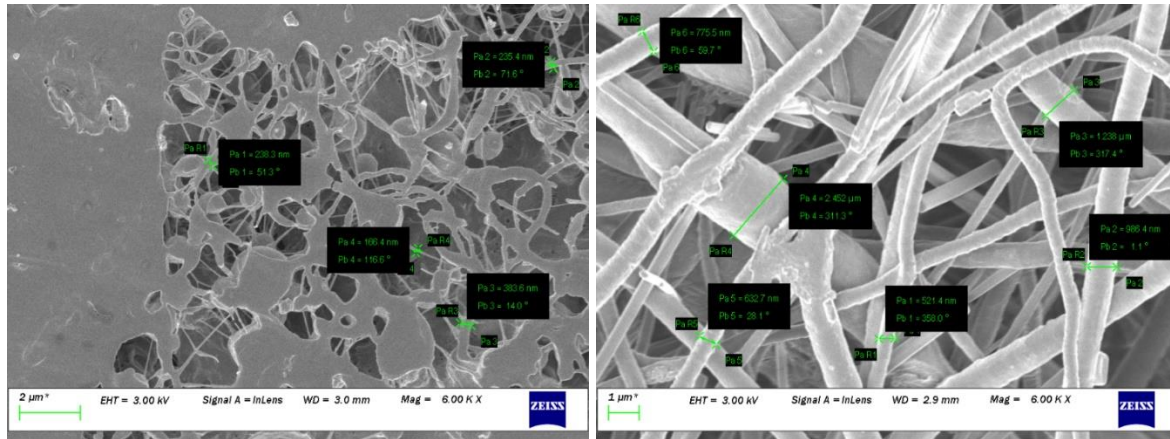
SEM images showing the mat edge fibre morphology for three layered nanofiber formulation, 1st layer 10% PEO, 2nd layer 5 and 1% PCL and 3rd layer 10% PCL with 10% Caffeine with 10 minutes overlapping time between the layers, lower side containig PEO polymer (left) and upper side containing PCl with Caffeine (right)

SEM images showing the mat edge fibre morphology for three layered nanofiber formulation, 1st layer 10% PEO, 2nd layer 5 and 1% PCL and 3rd layer 10% PCL with 10% Caffeine with 30 minutes overlapping time between the layers, lower side containig PEO polymer (left) and upper side containing PCl with Caffeine (right)

SEM image showing the fibre and bead diameter for formulation with three layer, 1st layer 10% PEO, 2nd layer 5 and 1% PCL and 3rd layer 10% PCL with 10% Caffeine with 10 minutes overlapping time between the layers, lower side containig PEO polymer (left) and upper side containing PCl with Caffeine (right)

SEM image showing the fibre and bead diameter for formulation with three layers, 1st layer 10% PEO, 2nd layer 5 and 1% PCL and 3rd layer 10% PCL with 10% Caffeine with 30 minutes overlapping time between the layers, lower side containig PEO polymer (left) and upper side containing PCl with Caffeine (right)